

**EFFECTS OF NUTRITIONAL MOLECULES IN
REGULATION OF ADIPOGENESIS AND KEY ADIPOGENIC
GENE EXPRESSION**

A Dissertation

Presented in Partial Fulfillment of the Requirements for the

Degree of Doctor of Philosophy

with a

Major in Animal Physiology

in the

College of Graduate Studies

University of Idaho

by

Shuhan Ji

Major Professor: Dr. Rodney A. Hill

Committee Members: Dr. Matthew Doumit; Dr. Onesmo Balemba; Dr. Min Du

Department Administrator: Dr. Mark McGuire

July 2015

AUTHORIZATION TO SUBMIT DISSERTATION

This dissertation of Shuhan Ji, submitted for the degree of Ph.D. with a major in Animal Physiology and titled “Effects of nutritional molecules in regulation of adipogenesis and key adipogenic gene expression” has been reviewed in final form. Permission, as indicated by the signatures and dates given below, is now granted to submit final copies to the College of Graduate Studies for approval.

Major Professor _____ Date _____

Dr. Rodney A. Hill

Committee
Members _____ Date _____

Dr. Matthew Doumit

_____ Date _____

Dr. Onesmo Balemba

_____ Date _____

Dr. Min Du

Department

Administrator _____ Date _____

Dr. Mark McGuire

ABSTRACT

Adipogenesis plays an important role in adipose tissue formation. Several transcriptional factors are involved in regulation of this complex process. Nutritional molecules, such as vitamin D and retinoic acid, have been reported as regulators of adipogenesis. The major aims of the present study were to investigate the mechanisms of vitamin D or retinoic acid regulation of adipogenesis and also the interaction between vitamin D or retinoic acid and adipogenic factors, such as peroxisome proliferator-activated receptor γ (PPAR γ) and CCAAT-enhancer-binding protein α (C/EBP α). The bioactive form of vitamin D, 1,25-dihydroxyvitamin D (1,25-(OH) $_2$ D $_3$) has been reported as a potential inhibitor of adipogenesis, and retinoic acid has also been shown as an inhibitor of adipogenesis. The inhibitory effect of both 1,25-(OH) $_2$ D $_3$ and retinoic acid on adipogenesis in 3T3-L1 cells was detected. Gene expression of the adipogenic key transcription factors PPAR γ and C/EBP α were inhibited by both high concentrations of 1,25-(OH) $_2$ D $_3$ (10 and 100 nM) and retinoic acid (100 and 1000 nM), and in contrast, gene expression of the other two C/EBP family members, C/EBP β and γ , were not influenced by any concentration of 1,25-(OH) $_2$ D $_3$ or retinoic acid. Fatty acid binding protein 4 (FABP4) gene expression showed a marked response to both 1,25-(OH) $_2$ D $_3$ and retinoic acid, even at the lower concentrations studied (0.1 and 1 nM of 1,25-(OH) $_2$ D $_3$ treatments, and 1 and 10 nM of retinoic acid treatments). Unlike 1,25-(OH) $_2$ D $_3$, retinoic acid had greater inhibitory impact on C/EBP α gene expression compared to PPAR γ . Both 1,25-(OH) $_2$ D $_3$ and retinoic acid had gradual inhibitory effects on the gene expression of stearoyl-coenzyme A desaturase 1 (SCD-1) compared to FABP4. C/EBP α promoter activity in response to 1,25-(OH) $_2$ D $_3$ (100 nM) or retinoic acid (1000 nM) treatments were tested in 3T3-L1 cells. The results showed that 1,25-(OH) $_2$ D $_3$ had little impact on the activity of the C/EBP α promoter, while retinoic acid appeared

to induce activation of the promoter, despite an overall inhibitory effect on *C/EBP α* mRNA concentration. This observation suggests that the actions of retinoic acid may be mediated through an mRNA degradative pathway. Gold-nanoconjugates linked with KDEL peptide was used to deliver siRNA against *C/EBP α* into 3T3-L1 cells. Transfection of gold-nanoconjugates into preadipocytes and mature adipocytes was observed by confocal microscopy. This result suggests that gold-nanoconjugates can be used as a delivery vector into mature adipocytes. Unfortunately, *C/EBP α* siRNA silencing was not detected on all the three time points measured, suggesting that further studies will be focused on optimizing time points, and cellular uptake trafficking and co-localization of gold-nanoconjugates/siRNA in adipocytes. Overall, adipogenesis was inhibited by both 1,25-(OH) $_2$ D $_3$ and retinoic acid treatments, and the gene expression of adipogenic transcription factors were inhibited in response to 1,25-(OH) $_2$ D $_3$ and retinoic acid treatments, suggesting that the mechanisms of 1,25-(OH) $_2$ D $_3$ and retinoic acid regulation of adipogenesis involved transcriptional regulation.

ACKNOWLEDGEMENTS

First of all, I would like to offer my sincere acknowledgements to Idaho Agricultural Experiment Station and the Department of Animal and Veterinary Science at the University of Idaho (UI). I am honored to be selected and given the opportunity to pursue a doctorate degree in Animal Physiology.

I am sincerely grateful to my major professor, Dr. Rodney A. Hill, for providing me with an environment that helped to improve my intellectual and scientific capabilities. Dr. Hill is a great professor for not only teaching me scientific knowledge and also providing me moral support, which helped me conquer all the difficulties in the process of completing my doctoral study. I also wish to thank my Ph.D committee members, Dr. Matt Doumit from the Department of Animal and Veterinary Science, UI, Dr. Onesmo Balemba from the Department of Biological Sciences, UI, and Dr. Min Du from the Department of Animal Sciences, Washington State University. I am very grateful for their encouragement, support, and suggestions. I would like to say to all my committee members, “Thank you very much for teaching and instructing me to become a good scientist in the future”.

I am greatly grateful to Mrs. Ann S. Norton for helping me with the microscopy experiments. Mrs. Ann S. Norton is the manager of UI optical imaging center and taught me lots of useful instructions on optical microscopy and fluorescence microscopy. I also would like to say “thank all of you very much” to many faculty members from the Department of Animal and Veterinary Science, UI. I would say “many thanks” to Paula Heaton, the administrative coordinator of the Department of Animal and Veterinary Science, UI, for helping me dealing

with the confusing paperwork and for answering my stupid questions during my first year and until now.

Finally, I would like to thank my family and friends for their encouragement and support. My parents, my mom, Xin Li, and my dad, Jun Ji, thank you so much for your support and trust. Thank you for raising me right, and encouraging me to pursue my dream. I could not make this far without both of you. I also want to thank my grandmother, Cunyu Hou, “thank you very much for helping my mom take care of me when I was little, and keeps loving me every day in my life”. All of my family make me whoever I am today, and I would like to share all my credits with all of them. No matter where I am, I will love them forever.

Sincerely,

Shuhan Ji

Department of Animal and Veterinary Science

University of Idaho

Moscow, ID, 83843

TABLE OF CONTENTS

AUTHORIZATION TO SUBMIT DISSERTATION.....	ii
ABSTRACT.....	iii
ACKNOWLEDGEMENTS.....	v
ABBREVIATIONS	xi
LIST OF FIGURES	xii
LIST OF TABLES.....	xv
CHAPTER I.....	1
LITERATURE REVIEW	1
MOLECULAR AND TRANSCRIPTIONAL REGULATION OF ADIPOGENESIS	1
INTRODUCTION OF ADIPOGENESIS.....	1
The value of fat in beef cattle	1
Physiological roles of the adipose tissues.....	3
Program of adipose cell development	5
Transcriptional control of adipogenesis	10
Cellular and hormonal regulation of adipogenesis	27
VITAMIN D.....	29
Vitamin D synthesis and metabolism	29
Vitamin D and adipogenesis.....	30
Vitamin A.....	34

Vitamin A metabolism.....	34
Vitamin A and adipogenesis.....	35
Vitamin A and body fat.....	36
GOLD NANOPARTICLES IN BIOMOLECULE DELIVERY	37
DIRECTING PEPTIDE	37
SMALL INTERFERING RNA.....	38
HYPOTHESES	40
OBJECTIVES	41
REFERENCES.....	42
CHAPTER II.....	71
REGULATION OF ADIPOGENESIS AND KEY ADIPOGENIC GENE EXPRESSION BY 1,25-DIHYDROXYVITAMIN D IN 3T3-L1 CELLS	71
ABSTRACT.....	71
INTRODUCTION.....	72
MATERIALS AND METHODS.....	75
RESULTS.....	82
DISCUSSION	109
ACKNOWLEDGEMENTS	119
REFERENCES.....	120
SUPPLEMENTARY FIGURES.....	125

CHAPTER III	131
ADIPOGENESIS AND KEY ADIPOGENIC GENE EXPRESSION RESPONSE TO RETINOIC ACID IN 3T3-L1 CELLS	131
ABSTRACT	131
INTRODUCTION.....	132
MATERIALS AND METHODS	134
RESULTS.....	141
DISCUSSION	156
ACKNOWLEDGEMENTS	161
REFERENCES.....	162
SUPPLEMENTARY FIGURES	167
CHAPTER IV	180
GOLD-KDEL EPTIDE-SIRNA NANOCONJUGATE-MEDIATED TRANSFECTION IN 3T3-L1 PREADIPOCYTES AND MATURE ADIPOCYTES.....	180
ABSTRACT	180
INTRODUCTION.....	181
MATERIALS AND METHODS	182
RESULTS.....	188
DISCUSSION	190
REFERENCES.....	193

CHAPTER V 198

CONCLUSIONS AND FUTURE DIRECTIONS..... 198

ABBREVIATIONS

PPAR γ	peroxisome proliferator-activated receptor γ
C/EBP α	CCAAT-enhancer-binding protein α
C/EBP β	CCAAT-enhancer-binding protein β
C/EBP δ	CCAAT-enhancer-binding protein δ
VDR	vitamin D receptor
RXR	retinoid X receptor
FABP4	fatty acid binding protein 4
SREBP-1c	sterol-regulatory element binding protein 1c
SCD-1	stearoyl-coenzyme A desaturase 1
Pref-1	preadipocyte factor-1
EEF2	eukaryotic translation elongation factor 2

LIST OF FIGURES

Figure 1.1 The stages of adipocyte differentiation	6
Figure 1.2 Transcriptional regulation of adipogenesis	8
Figure 1.3 Putative functions of fatty acid binding protein (FABP) in the cells	26
Figure 1.4 Vitamin D and adipogenesis.....	33
Figure 1.5 Chemical structures of some biological active retinoids	34
Figure 2.1 Oil red o staining in 3T3-L1 cells.....	83
Figure 2.2 PPAR γ mRNA and protein expression in differentiation medium	85
Figure 2.3 Real-time PCR quantification of PPAR γ gene expression in 3T3-L1 cells in response to treatments.....	87
Figure 2.4 C/EBP α mRNA and protein expression in differentiation medium	90
Figure 2.5 Real-time PCR quantification of C/EBP α gene expression in 3T3-L1 cells in response to treatments.....	92
Figure 2.6 Real-time PCR quantification of VDR gene expression in 3T3-L1 cells in response to treatments.....	95
Figure 2.7 Real-time PCR quantification of C/EBP β gene expression in 3T3-L1 cells in response to treatments.....	97
Figure 2.8 Real-time PCR quantification of C/EBP δ gene expression in 3T3-L1 cells in response to treatments.....	99
Figure 2.9 Real-time PCR quantification of FABP4 gene expression in 3T3-L1 cells in response to treatments.....	101
Figure 2.10 Real-time PCR quantification of SREBP-1c gene expression in 3T3-L1 cells in response to treatments.....	103

Figure 2.11 Real-time PCR quantification of SCD-1 gene expression in 3T3-L1 cells in response to treatments.....	105
Figure 2.12 Real-time PCR quantification of Pref-1 gene expression in 3T3-L1 cells in response to treatments.....	107
Figure 2.13 Relative luciferase activity of C/EBP α promoter activity in response to treatments.....	109
Supp 2.1 PPAR γ protein expression.....	125
Supp 2.2 C/EBP α protein expression.....	128
Figure 3.1 Real-time PCR quantification of PPAR γ gene expression in 3T3-L1 cells in response to treatments.....	143
Figure 3.2 Real-time PCR quantification of C/EBP α gene expression in 3T3-L1 cells in response to treatments.....	1467
Figure 3.3 Real-time PCR quantification of FABP4 gene expression in 3T3-L1 cells in response to treatments.....	149
Figure 3.4 Real-time PCR quantification of SREBP-1c gene expression in 3T3-L1 cells in response to treatments.....	151
Figure 3.5 Real-time PCR quantification of SCD-1 gene expression in 3T3-L1 cells in response to treatments.....	153
Figure 3.6 Real-time PCR quantification of Pref-1 gene expression in 3T3-L1 cells in response to treatments.....	155
Supp 3.1 Oil Red O staining in 3T3-L1 cells.....	167
Supp 3.2 PPAR γ protein expression.....	169

Supp 3.3 C/EBP α protein expression.....	172
Supp 3.4 Real-time PCR quantification of C/EBP β gene expression in 3T3-L1 cells in response to treatments.....	172
Supp 3.5 Real-time PCR quantification of C/EBP δ gene expression in 3T3-L1 cells in response to treatments.....	177
Supp 3.6 Real-time PCR quantification of C/EBP δ gene expression in 3T3-L1 cells in response to treatments.....	179
Figure 4.1 Fluorescence image of Au-nanoconjugates in 3T3-L1	188
Figure 4.2 mRNA knockdown of C/EBP α by Au-nanoconjugates	189

LIST OF TABLES

TABLE 2.1 Primers And Probes	79
TABLE 3.1 Primers And Probes	139
TABLE 4.1 Sequences and Purities of Peptides and siRNAs	187

CHAPTER I

LITERATURE REVIEW

MOLECULAR AND TRANSCRIPTIONAL REGULATION OF ADIPOGENESIS

Introduction of Adipogenesis

The value of fat in beef cattle

In the beef cattle industry, adipocyte differentiation and adipose physiology are directly associated with both the quality and the value of the meat production [1]. The intramuscular fat tissue is synonymous with marbling, which influences the tenderness and palatability of beef product [2]. The subcutaneous fat thickness is also important for grading beef carcasses, and is also related to palatability [3]. Understanding the mechanisms of regulating adipocyte differentiation and adipose deposition via manipulating the expression of key adipogenic genes is very important in improving beef quality and saving economic cost in beef cattle industry.

Adipose tissue is distributed in different parts (fat depots) in an animal's body, such as subcutaneous, intramuscular, intermuscular, peri-renal, and omental depots. Subcutaneous and intermuscular fat depots form the largest portion of the whole body fat [4]. Size of the adipocytes from various fat depots was reported as follows: peri-renal > omental > subcutaneous > intermuscular > intramuscular > brisket depots [5, 6]. Peri-renal and omental adipocytes were reported to have more lipogenic enzyme activity than adipocytes from subcutaneous and intermuscular depots [7]. The subcutaneous adipocytes and intramuscular adipocytes contain lipogenesis and lipogenic enzymes, such as glucose 6-phosphate dehydrogenase, fatty acid synthetase, pentose cycle reductase and NADP-malate dehydrogenase [6, 8]. Thus, intramuscular and subcutaneous adipose tissues play important roles in triglyceride formation and fat storage.

Beef carcasses can be categorized by quality grade and yield grade. The amount of intramuscular fat tissue contributes to marbling scores and influences the quality and palatability of beef [2]. Levels of marbling and subcutaneous fat are important in determining quality grade and yield grade respectively [9]. The size of adipocytes in intramuscular fat depots is a factor that impacts the amount of marbling [8]. Marbling scores are categorized as Devoid, Practically Devoid, Trace, Slight, Small, Modest, Moderate, Slightly Abundant, Moderately Abundant and Abundant. Based on the level of marbling, the United States Department of Agriculture (USDA) categorizes beef quality into eight different grades. Prime and Choice grades are considered as higher quality beef and have more desirable marbling scores than Select and Standard grades in relatively younger cattle. For carcasses from older cattle, Commercial and Utility grades have more

marbling than Cutter and Canner grades. Yield grade is determined by the muscle and fat ratio and has a range of 1 to 5. Beef having a yield grade of 5 would have less muscle and more fat. Studies are needed to understand the mechanisms that influence the amount of intramuscular adipocytes by regulating expression of key adipogenic genes in adipogenesis.

Physiological roles of adipose tissues

For decades, adipose tissue was considered an inert mass of stored energy with some advantageous properties, such as its functions as an insulating substance and as a mechanical support for more important structures [10]. However, in the past fifteen years, interest of studies in adipose tissue has been shifted from its physiology to its developmental biology. The discovery of leptin in 1994 showed a growing awareness that adipocytes are essential regulators of whole-body energy homeostasis. These cells secrete several proteins that regulate processes such as blood pressure, immune function, energy balance and angiogenesis [11]. Although many cell types contain esterified lipids, adipocytes are the only cell type in maintaining the quantity of lipid that they can store, and quick releasing these calories for use by other organs. Another reason for the surge in interest in adipocytes is the realization that we are in the early stages of a global wave of obesity with the consequent increase in associated morbidity and mortality [12]. Moreover, obesity is characterized by an increase in lipid accumulation and is the leading risk-factor for the development of Type 2 diabetes [13].

There are two types of adipocyte in mammals, termed white adipose tissue (WAT) and brown adipose tissue (BAT), which differ in several important properties. WAT functions as a storage tissue of extra food and its further utilization during starving periods [14]. WAT also produces hormones such as leptin and adiponectin that play important roles in lipid metabolism [15]. On the other hand, BAT store less lipid and has more mitochondria than WAT, and is rich in uncoupling proteins (UCPs) and primarily participates in heat production and maintenance of body temperature (adaptive thermogenesis) [16]. Brown adipocytes express almost all the genes that are expressed in white adipocytes, however, they also express some distinct genes, including uncoupling protein-1 (UCP1), which allows energy to be dissipated as heat without generating ATP. Most brown adipose tissue (BAT) in rodents is localized to the interscapular region. Human have large depots of brown- adipose tissue in infancy, but only small amounts that are dispersed throughout depots of WAT persist in adults [10].

Both brown adipogenesis and white adipogenesis require peroxisome proliferator-activated receptor γ (PPAR γ) and CCAAT-enhancer-binding proteins (C/EBPs). Interesting, although inhibition or decrease of C/EBP α blocks development of most white-adipose tissue, the influence on brown-adipose tissue are less marked [17]. Conversely, the ablation of both C/EBP β and C/EBP δ results in significantly decreased amounts of UCP1 in brown-adipose tissue, even though the amounts of C/EBP α are normal [18].

In physiological terms, brown adipose tissue is thought to function in two major contexts: defense against cold and protection against obesity. Despite large mammals such as humans have less obvious brown adipose depots than smaller mammals such as rodents, it is clear that BAT does exist in humans, and they possess the necessary molecular components to dissipate energy in the form of heat [8]. Among WAT, adipocytes from different locations can have distinct molecular and physiological properties [19, 20]. For instance, Adipocytes in visceral depots are sensitive to lipolytic stimuli, whereas adipocytes from structural depots (for example, around the eyes and in the heel pads) do not release stored lipid easily. Moreover, increased visceral adipose tissue is related with an increased risk of insulin resistance and cardiovascular disease, whereas increased subcutaneous adipose tissue is not.

Program of adipose cell development

Adipogenesis

Adipogenesis is a complex process including several steps. Adipose tissue is formed from its precursor cells named adipoblasts [21, 22]. Adipoblasts arise from multipotent stem cells through rapid cell division. Multipotent stem cells are not committed to undergo adipogenesis, but have multiple potentials to become either adipoblasts, chondroblasts, osteoblasts or myoblasts [23]. The mechanism by which multipotent stem cells become adipoblasts is not completely characterized. Adipoblasts differ from multipotent stem cells and are committed to become adipose tissue, and this stage in adipogenesis is called 'Cell Determination' [22]. After these cells undergo multiple cell division cycles, adipoblasts

become ‘preadipocytes’, and this stage is called ‘Exponential Growth Phase’ [24]. Preadipocytes appear as elongated fibroblast-like cells in morphology, and at this stage, cells reach confluence *in vitro* conditions and stop cell division through mechanisms associated with ‘cell-cell contact’ [22]. Further, *in vitro*, addition of adipogenic differentiation medium induces preadipocytes to become mature adipocytes. Mature adipocytes do not have the capability to undergo cell division and are named as ‘terminally differentiated’ cells (Fig. 1.1).

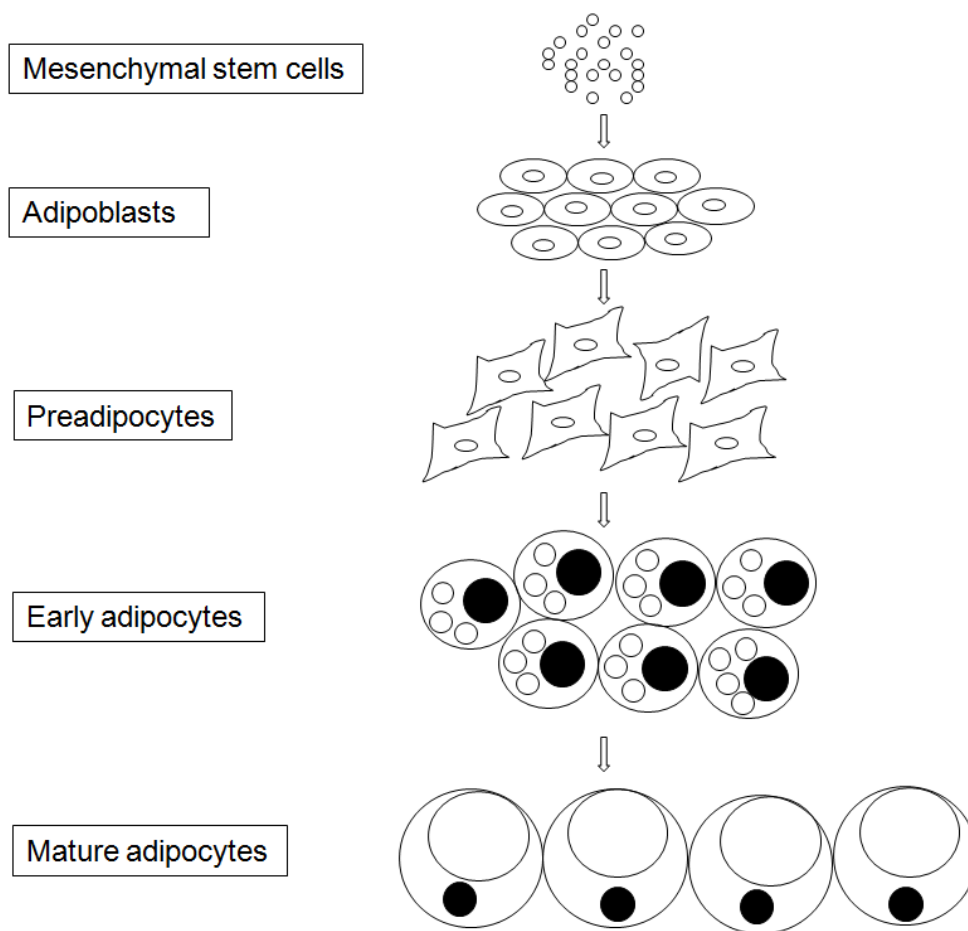


Figure 1.1: The stages of adipocyte differentiation

During the process of adipogenesis, preadipocytes differentiate to form mature adipocytes to achieve lipid accumulation. The transcriptional control of adipocyte differentiation requires a sequential series of gene expression events and activation of a number of key signaling pathways (Fig. 1.2). This cascade starts with the induction of CCAAT/enhancer – binding protein β and δ (C/EBP β and C/EBP δ). These two proteins then induce the expression of nuclear receptor peroxisome proliferator – activated receptor γ (PPAR γ), which in turn induces C/EBP α expression [25]. Once expressed, C/EBP α activity positively feeds back on PPAR γ activity. These two factors enhance each other's expression and maintain the differentiated state [26]. Sterol-regulatory element binding protein 1c (SREBP-1c) is another notable key adipogenic gene [27]. Increased expression of SREBP-1c leads to activation of PPAR γ by inducing its expression and by increasing the production of an endogenous PPAR γ ligand. All these transcriptional factors are necessary for the terminally differentiated phenotype.

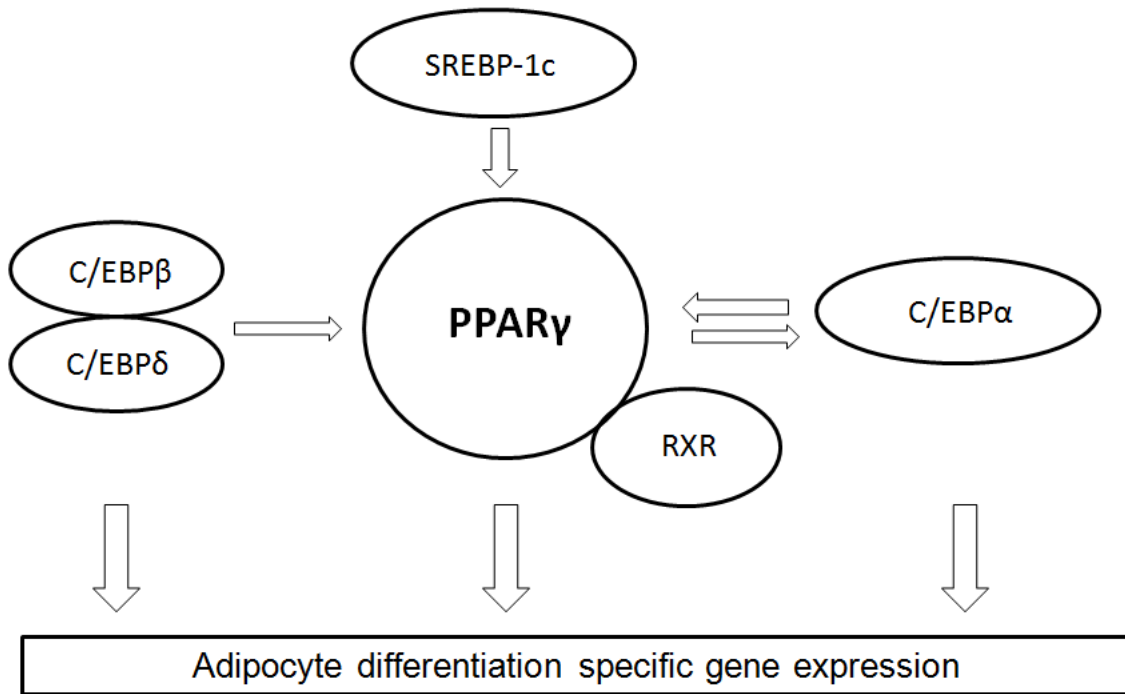


Figure 1.2: Transcriptional regulation of adipogenesis (PPAR γ , Peroxisome proliferator activated receptor γ ; C/EBP α , CCAAT/enhancer binding protein α ; C/EBP β , CCAAT/enhancer binding protein β ; C/EBP δ , CCAAT/enhancer binding protein δ ; SREBP-1c, sterol regulatory element binding protein 1c; RXR, retinoid X receptor)

Adipose tissue formation

Adipose tissues are different from many other tissues in that they occur in multiple, dispersed sites around the body [8]. Generally speaking, most adipose tissues form at sites rich in loose connective tissues, such as the subcutaneous layers between the dermis and muscle. However, fat deposits also form around the heart, kidneys, and other internal organs [28]. One interesting feature of fat cell development is that it tends to occur in clusters. This phenomenon is observed both *in vivo* and *in vitro*. One possible explanation is that the expression of a recruitment factor by mature adipocytes, ensures that where one adipocyte develops, others will follow and be induced as well. There is actually evidence for such a factor, as conditioned media from mature adipocytes has been shown to induce the differentiation of preadipocytes in culture [29]. This factor has not been isolated, however, it is has been shown that the addition of triglycerides and fatty acids to unconditioned media does not mimic the effect.

Growth of adipose tissue mass *in vivo* involves two distinct processes: hypertrophy (because of lipid synthesis and the subsequent increase in the size of adipocytes) and hyperplasia (because of proliferation, when preadipocyte and adipocyte numbers increase) [30]. Two theories were proposed to explain the process of adipose tissue accumulation in mammalian bodies. It was once believed that animals have a specific number of adipocytes at birth and this number of adipocytes does not change during the entire lifetime [31, 32]. According to this theory, 'critical period theory' [21, 32], there are two steps during the process of adipose tissue accumulation. The first step, in pre-adult, adipoblast cells undergo

cell division (hyperplasia), resulting in an increase of cell number. Later in the adult phase, cells do not undergo cell division and this phase is characterized by a marked increase in lipid accumulation causing enlargement of adipocytes (hypertrophy). Another theory to explain the process of accumulation of adipose tissue in animals was proposed by Faust *et al.* in 1978, termed as ‘maximum fat cell size theory’ [33]. According to this theory, the number of adipocytes in animals is not constant and adipose tissue accumulation occurs both through hypertrophy and hyperplasia. Adipoblasts undergo mitotic cell division and then stop cell division after reaching a particular point. Then a portion of cells start to accumulate lipid droplets and become mature adipocytes. After these cells reach a specific size, called ‘maximum fat cell size’, the remaining precursor Adipoblast cells undergo cell division and start to become new adipoblast cells, and this process causes an increase in the number of cells in adipose tissue [32].

Transcriptional control of adipogenesis

Peroxisome Proliferator-activated Receptor γ (PPAR γ)

The PPAR family is a group of transcriptional factors that belongs to the nuclear hormone receptor superfamily. These transcriptional factors heterodimerize with another nuclear hormone receptor, retinoid X receptor (RXR), bind to the response elements of target gene promoters and function as active transcriptional factors [34]. When PPARs are heterodimerized with RXR, the complex is activated and transported to the nucleus to bind to specific sequences in promoter regions (termed as PPAR response elements, PPREs) of downstream target genes, activating their transcription [35-37]. The molecular structure of

PPARs has two highly conserved functional domains, the DNA binding domain (DBD) and the ligand binding domain (LBD). The DBD contains two zinc-finger motifs which bind to PPRE of target gene regulatory regions (37). LBD binds to a variety of natural and synthetic ligands of PPARs and this process is important in PPAR activation. Fatty acids such as linoleic acid, linolenic acid, and arachidonic acid have been reported as natural ligands of PPARs. Some antidiabetic drugs, such as troglitazone, rosiglitazone and pioglitazone, are reported as potential synthetic ligands of PPAR γ [37].

There are three major isoforms: PPAR α , PPAR δ , and PPAR γ [36]. These three isoforms have specific roles in lipid metabolism. Notably, PPAR γ plays an important role in triglyceride synthesis and adipocyte differentiation processes [38]. In addition, PPAR γ also has a role in increasing expression of mitochondrial uncoupling proteins (UCPs) [39]. PPAR γ has two protein isoforms, PPAR γ 1 and PPAR γ 2, due to differential promoter usage and mRNA splicing. PPAR γ 2 has an additional 30 amino acids compared to PPAR γ 1 at the N-terminus [40-42]. PPAR γ 2 is expressed predominantly in adipose tissue, and is expressed at very high levels [35, 43]. However, PPAR γ 1 occurs in different tissues, such as heart, muscle, intestine, liver, kidney, pancreas and spleen [44, 45]. Activation of PPAR γ expression occurs downstream of C/EBP β and C/EBP δ transcription during the cascade of adipogenesis, and upstream of C/EBP α . In contrast to the role of PPAR γ in triglyceride formation, PPAR α was reported to play a critical role in β -oxidation of fatty acids. PPAR α is abundant in brown adipose tissue and liver, and is less abundantly present in kidney, heart, skeletal muscle and brown fat [36]. PPAR δ is expressed in brain, muscle, adipose

tissue and skin. PPAR δ plays a role in muscle and fat metabolism and clearance of excess cholesterol [46].

PPAR γ plays a crucial role in the function of many adipogenesis-specific genes, and PPAR γ binding is absolutely required for the function of the adipogenic selective enhancers for *FABP4* gene in cultured adipocytes [47]. In addition to its role in inducing *FABP4* expression, PPAR γ activates the promoters of many other adipogenic genes. The expression of phosphoenolpyruvate carboxykinase (PEPCK) in adipocytes was reported to require PPAR γ binding [47]. Another study published by Tontonoz *et al.* in 1994 indicated that forced expression of PPAR γ is sufficient to induce adipocyte differentiation in fibroblasts [48], and no factor has been discovered that induces adipogenesis in the absence of PPAR γ . These findings are consistent with the observation that most pro-adipogenic factors seem to function at least in part by inducing PPAR γ expression or activity. PPAR γ is both necessary and essential for adipogenesis [16].

Efforts to identify the endogenous PPAR γ ligand have not been successful. Cyclic AMP (cAMP)-dependent ligand activity was found in 3T3-L1 cells in the first two days of differentiation, after which this activity quickly declined [49]. This interesting finding demonstrates that ligand activation of PPAR γ is required to induce adipogenesis, but not to maintain PPAR γ -dependent gene expression in mature adipocytes. Other studies have reported that the transcription factors SREBP-1c and C/EBP β are upstream of PPAR γ in

the process of adipogenesis, and can increase PPAR γ ligand production [50, 51], but these results have not led to the identification of a definitive endogenous PPAR γ agonist.

PPAR γ is not only crucial for adipogenesis but is required for maintenance of the differentiated state as well. Adenoviral introduction of a dominant-negative PPAR γ into mature 3T3-L1 adipocytes causes de-differentiation with reduction of lipid accumulation and decreased expression of adipogenic factor genes [52]. In vivo, inducible knockout of PPAR γ in differentiated adipocytes results in adipocyte death, followed by generation of new adipocytes [53].

CCAAT/enhancer-binding protein (C/EBP) family

The C/EBPs are members of the basic-leucine zipper class of transcription factors. Six isoforms have been described, all of which act as homo- and/or heterodimers formed via a highly conserved bZIP domain [54]. Their tissue distribution is not limited to adipose tissue [55], and a role for C/EBP proteins has been demonstrated in the terminal differentiation of granulocytes [56] and hepatocytes [57, 58]. C/EBPs also play an important role in resistance to infection [59] and in the tissue response to injury [58], in addition to transactivating a wide variety of target genes.

During adipogenesis, expression of several C/EBP family members can be regulated at many levels, including transcriptionally, as measured by mRNA levels in cell [60].

Actually, cAMP a well-known inducer of adipogenesis *in vitro* and a component of most pro-differentiative regimens, can enhance both C/EBP α and C/EBP β expression [55, 61]. Moreover, alternative translational start sites yield multiple isoforms of some of the C/EBPs, including C/EBP α and β . For instance, the 42-kD C/EBP α isoform is a stronger transcriptional activator than the 30-kD C/EBP α isoform, and the p42/p30 ratio increases during the process of adipogenesis [62]. Studies like these do not prove that translation is a regulated step in adipocyte formation, but they at least show the possibility. Similarly, the amount of the 20-kD isoform of C/EBP β decreases during adipogenesis compared to the 32-kD active isoform [63]. Post-translational regulation of C/EBPs, particularly changes in phosphorylation, can modify the activity of C/EBP proteins as well. Finally, the activity of C/EBPs can be modulated by the presence of other family members, for example, C/EBP ξ (also known as CHOP or Gadd 153) cannot bind DNA by itself but does dimerize with other C/EBPs, then acting as a natural dominant-negative inhibitor of C/EBP activity [64].

Regulated expression is seen for several C/EBPs during adipogenesis, and recent gain- and loss-of-function studies demonstrate that these proteins have important impact on adipocyte differentiation. In the process of adipogenesis, mRNA levels and protein levels of C/EBP β and C/EBP δ are induced early, and transiently [55, 65, 66]. On the other hand, C/EBP α is induced later in the adipogenesis process, slightly preceding the induction of most of the adipogenic genes. The inhibitory factor C/EBP ξ is suppressed during the induction process of adipogenesis, however, it returns when differentiation has progressed

almost to completion [65]. This isoform may therefore act as a brake on the adipogenesis program after important events have been initiated.

C/EBP α induces many adipocyte genes directly, and *in vivo* studies indicate an important role for this factor in the development of adipose tissue. Animals that carry a homozygous deletion of the C/EBP gene have dramatically decreased fat accumulation in WAT and BAT pads [57]. Analysis of C/EBP α ^{-/-} mice is complicated by profound hypoglycaemia and perinatal lethality and requires restoration of hepatic C/EBP α levels by liver-specific rescue. These mice are almost completely devoid of white-adipose tissue (except within the mammary gland) [17]. Mice in which the C/ebpa locus is replaced by C/ebpb are viable and do not lose normal liver function, but have reduced amounts of WAT [67]. In both these C/ebpa^{-/-} models, the development of BAT is delayed, but is mostly normal in amounts. The involvement of C/EBP α in adipogenesis is also strongly supported by *in vitro* studies. Overexpression of C/EBP α in 3T3-L1 preadipocytes induces their differentiation into mature adipocytes [68, 69], and the expression of C/EBP α antisense RNA in these cells blocks the adipocyte differentiation process [70].

C/EBP β is crucial for adipogenesis in immortalized pre-adipocyte lines, but its effect is less obvious in embryonic fibroblasts. Ectopic expression of C/EBP β is sufficient to induce 3T3-L1 preadipocytes differentiation in the absence of hormonal inducers. Similar studies with C/EBP δ indicated that in the presence of ectopic expression of C/EBP δ , cells still require prodifferentiative agents, but adipogenesis is accelerated [66]. C/EBP β may also

predispose cells to adipocytic lineage as well as promote their differentiation. Ectopic expression of C/EBP β (but not C/EBP δ) in NIH 3T3 fibroblasts is permissive for γ adipogenesis in the presence of hormonal inducers [71]. Embryonic fibroblast lacking either C/EBP β or C/EBP δ showed slight decreases in adipogenic potential, however, cells lacking both C/EBP β and C/EBP δ were severely blocked from developing from preadipocytes to adipocytes [72]. C/EBP β -deficient mice have reduced adiposity, however, this influence might be the result of abnormal lipogenesis and not reduced adipogenesis *per se*. It is also possible that C/EBP δ can compensate for the lack of C/EBP β , because when double-knockout C/ebpb and C/ebpd, mice show a greater reduction in adipose tissue mass [72]. Approximately 85% of these animals die in the perinatal period of unknown causes, and the remaining 15% that survive have sharply reduced BAT and smaller decreases in WAT [72]. C/EBP β and C/EBP δ promote adipogenesis at least in part by inducing C/EBP α and PPAR γ . The amounts of C/EBP α and PPAR γ mRNA are normal in the remaining adipocytes of these double-knockout mice in contrast to C/EBP β - and C/EBP δ -deficient MEFs, which do not express C/EBP α and PPAR γ . These results suggest that there might be factors that allow some cells to escape the developmental requirement for C/EBP β and C/EBP δ *in vivo*. Interestingly, the reduction of BAT appears to be from decreased lipid accumulation, and the reduction in WAT is reported to involve reduced cell numbers, with normal size, morphology, and gene expression profiles in those white adipocytes that do differentiate. Other C/EBP isoforms, including C/EBP ξ and C/EBP γ , seem to suppress adipogenesis, perhaps via heterodimerization with C/EBP β , and then inactivate it.

Moreover, despite the importance of C/EBPs in the process of adipogenesis, these transcriptional factors clearly cannot function efficiently without PPAR γ . For example, C/EBP β cannot induce expression of C/EBP α in the absence of PPAR γ , which is required to release histone deacetylase-1 (HDAC1) from the C/ebpa promoter [73]. Furthermore, the ectopic expression of C/EBP α cannot rescue adipogenesis in Pparg^{-/-} fibroblasts [9]. However, C/EBP α has an important role in differentiated adipocytes. Study of expression of exogenous PPAR γ in C/EBP α -deficient cells showed that, although C/EBP α is not required for accumulation of lipid and the expression of many adipocyte genes, it is necessary for the acquisition of insulin sensitivity [74, 75].

Kruppel-like factors (KLFs)

The KLFs are a large family of C2H2 zinc-finger proteins that regulate proliferation, apoptosis, and differentiation. KLF genes are expressed in adipose tissue, the variability in their expression patterns during adipogenesis, and their effects on adipocyte development and gene expression indicate that a cascade of KLFs function during adipogenesis. KLF15 was the first family member that was shown to regulate adipocyte biology. KLF15 promotes adipocyte differentiation [76] and induces expression of the insulin-sensitive glucose transporter-4 (GLUT4) [77]. Another family member, KLF5, is induced early during the process of adipogenesis by C/EBP β and C/EBP δ , both of which directly bind to the *KLF5* promoter [78]. KLF5 binds to and activates the *PPAR γ* promoter, functioning in concert with C/EBPs. *KLF5*^{-/-} mice have reduced adipose tissue early in postnatal life, but rebounded with normal mice by the fourth week of life, KLF6 inhibits the expression of

delta-like-1/pre-adipocyte factor-1 (DLK1/Pref-1) in 3T3-L1 cells and fibroblasts. Although forced expression of KLF6 is not sufficient to promote adipogenesis, adipocytes with reduced amounts of KLF6 show decreased adipogenesis [79]. However, not all KLFs promote adipocyte differentiation. For example, KLF2 and KLF7, are both anti-adipogenic factors. KLF2 inhibits the activity of *PPAR* γ 2 promoter [80-82].

Adipocyte determination and differentiation factor/sterol-regulatory element binding protein 1c (ADD1/SREBP-1c)

ADD1/SREBP-1c is a member of the basic helix-loop-helix (bHLH) family of transcription factors [16]. This family has been implicated in tissue specific gene regulation, particularly in muscle, which shares a mesodermal origin with fat. ADD1/SREBP-1c was isolated independently as a factor from adipocytes that bound to E box sequence motifs [83, 84] and as a liver component that bound to sterol-regulatory-elements (SREs) in cholesterol regulatory genes [85]. ADD1/SREBP-1c is induced during adipogenesis and is also regulated by fasting and refeeding in vivo [86, 87]. The induction during refeeding most likely represents insulin regulation, because insulin regulates ADD1/SREBP-1c expression in cultured adipocytes.

Full-length ADD1/SREBP-1c is an inactive molecule bound to the membrane of the endoplasmic reticulum (ER). Sterol depletion can lead to proteolytic cleavage, nuclear translocation, and transcriptional activity of the SREBPs in liver, however, the pathway of

ADD1/SREBP-1c activation in adipocytes remains to be determined. It is known that activated ADD1/SREBP-1c can regulate a variety of genes linked to fatty acid and triglyceride metabolism including fatty acid synthase, acetyl-coA carboxylase, and glycerophosphate acyltransferase-1 and -2, suggesting that ADD1/SREBP-1c is a key link between nutritional changes and the lipogenic gene program.

In addition, ADD1/SREBP-1c can regulate adipogenesis, although not as robustly as PPAR γ or the C/EBPs. The role of ADD1/SREBP-1c in adipogenesis was indicated by the observation that the expression of mRNA encoding this factor was induced dramatically when cultured preadipocytes were stimulated to undergo differentiation [87]. Overexpression of ADD1/SREBP-1c in 3T3-L1 preadipocytes in the presence of hormonal cocktail inducers of differentiation results in accelerating the expression of adipogenic key genes and lipid accumulation as compared to control cells. Moreover, ectopic expression of ADD1/SREBP-1c in undetermined fibroblasts results in some adipose conversion, but only under conditions strongly permissive for adipogenesis, likely by directly inducing *PPAR γ* gene expression via E box motifs present in the PPAR γ promoter [41]. A dominant-negative ADD1/SREBP-1c has also been reported to inhibit 3T3-L1 preadipocyte differentiation [87]. Interestingly, conditioned medium from cells expressing ADD1/SREBP-1c can activate PPAR γ -mediated transcription [51], suggesting that ADD1/SREBP-1c is also involved in the production of an endogenous PPAR γ ligand.

Fatty Acid-binding Proteins (FABPs)

The intracellular fatty acid-binding proteins (FABPs) were discovered in the early 1970s as abundant cytoplasmic proteins which were 14-15 kDa proteins, and bind hydrophobic ligands, such as saturated and unsaturated long-chain fatty acids, eicosanoids and other lipids, with high affinity [88-91]. Different members of the FABP family exhibit various tissue expression patterns, and are expressed abundantly in tissues involved in active lipid metabolism. Until now, there are at least nine members that have been identified, liver FABP (FABP1, L-FABP), intestinal FABP (FABP2, I-FABP), heart FABP (FABP3, H-FABP, MDGI), adipocyte FABP (FABP4, aP2), epidermal FABP (FABP5, E-FABP, PA-FABP, MDGI), ileal FABP (FABP6, II-FABP, I-BABP, gastrotropin), brain FABP (FABP7, B-FABP, MRG), myelin FABP (FABP8, M-FABP, PMP2), and Testis FABP (FABP9, T-FABP) [92]. FABPs have a wide range of sequence diversity, from 15% to 70% sequence identity between different members [93], however, all known FABPs share almost identical three dimensional structures [92].

As small intracellular proteins, FABPs appear to access the nucleus under certain conditions, and potentially target fatty acids to transcriptional factors, such as members of the PPAR family, PPAR α , PPAR δ and PPAR γ , in the nuclear lumen [94]. FABP1, FABP3, and FABP5 themselves are regulated by these transcriptional factors, which are liganded by fatty acids or other hydrophobic agonists [95-97]. FABP1 and PPAR α physically interact, thus, it has been suggested that FABP1 could be considered a co-activator in PPAR-mediated gene regulation [98]. In a similar way, FABP5 interacts with PPAR δ and

FABP4 interacts with PPAR γ [97]. Recent studies indicate that continuous nucleocytoplasmic shuttling may underlie transcriptional activation of PPAR γ by FABP4 [99]. However, actions of FABP4 also provided a negative feedback to terminate PPAR γ action, and the absence of FABP4 resulted in enhanced nuclear hormone receptor activity in the macrophage [100].

FABP1, also known as liver FABP, is abundant in the liver cytoplasm, and is also expressed in pancreas, intestine, kidney, lung and stomach [46]. In the liver, 5% of all cytosolic proteins (in hepatocytes) are FABP1 [101]. The promoter of FABP1 gene contains a peroxisome-proliferator response element, and accordingly the mRNA levels are increased by fatty acids, dicarboxylic acids, and retinoic acid [40]. Unlike the other members in the FABP family, FABP1 can bind two ligands simultaneously via two different binding sites with high and low affinities [102]. Peroxisome proliferators always bind FABP1 with low affinity, whereas the strength of binding with fatty acids depends on which affinity site is utilized. This property of FABP1 is suggested to act as a feature enabling ligand delivery through interactions with target receptors. In addition to binding fatty acids, such as oleic acid, FABP1 can carry acyl-coenzyme A, eicosanoids, lysophospholipids, carcinogens, anticoagulants, such as warfarin, and haem, making it probably the most versatile chaperone in terms of its ligand repertoire [40]. Moreover, recent studies showed that fatty acid induced expression of FABP1 happens in the proximal tubules and indicated that urinary FABP1 in humans might be used as a clinical marker that can help predict and monitor the progression of renal diseases [103].

FABP2, also known as intestinal FABP, is expressed in the epithelium of the small intestine. Another two FABPs, FABP1 and FABP6 (also known as ileal-FABP) are present in small intestine as well, although they are distributed in different segments [104]. FABP1 is mostly expressed in the proximal region, and FABP6 is restricted in the distal part of the small intestine. FABP2 is expressed throughout the intestine, but mostly in the distal segment. It is difficult to estimate the individual contributions of these proteins to lipid absorption and metabolism at the sites where they are present, and more work is needed in this regard. FABP2-deficient mice were viable and fertile, and fat absorption affected by FABP2 and compensation by FABP1 and FABP6 were not observed [105]. Both genders of mice with FABP2-deficiency exhibited increased plasma levels of insulin, but glucose levels remain normal. Male mice lacking FABP2 gained more weight, had larger livers and had significantly higher triglyceride levels regardless of diet. Female FABP2-deficient mice gained less weight, and had smaller livers on a high-fat diet, and exhibited no difference in plasma triglyceride levels. Although the pathway responsible for these gender differences remain unclear, it appears that fatty-acid uptake can be mediated by the remaining FABPs, possibly FABP1 and FABP6, without the need for increased total amounts of FABPs to compensate for the lack of FABP2.

FABP3, also known as heart FABP, has been isolated from several different tissues, including heart, skeletal muscle, brain, renal cortex, lung, testis, aorta, adrenal gland, brown adipose tissue and ovary [46, 88, 93, 101]. The level of FABP3 is impacted by exercise, PPAR α agonists and testosterone [40, 89, 90, 106]. In muscle cells, FABP3 plays a role in the uptake of fatty acids and their subsequent transport towards the mitochondrial

β -oxidation system, and increasing fatty acids exposure in vitro and in vivo caused an increase of FABP3 expression [88, 91]. Conditions with elevated plasma lipids may result in increased FABP3 levels in myocytes, as seen in endurance training [88, 91]. Studies in FABP3-deficient mice indicate that the uptake of fatty acids is severely inhibited in the heart and skeletal muscle, whereas plasma concentrations of free fatty acids are increased [107]. Cardiac and skeletal muscle metabolism is reported to switch from fatty-acid oxidation to glucose oxidation when there is an inability to obtain sufficient amounts of fatty acids [108, 109]. Consequently, FABP3-deficient mice were rapidly fatigued and exhausted by exercise, showing a reduced tolerance to physical activity. Localized cardiac hypertrophy was also observed in the older animals [107].

FABP4, also known as adipocyte FABP, was first detected in mature adipocytes and adipose tissue [92, 93]. This protein has been named adipocyte P2 (aP2), because of its highly similar sequence (67%) to peripheral myelin protein 2 (FABP8) [93]. FABP4 is the best characterized isoform among the entire FABP family. Expression of FABP4 is highly regulated during the processes of adipocyte differentiation, and its mRNA is transcriptionally controlled by fatty acids, PPAR γ agonists and insulin [101,106]. *FABP4*-deficient mice showed reduced hyperinsulinaemia and insulin resistance in the context of both dietary and genetic obesity, however, the effect of FABP4 on insulin sensitivity was not observed in lean mice [110, 111]. In adipocytes, the loss of FABP4 was compensated for by overexpression of FABP5, which is present in the normal adipocyte but only in extremely small amounts. Adipocytes obtained from *FABP4*-deficient mice have reduced efficiency of lipolysis in vivo and in vivo [112-114]. This was initially attributed to the

ability of FABP4 to bind and activate hormone-sensitive triglyceride lipase (HSL), however, the definitive links between HSL activation and FABP4 have not been demonstrated *in vivo*. The potential mechanisms responsible for alterations in lipolysis in *FABP4* deficiency also requires further study. Recent studies have showed that FABP4 is expressed in macrophages during their differentiation from monocytes, and following activation with phorbol 12-myristate 13-acetate, lipopolysaccharide, PPAR γ agonists and oxidized low-density lipoprotein [115-119]. FABP4 expression in macrophages was suppressed by a cholesterol-lowering statin *in vitro* [120]. Notably, adipocytes express much higher levels of FABP4 compared to macrophages (approximately 10,000-fold) [121]. In macrophages, FABP4 modulates inflammatory responses and cholesterol ester accumulation [115].

FABP5, also known as epidermal FABP, is expressed most abundantly in epidermal cells of the skin. It is also present in other tissues, such as the tongue, adipose tissue (macrophages), dendritic cells, mammary gland, kidney, brain, liver, lung and testis [46, 106, 122]. As all these tissues express other FABP members, the exact function of FABP5 is difficult to explore. The ratio of FABP4 to FABP5 in adipocytes isolated from normal mice was about 99:1 [123], however, the ratio changes to 1:1 in the macrophage under physiological conditions [115]. These two proteins have 52% amino acid similarity and bind various fatty acids and synthetic compounds with similar selectivity and affinity [101]. Studies with *FABP4*^{-/-} mice showed that FABP5 expression was dramatically increased in adipocytes, but not in macrophages [110, 115]. Transgenic mice over-expressing *FABP5* gene in adipose tissue showed a minor phenotype with enhanced basal and hormone-

stimulated lipolysis [124]. When fed a high-fat diet, adipose tissue-specific FABP5 over-expressed in transgenic mice resulted in a reduction in systemic insulin sensitivity [125]. On the other hand, absence of FABP5 in these mice led to a modest increase in insulin sensitivity [125]. The adipocytes in *FABP4*^{-/-} mice showed an increased capacity of insulin-dependent glucose transport. Except for FABP5 expression increasing in liver, no compensatory increase was observed in the expression of FABP3, FABP4, or FABP7 in adipose tissue, tongue, brain or testis in FABP5-deficient mice [125].

FABP7, also known as brain FABP, is expressed in various regions of the mouse brain in the mid-term embryonic stage, but the expression decreases as differentiation progresses [126]. This protein is strongly expressed in radial glia cells of the developing brain, especially in the pre-perinatal stage, but only weakly in mature glia of the white matter. Neurons of the grey matter express FABP3 and FABP5, but not FABP7. FABP7 has strong affinity for n-3 polyunsaturated fatty acids, in particular, docosahexaenoic acid. This long-chain fatty acid is an important nutrient for the nervous system, and it has been considered a natural ligand for FABP7 [127]. Moreover, similarly to FABP3 [128, 129], FABP7 is prominently expressed in the mammary gland, and its over-expression inhibited tumor growth in a mouse breast cancer model [130, 131].

Overall, the functions of FABPs are transport of lipids to specific compartments in cells, such as to the lipid droplet for storage, to the endoplasmic reticulum for signaling, trafficking and membrane synthesis, to the mitochondria or peroxisome for oxidation, to

cytosolic or other enzymes to regulate their activity, to the nucleus for lipid-mediated transcriptional regulation, or even outside the cells to signal in an autocrine or paracrine manner (Fig. 3) [45].

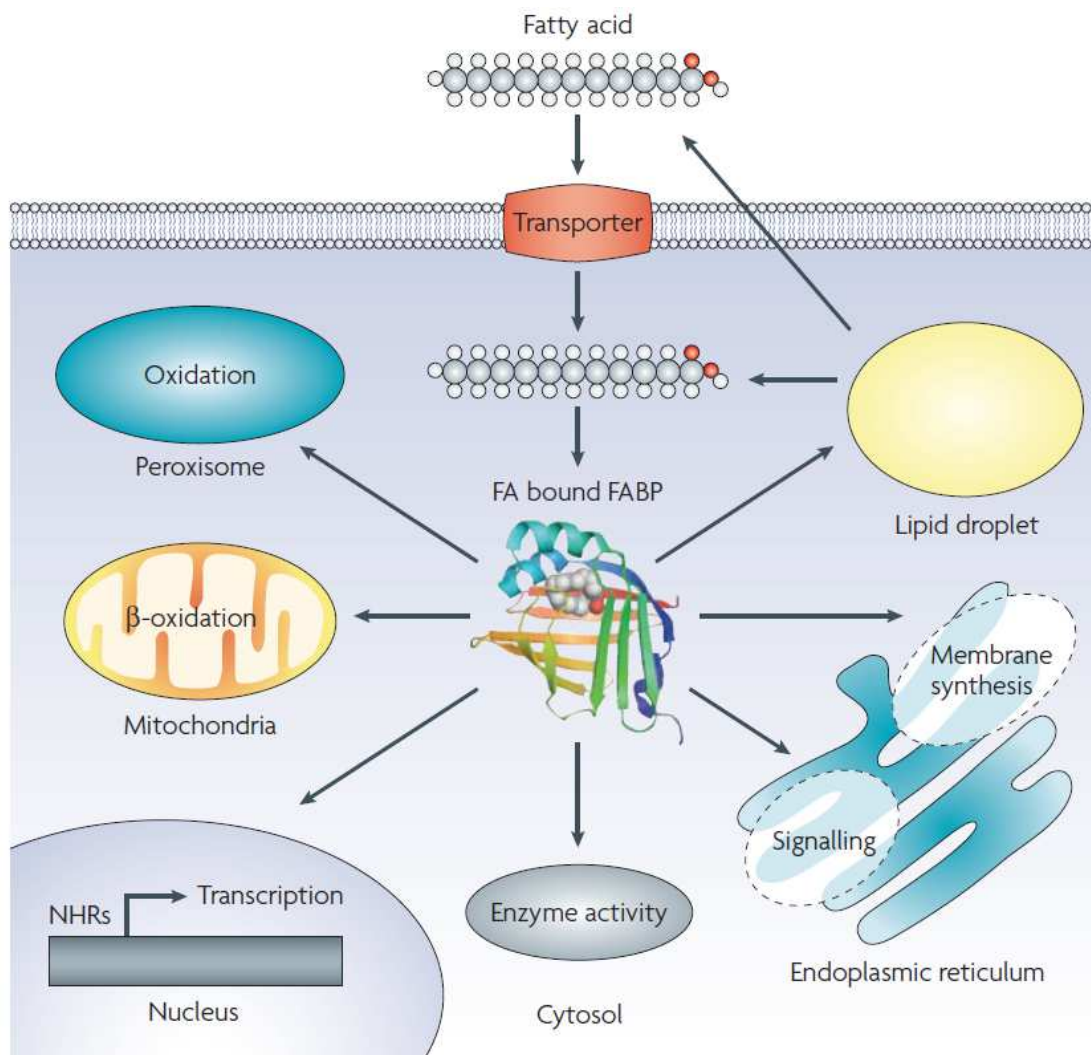


Figure 3: Putative functions of fatty acid binding protein (FABP) in the cells (This figure is copied/cited from reference [45])

Cellular and hormonal regulation of adipogenesis

Inducers of adipogenesis

The earliest observations revealed that efficient differentiation in vitro required insulin. Insulin increased the percentage of cells that differentiate and also increases the amount of lipid accumulation in every adipocyte [132]. Insulin also has potent anti-apoptotic activity [133]. Preadipocytes have been reported express a few insulin receptors [134]. The impact of insulin on differentiation has been indicated to occur through cross-activation of the Insulin-like growth factor 1 (IGF-1) receptor, which explains why pharmacological doses of insulin are required to produce the desired effect. IGF-1 is also a critical component of fetal calf serum [135], and supplementation with this factor enables differentiation to proceed in serum-free medium [136].

Glucocorticoids have also been used for many years to induce optimal differentiation of cultured preadipocytes and primary adipocytes. In most of these studies, glucocorticoids are administered in the form of dexamethasone (Dex). Dex is believed to operate through activation of the glucocorticoid receptor (GR), which is a nuclear hormone receptor in the same large superfamily as PPAR γ . The transcriptional targets of GR in adipogenesis are not yet clear. Dex has been shown to induce C/EBP β , which may account for some of its adipogenic activity [137]. However, even when C/EBP β is overexpressed in preadipocytes, Dex is still required to induce adipogenesis, indicating a more complex role of this compound. Studies have shown that DEX can reduce expression of preadipocytes factor-1 (Pref-1), a negative regulator of adipogenesis. Constitutive expression of Pref-1 blocks the

pro-differentiation action of Dex, and antisense-mediated reduction in Pref-1 decreases the dose of Dex required for differentiation to occur [138].

There are other hormones that have an influence on adipogenesis. Growth hormone can clearly induce adipogenesis in a variety of cultured preadipocyte lines, but does not have effects in primary preadipocyte cultures [139-142]. Actually, differentiation of the primary cells appears to be inhibited by growth hormone. This is consistent with the observation that humans with growth hormone deficiency have normal adipose stores and can be obese. Thyroid hormone [143], retinoic acid [144], and various prostaglandins [136] are among of other hormones that have influence in adipogenesis *in vitro*, but for which there is scant evidence to support such a function *in vivo*.

Inhibitors of adipogenesis

A variety of cytokines including IL-1, TNF- α , and some other proinflammatory molecules have been found to inhibit adipocyte differentiation in most cultured preadipocyte lines, and can dedifferentiate mature adipocytes [145, 146]. The suppression of adipocyte lipoprotein lipase was used as a bioassay in the purification of cachectin, which was ultimately identified as TNF- α [147]. Moreover, several growth factors can potentially inhibit adipogenesis, including epidermal growth factor (EGF), platelet-derived growth factor (PDGF) and fibroblast growth factor (FGF) [148-150].

This inhibitory effect on adipogenesis is likely to be mediated by activation of the classic mitogen-activated protein (MAP) kinases, ERK 1 and 2. These kinases, as well as JNK MAP kinase, directly phosphorylate PPAR γ 2 at Ser112 in the amino-terminal domain (Ser82 of PPAR γ 1), and repress its adipogenic activity [151-155]. RXR, the obligate heterodimerization partner of PPAR γ , is also phosphorylated and subsequently inhibited by MAP kinases [156].

Adipogenesis can also be regulated by the expression of a trans-membrane molecule, Pref-1. This molecule is present in preadipocytes, but is down-regulated during adipocyte differentiation [157]. When expressed ectopically in transmembrane form, Pref-1 inhibits adipogenesis. Moreover, Pref-1 can also be released from cells as a soluble molecule, and this form also has inhibitory effect [158], which opens the possibility that Pref-1 may be an autocrine or paracrine regulator of adipogenesis.

Vitamin D

Vitamin D synthesis and metabolism

Vitamin D was discovered nearly a century ago as the nutrient that prevented rickets, a devastating skeletal disease characterized by under-mineralized bones [159]. Since that time, the concept of vitamin D and its most bioactive derivative, 1,25-dihydroxyvitamin D₃ (1, 25 - (OH)₂D₃), has evolved from that of an essential micronutrient to that of a hormone involved in a complex endocrine system that directs mineral homeostasis,

protects skeletal integrity, and regulates cell growth and differentiation in a diverse array of tissues [160]. 1, 25 - (OH)₂D₃ acts in concert with PTH to tightly regulate the concentration of serum calcium and phosphate, thereby maintaining proper skeletal mineralization. A major function of 1, 25 - (OH)₂D₃ is to promote intestinal absorption of calcium and phosphate. Moreover, it also has direct effects on bone [161], in which continuous remodeling must occur to sustain structural integrity.

During exposure to sunlight, ultraviolet B (UVB) photons penetrate into the skin and are absorbed by 7-dehydrocholesterol, inducing the formation of pre-vitamin D. This is an unstable form of vitamin D that quickly undergoes rearrangement to form vitamin D₃ (cholecalciferol). Vitamin D₂ (ergocalciferol) is the form of vitamin D that occurs in plants and is used to fortify certain foods such as fluid milk. Both vitamin D forms eventually enter the circulation bound to a vitamin D-binding protein and are metabolized in the liver by the vitamin d-25-hydroxylase enzyme (25-OHase or CYP27A1) to 25-hydroxyvitamin D (calcidiol), the main vitamin D form circulating in plasma and a substrate for production of the hormonally active metabolite 1,25-dihydroxyvitamin D (calcitriol) [162].

Vitamin D and adipogenesis

Increasing evidence suggests there is a potential link between obesity and vitamin D insufficiency [162]. The bioactive metabolite of vitamin D is 1, 25 - (OH)₂D₃, which acts as a steroid hormone and a high-affinity ligand for the vitamin D receptor (VDR). The 1,

25 - (OH)₂D₃ activated VDR can form a heterodimer with the retinoid C receptor (RXR), which can bind to vitamin D response elements in various genes [163], and this heterodimer formation may result in a competition with PPAR γ binding with RXR[164]. The competition can inhibit the expression of PPAR γ , which is a key regulator of adipogenesis, and inhibit the development of adipocyte maturation [163]. Therefore, the 1, 25 - (OH)₂D₃ and VDR may play an important role in regulating adipogenesis. The vitamin D receptor is expressed very early in adipogenesis in 3T3-L1 cells. The VDR expression level reaches the maximum during the first 6 h after induction of differentiation, then declines and disappears in 2 days [165]. This creates a short window of opportunity for 1, 25 - (OH)₂D₃ to influence the differentiation process of pre-adipocyte into mature adipocyte.

C/EBP β and C/EBP δ are expressed in the early period of adipogenesis, and can regulate PPAR γ and C/EBP α expression (Fig. 1.4). ETO/MTG8, a transcriptional corepressor, is expressed in preadipocytes as an inhibitor of C/EBP β function and down-regulated via insulin signaling in early adipogenesis [166]. When overexpressed, ETO/MTG8 played a potent role of inhibiting adipogenesis via its ability to directly interact with C/EBP β and inhibited its function on activating the C/EBP α promoter [166]. In the absence of 1, 25 - (OH)₂D₃, ETO/MTG8 expression level decreased rapidly in the first 12 h [165]. But in the presence of 1, 25 - (OH)₂D₃, ETO/MTG8 expression level was maintained throughout adipogenesis and increased after Day 1, and the high level of ETO/MTG8 inhibited C/EBP β function[165]. This may be another contributing mechanism to the actions of 1, 25 - (OH)₂D₃ inhibiting adipogenesis. However, the role of C/EBP β in 1, 25 - (OH)₂D₃ – induced inhibition of PPAR γ and C/EBP α is controversial. Blumberg et al [165] found that

1, 25 - (OH)₂D₃ blocks adipogenesis by down-regulating both C/EBP β mRNA expression level and C/EBP β nuclear protein level. In contrast, Juan Kong and Yan Chun Li [167] found that the C/EBP β mRNA expression level after the initiation of differentiation was not affected by 1, 25 - (OH)₂D₃ in 3T3 cells. These two studies were conducted in 3T3-L1 cells, and the concentrations of dexamethasone and insulin in protocols of differentiation media were not the same. This may influence the response of C/EBP β to 1, 25 - (OH)₂D₃ treatment. However, the specific reason for this apparent discrepancy is not clear, and the role of C/EBP δ in the 1, 25 - (OH)₂D₃ inhibition effect is unknown. When cattle are exposed to sunlight, plasma vitamin D will increase [168]. With the inhibition effect of vitamin D on adipogenesis, this may explain that meat quality declines in summer. Therefore, understanding 1, 25 - (OH)₂D₃ effect on bovine adipocyte differentiation is very important for the beef industry.

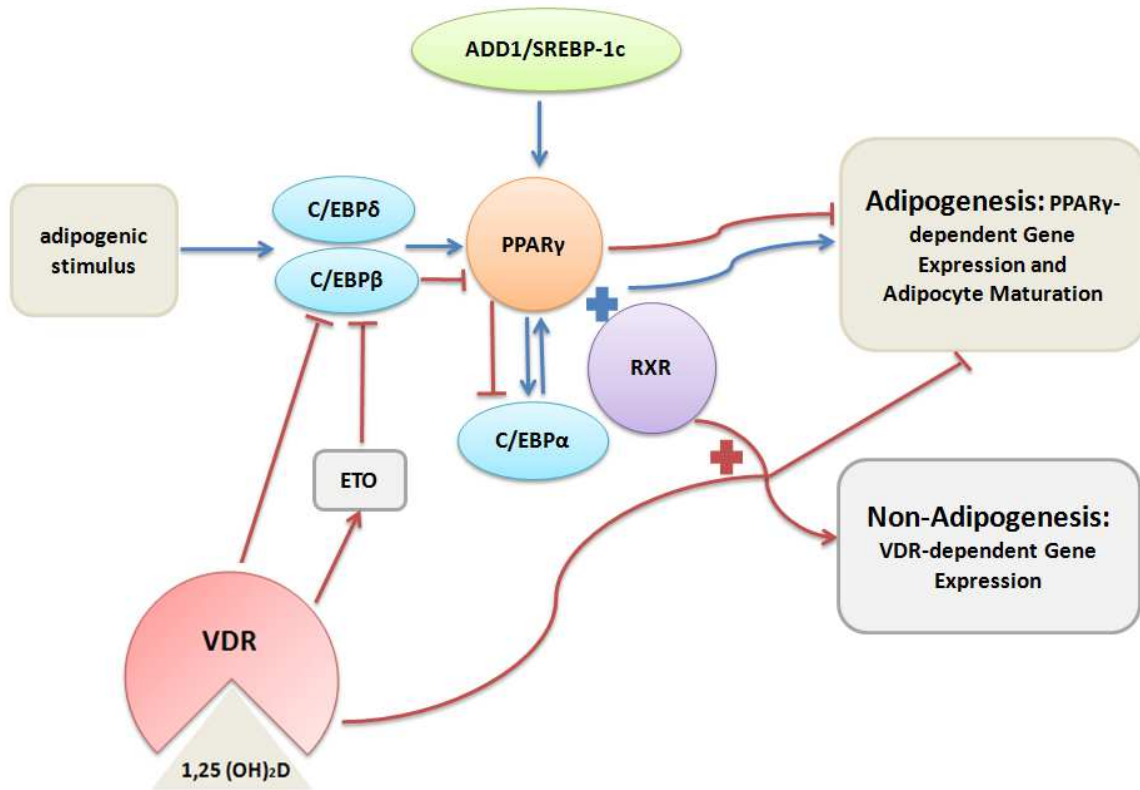


Fig. 1.4 Vitamin D and adipogenesis. 1, 25 - (OH)₂D₃ blocks adipogenesis by down regulating CCAAT-enhancing binding protein β (C/EBP β) expression. 1, 25 - (OH)₂D₃ also up-regulates the expression of ETO, the C/EBP β corepressor, which would further inhibit the action of any remaining C/EBP β . 1, 25 - (OH)₂D₃ forms a heterodimer with the retinoid X receptor (RXR), and competes with PPAR γ to form a heterodimer with RXR.

Vitamin A

Vitamin A metabolism

There are three main forms of vitamin A in the body, the hydroxyl form (retinol), the aldehyde form (retinal) and the carboxylic form (retinoic acid, RA) (Fig. 1.5). These three vitamin A vitamers and their metabolites together play a critical role in a variety of essential life processes, including vision, hematopoiesis, reproduction and manipulation of the growth and differentiation of a variety of cell types [169]. Except for vision, which requires retinal, the active formation of vitamin A in the other processes is retinoic acid (RA) [170].

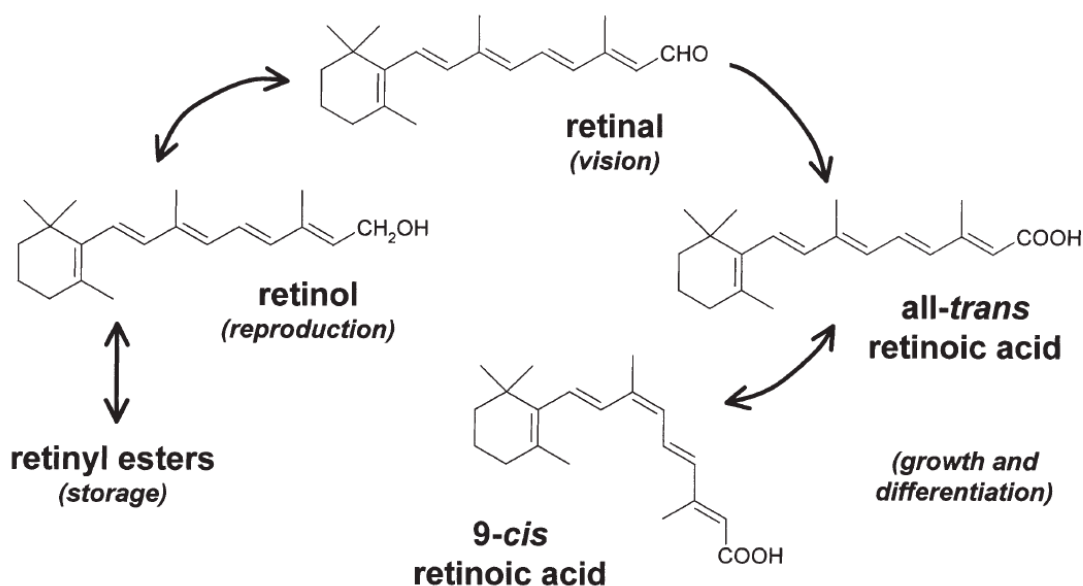


Fig. 1.5 Chemical structures of some biologically active retinoids. Retinol appears to be essential for fertility and may be stored as retinyl esters or converted to the aldehyde form (retinal). The latter is required for the vision process and can be converted into all-trans-retinoic acid (RA) through an irreversible oxidation. All-trans RA and its natural isomers are responsible for most of the effects of vitamin A on cell growth and differentiation. (This figure is copied/cited from reference [169])

Most of the biological effects of RAs involve the activation of ligand-dependent transcription factors of the nuclear hormone receptor superfamily, the retinoid receptors. Two types of these receptors are known: the retinoic acid receptors (RARs), which are responsive to both all-trans RA and 9-cis RA, and the retinoid receptors (RXRs), which are responsive to the 9-cis RA isomer specifically. Three subtypes of RARs (RAR α , RAR β and RAR γ) and RXRs (RXR α , RXR β and RXR γ) have been described in mammalian tissues, which are encoded by different genes and show distinct developmental- and tissue-specific regulated expression [171, 172].

Vitamin A and adipogenesis

RA with high concentration (1-10 μ M) was considered as a potent inhibitor of adipocyte differentiation 30 years ago [173], and a dietary deficit in vitamin A results in increased adipogenesis [174]. The mechanisms of RA inhibition effect on adipogenesis are multiple. First, RA can interfere with the transcriptional activities of C/EBP β , and then block the C/EBP β -mediated induction of downstream adipogenic key gene expression, notably PPAR γ and C/EBP α [175]. Second, RA can strongly up-regulate retinoic acid receptor (RAR) expression and inhibit retinoid X receptor (RXR) expression in 3T3-L1 cells [176]. Ziouzenkova et al [177] found that retinaldehyde, a precursor for retinoic acid formation, inhibited adipogenesis and suppressed PPAR γ and RXR responses. Kawada et al [178] also found that carotenoids and retinoids (precursors of RA) inhibited adipogenesis via up-regulating RAR and suppressing PPAR γ . Therefore, RA may influence PPAR γ activity through disturbing PPAR γ and RXR heterodimer formation. However, low concentrations

of RA (1-10 nM) were found to stimulate adipogenesis of preadipocytes [179]. But, the mechanism of the low concentration RA stimulating adipocyte differentiation has not been determined. Therefore, understanding the mechanism of RA regulation of adipogenesis is useful for helping to control body fat and to manipulate meat quality in the beef industry.

Vitamin A and body fat

In adult NMRI male mice, acute RA treatment (100 mg of all-trans RA/kg body weight, during the 4 days preceding death) triggered a 12% reduction of body weight that could not be completely accounted for by the observed changes in energy intake [180-182], and a strong reduction of body fat content (the combined weight of interscapular BAT, epididymal WAT and inguinal WAT was reduced by 46% in the RA-treated animals, as compared with control animals) [182]. RA-induced reduction of adiposity correlated with down-regulation of the expression of transcription factors controlling adipocyte differentiation and metabolism, notably PPAR γ , in both WAT and BAT depots [182] and with an up-regulation of the expression of UCPs in BAT and muscle. Reduced adipogenesis/lipogenesis and enhanced lipolysis and apoptosis in fat depots, together with enhanced whole body thermogenesis, are all likely to contribute to the reduced adiposity of RA-treated animals.

Gold Nanoparticles in Biomolecule Delivery

Gold nanoparticles (AuNPs) have been investigated for centuries because of their unique characteristics, realized and potential applications in biology, catalysis and nanotechnology [183]. In the past decade, scientists have generally developed two kinds of gold-based nanoconjugates: homofunctionalized and heterofunctionalized AuNPs. Homofunctionalized AuNPs are conjugated by one form of biomolecule such as peptides [184-188], oligonucleotides (ONs) [189, 190], or antibodies [191]. Heterofunctionalized AuNPs combine two or more biomolecules including ONs and antibodies [192], bovine serum albumin (BSA) and peptide [193], protein-stabilized peptides and ONs [194], peptides and ONs [195], alkyl chains and plasmid [196], polyethylene glycol (PEG) and peptides [197], PEG and ONs [198], PEG and small interfering RNA (siRNA) [199, 200], polyethyleneimine (PEI) and siRNA [201-203], or oligoethylene glycol (OEG) and siRNA [204]. These studies provide evidence that AuNPs could be used as nanocarriers for drug delivery and gene regulation, suggesting their great potential for further development and use in genetic manipulation.

Directing Peptide

The specific target of AuNPs can be controlled by directing peptides. The directing peptides can target to certain organelles. Several peptide-specific pathways have been suggested to facilitate receptor-mediated uptake of gold-peptide nanoconjugates [186, 193]. For instance, Transactivator of Transcription (TAT) contains a putative cell penetrating peptide (CPP) sequence that has been shown to be effective for intracellular conjugate

delivery [187, 193, 205]. The carboxy-terminal sequence Lys-Asp-Glu-Leu (KDEL) or His-Asp-Glu-Leu (HDEL in yeast) was first detected in resident soluble proteins of the endoplasmic reticulum (ER) as a retention signal [206], but later it was found that the KDEL sequence is also a retrieval signal [207]. It has been reported that the KDEL receptor ERD2 exists mainly in Golgi-like structures, particularly in the cis-Golgi network in several immunofluorescence [208-211] and immunoelectronmicroscopy studies [207, 212]. The KDEL signal is recognized by ERD2, which targets its ligands to the retrograde COPI-mediated transport pathway, and cycles between the Golgi complex and the ER [209, 213, 214]. Extra-cellular KDEL peptides can be internalized, reaching Golgi-like structures within 30 min and finally localize at the ER between 30-90 min [215]. Recently, KDEL peptides have been reported used as the directing peptides and linked to AuNPs, and showed high efficiency of AuNPs and siRNA delivery [188, 216].

Small Interfering RNA

Small interfering RNAs (siRNAs) are short stretch (19-30 nucleotides) double stranded RNAs that are able to target and cleave complementary mRNA in the cytoplasm [217]. SiRNAs are produced from long pieces of double-stranded RNA cleaved by the enzyme Dicer. Once siRNA is present in the cytoplasm, it is incorporated into a protein complex called RNA-induced silencing complex (RISC) [218]. RISC contains a multi-functional protein called Argonaute 2 that can unwind the siRNA and cleave the sense strand of siRNA [219]. The antisense strand of siRNA will remain in the activated RISC and selectively degrades its complementary mRNA [220]. After cleavage of one mRNA, the

activated RISC can move on to target additional mRNAs [221], which ensures a therapeutic effect for 3-7 days in rapidly dividing cells and for several weeks in non-dividing cells [222]. As naked siRNA is too large and too negatively charged to cross cell membranes, and is also easily degraded by endogenous enzyme, many efforts on siRNA effective delivery have been made in the past decade. Promising siRNA carriers have been developed currently including cationic CPPs [223-226], polymers [227-230], lipid-based materials [231-234] and nanoparticles such as silica [235-237], iron oxide [238, 239], gold nanoparticles [240] and quantum dots [241-244]. Although AuNPs have been investigated for drug delivery in the past decades, their use as siRNA delivery agents has been studied for only 5 years. Different strategies employed for AuNP mediated siRNA delivery include siRNAs conjugation with AuNP via 1) Au-S chemistry or 2) electrostatic interactions [240]. Here in the proposed study, we will form siRNA-gold nanoconjugates via Au-S bonds as reported previously [188].

Hypotheses

Adipogenesis plays a key role in metabolic homeostasis and nutrient pathways, and this process requires both lipid storage and adipocyte development. Adipocyte differentiation is regulated by a cascade of interactions of many transcriptional factors. Of all of the nuclear factors which influence the adipogenic process, two nuclear factor families have received the most attention as follows: the CCAAT enhancer-binding proteins (C/EBPs) and the peroxisome proliferator-activated receptors (PPARs). There are also some extracellular factors, for example, 1, 25-dihydroxyvitamin D (1, 25 - (OH)₂D₃) and retinoic acid (RA), which can modulate adipogenesis. However, the specific regulation mechanisms of these molecules in adipogenesis are not clearly determined. The present studies focus on the effect of 1, 25 - (OH)₂D₃ and RA in regulation of adipogenesis, and also the interaction between these molecules and the promoter region of key adipogenic genes.

There are three parts of the hypotheses that pertain to the next three chapters, chapter II, III, and IV, respectively.

For chapter II, the hypotheses are as follows:

- ① lipid accumulation is inhibited by 1, 25-dihydroxyvitamin D treatments;
- ② the expression of adipogenic key genes are regulated by 1, 25-dihydroxyvitamin D;
- ③ different concentrations of 1, 25-dihydroxyvitamin D have various impact on adipogenesis.

For chapter III, the hypotheses are as follows:

- ① lipid accumulation is inhibited by retinoic acid treatments;
- ② the expression of adipogenic key genes are regulated by retinoic acid;
- ③ different concentrations of retinoic acid have different effect on adipogenesis.

For chapter IV, the hypotheses are as follows:

- ① Au-peptide nanoconjugates transfects into pre- (day 0) 3T3-L1 cells;
- ② Au-peptide nanoconjugates transfects into post- (day 6) 3T3-L1 cells;
- ③ Au-peptide-siRNA/C/EBP α inhibits adipocyte differentiation.

Objectives

For the chapter II, the objectives are:

- ① investigate the influence on adipogenesis by 1, 25-dihydroxyvitamin D treatments;
- ② investigate the influence on the expression of adipogenic key genes by 1, 25-dihydroxyvitamin D treatments;

For the chapter III, the objectives are:

- ① investigate the influence on adipogenesis by retinoic acid treatments;
- ② investigate the influence on the expression of adipogenic key genes by retinoic acid treatments;

For chapter IV, the objectives are:

- ① preparation of gold-peptides nanoconjugates;
- ② investigate the cellular uptake of gold-peptide nanoconjugates by both pre- and post-adipocytes;
- ③ investigate regulation of adipogenesis by gold-peptide nanoconjugates.

References

1. Ritchie HD, Rust SR, Merkel RA, Bergen WG (1993) Getting rid of excess fat is not an easy task. *Feedstuffs* 65: 13-16
2. Wheeler TL, Cundiff LV, Koch RM (1994) Effect of marbling degree on beef palatability in *Bos Taurus* and *Bos indicus* cattle. *J Anim Sci* 72: 3145-3151
3. Dolezal HG, Smith GC, Savell JW, Carpenter ZL (1982) Comparison of subcutaneous fat thickness, marbling and quality grade for predicting palatability of beef. *Food Science* 47 (2): 397-401
4. Gregoire FM, Smas CM, Sul HS (1998) Understanding adipocyte differentiation. *Physiol Rev* Jul 78:783-809
5. Macdougald OA, Lane MD (1995) Transcriptional regulation of gene-expression during adipocyte differentiation. *Annu Rev Biochem* 64: 345-373
6. Taylor SM, Jones PA (1979) Multiple new phenotypes induced in 10T1/2 and 3T3 cells treated with 5-azacytidine. *Cell* Aug 17: 771-779
7. Boone C, Mourot J, Gregoire F, Remacle C (2000) The adipose conversion process: Regulation by extracellular and intracellular factors. *Reprod Nutr Dev* Jul-Aug 40: 325-328
8. Rosen ED and Spiegelman BM (2000) Molecular regulation of adipogenesis. *Annu. Rev. Cell Dev. Biol* 16:145-171
9. Rosen ED, Hsu H, Wang X, Sakai S, Freeman MW, Gonzalez FJ, Spiegelman BM (2002) C/EBP α induces adipogenesis through PPAR γ : a unified pathway. *Genes Dev* 16:22-26

10. Rosen ED, MacDougald OA (2006) Adipocyte differentiation from the inside out. *Nature Reviews Molecular Cell Biology* 7:885-896
11. Lau DC, Dhillon B, Szmitko PE, Verma S (2005) Adipokines: molecular links between obesity and atherosclerosis. *Am. J. Physiol. Heart Circ. Physiol* 288: 2031-2041
12. Ogden CL et al. (2006) Prevalence of overweight and obesity in the United States, 1999-2004. *JAMA* 295: 15499-1555
13. Matsuo T, Matsuo M, Kasai M, Kasai M, Takeuchi H (2001) Effects of a liquid diet supplement containing structured medium- and long- chain triacylglycerols on body fat accumulation in healthy young subjects. *Asia Pac J Clin Nutr* 10: 46-50
14. Faust IM, Johnson PR, Stern JS, Hirsch J (1978) Diet-induced adipocyte number increase in adult rats: A new model of obesity. *Am J Physiol* Sep 235: E279-286
15. Laudet V, Hanni C, Coll J, Catzeflis F, Stehelin D (1992) Evolution of the nuclear receptor gene superfamily. *EMBO J.* Mar 11: 1003-1013
16. Rosen ED, Walkey CJ, Puigserver P, Spiegelman BM (2000) Transcriptional regulation of adipogenesis. *Genes Dev* Jun 1; 14: 1293-1307
17. Linhart HG et al. (2001) C/EBP α is required for differentiation of white, but not brown, adipose tissue. *Proc. Natl Acad. Sci. USA* 98:12532-12537
18. Ranaka T, Yoshida N, Kishimoto T, Akira S (1997) defective adipocyte differentiation in mice lacking the C/EBP β and/or C/EBP δ gene. *EMBO J.* 16: 7432-7443
19. Giorgino F, Laviola L, Eriksson JW (2005) Regional differences of insulin action in adipose tissue: insights from in vivo and in vitro studies. *Acta Physiol. Scand* 183: 13-30

20. Gesta S et al. (2006) Evidence for a role of developmental genes in the origin of obesity and body fat distribution. *Proc. Natl Acad. Sci. USA* 103: 6676-6681
21. Gregoire FM, Smas CM, Sul HS (1998) Understanding adipocyte differentiation. *Physiol Rev* 78:783-809
22. Tiraby C, Langin D (2003) Conversion from white to brown adipocytes: A strategy for the control of fat mass? *Trends Endocrinol Metab* Dec 14:439-441
23. Kokta TA, Dodson MV, Gertler A, Hill RA (2004) Intercellular signaling between adipose tissue and muscle tissue. *Domest Anim Endocrinol* Nov 27:303-301
24. Himms-Hagen J (1990) Brown adipose tissue thermogenesis: Interdisciplinary studies. *FASEB J* Aug 4: 2890-2898
25. Hirsch J and Batchelor B (1976) Adipose tissue cellularity in human obesity. *Clin Endocrinol Metab* 5:299-311
26. Brook CG (1972) Evidence for a sensitive period in adipose-cell replication in man. *Lancet* Sep 23; 2: 624-627
27. Johnson RP, Francendese, AA (1985) Cellular regulation of adipose tissue growth. *J. Anim Sci* 61:57-75
28. Netter FH (1989) *Atlas of Human anatomy* Summit, NJ: Ciba-Geigy
29. Shillabeer G, Forden JM, Lau DC W (1989) Induction of preadipocytes differentiation by mature fat cells in the rat. *J. Clin. Invest.* 84: 381-387
30. Desvergne B, Michalik, L, and Wahli W (2006) Transcriptional regulation of metabolism. *Physiol Rev* 86: 465-514
31. Berger J and Moller DE (2002) The mechanisms of action of PPARs. *Annu Rev Med* 53: 409-435

32. Rosen ED and Spiegelman BM (2001) PPARgamma: a nuclear regulator of metabolism, differentiation, and cell growth. *J Biol Chem* Oct 12; 276: 37731-37734
33. Kelly LJ, Vicario PP, Thompson GM, Candelore MR, Doebber TW, Ventre J, Wu MS, Meurer R, Forrest MJ, Conner MW, Cascieri MA, Moller DE (1998) Peroxisome proliferator-activated receptors gamma and alpha mediate in vivo regulation of uncoupling protein (UCP-1, UCP-2, UCP-3) gene expression. *Endocrinology* Dec 139: 4920-4927
34. Fajas L, Auboeuf D, Raspe E, Schoonjans K, Lefebvre AM, Saladin R, Najib J, Laville M, Fruchart JC, Deeb S, Vidal-Puig A, Flier J, Briggs MR, Staels B, Vidal H, Auwerx J (1997) The organization, promoter analysis, and expression of the human PPARgamma gene. *J Biol Chem* Jul 25; 272: 18779-18789
35. Braissant O, Foufelle F, Scotto C, Dauca M, Wahli W (1996) Differential expression of peroxisome proliferator-activated receptors (PPARs): tissue distribution of PPAR-alpha, -beta, and -gamma in the adult rat. *Endocrinology* Jan 137:354-366
36. Escher P, Braissant O, Basu-Modak S, Michalik L, Wahli W, Desvergne B (2001) Rat PPARs: quantitative analysis in adult rat tissues and regulation in fasting and refeeding. *Endocrinology* Oct 142:4195-4202
37. Evans RM (2003) Keio Medical Science Prize commemorative lecture. PPARs and the complex journey to obesity. *Keio J Med* Jun 53: 53-58
38. Ockner RK, Manning JA, Poppenhausen RB, Ho WKL (1972) A binding protein for fatty acids in cytosol of intestinal mucosa, liver, myocardium, and other tissues. *Science* 177: 56-58

39. Mishkin S, Stein L, Gatmaitan Z, Arias IM (1972) The binding of fatty acids to cytoplasmic proteins: Binding to Z-protein in liver and other tissues of the rat. *Biochem. Biophys. Res. Commun* 47: 997-1003
40. Coe NR, Bernlohr DA (1998) Physiological properties and functions of intracellular fatty acid-binding proteins. *Biochim. Biophys. Acta* 1391: 287-306
41. Fajas L, Schoonians K, Gelman L, Kim JB, Najib J, et al. (1999) Regulation of peroxisome proliferator-activated receptor γ expression by adipocyte differentiation and determination factor 1/sterol regulatory element binding protein 1: implications for adipocyte differentiation and metabolism. *Mol. Cell. Biol.* 19:5495-5503
42. Zhu Y, Qi C, Korenberg JR, Chen XN, Noya D, et al. (1995) Structural organization of mouse peroxisome proliferator-activated receptor γ (mPPAR γ) gene: alternative promoter use and different splicing yield two mPPAR γ isoforms. *Proc. Natl. Acad. Sci. USA* 92:7921-7925
43. Tontonoz P, Graves RA, Budavari AI, Erdjument-Bromage H, Lui M, et al. (1994) Adipocyte-specific transcription factor ARF6 is a heterodimeric complex of two nuclear hormone receptors, PPAR γ and RXR α . *Nucleic Acids Res* 22:5628-5634
44. Zimmerman AW, Veerkamp JH (2002) New insights into the structure and function of fatty acid-binding proteins. *Cell Mol. Life Sci.* 59: 1096-1116
45. Furuhashi M, Hotamisligil CS (2008) Fatty acid-binding proteins: Role in metabolic diseases and potential as drug targets. *Nature Rev Drug Discovery* Jun 7: 489-503
46. Chmurzynska A (2006) The multigene family of fatty acid-binding proteins (FABPs): function, structure and polymorphism. *J Appl Genet* 47: 39-48

47. Tontonoz P, Hu E, Devine J, Beale EG, Spiegelman BM (1995) PPAR γ 2 regulates adipose expression of the phosphoenolpyruvate carboxykinase gene. *Mol. Cell. Biol.* 15: 351-357
48. Tontonoz P, Hu E, Spiegelman BM (1994) Stimulation of adipogenesis in fibroblasts by PPAR γ 2, a lipid-activated transcription factor. *Cell* 79:1147-1156
49. Tzamelis I et al. (2004) regulated production of a peroxisome proliferator-activated receptor- γ ligand during an early phase of adipocyte differentiation in 3T3-L1 adipocytes. *J. Biol. Chem.* 279:36093-36102
50. Hamm JK, Park BH, Farmer SR (2001) A role for C/EBP β in regulating peroxisome proliferator-activated receptor γ activity during adipogenesis in 3T3-L1 preadipocytes. *J. Biol. Chem.* 276: 18464-18471
51. Kim JB, Wright HM, Wright M, Spiegelman BM (1998) ADD1/SREBP1 activates PPAR γ through the production of endogenous ligand. *Proc. Natl. Acad. Sci. USA* 95:4333-4337
52. Tamori Y, Masugi J, Nishino N, Kasuga M (2002) Role of peroxisome proliferator-activated receptor γ in maintenance of the characteristics of mature 3T3-L1 adipocytes. *Diabetes* 51: 2045-2055
53. Imai T et al. (2004) Peroxisome proliferator-activated receptor γ is required in mature white and brown adipocytes for their survival in the mouse. *Proc. Natl. Acad. Sci. USA* 101: 4543-4547
54. Lekstrom-Himes J, Xanthopoulos KG (1998) Biological role of the CCAAT/enhancer-binding protein family of transcription factors. *J. Biol. Chem.* 273: 28545-28548

55. Cao Z, Umek RM, McKnight SL (1991) Regulated expression of three C/EBP isoforms during adipose conversion of 3T3-L1 cells. *Genes Dev* 5: 1538-1552
56. Zhang DE, Zhang P, Wang ND, Hetherington CJ, Darlington GJ, Tenen DG (1997) Absence of granulocyte colony-stimulating factor signaling and neutrophil development in CCAAT enhancer binding protein alpha-deficient mice. *Proc. Natl. Acad. Sci.* 94: 569-574
57. Wang ND, Finegold MJ, Bradley A, Ou CN, Abdelsayed SV, Wilde MD, Taylor LR, Wilson DR, Darlington GJ (1995) Impaired energy homeostasis in C/EBP alpha knockout mice. *Science* 269: 1108-1112
58. Flodby P, Barlow C, Kylefjord H, Ahrlund-Richter L, Xanthopoulos KG (1996) Increased hepatic cell proliferation and lung abnormalities in mice deficient in CCAAT/enhancer binding protein alpha/ *J. Biol. Chem.* 271: 24753-24760
59. Yamanaka R, Barlow C, Lekstrom-Himes J, Castilla LH, Liu PP, Eckhaus M, decker T, Wynshaw-Boris A, Xanthopoulos KG (1997) Impaired granulopoiesis, myelodysplasia, and early lethality in CCAAT/enhancer binding protein epsilon-deficient mice. *Proc. Natl. Acad. Sci.* 94: 13187-13192
60. Rosen ED, Walkey CJ, Puigserver P et al. (2000) Transcriptional regulation of adipogenesis. *Genes Dev* 14: 1293-1307
61. Tang QQ, Jiang MS, Kane MD (1999) Repressive effect of Sp1 on the C/EBP alpha gene promoter: Role in adipocyte differentiation. *Mol. Cell. Biol.* 19: 4855-4865
62. Lin FT, MacDougald OA, Diehl AM, Lane MD (1993) A 30-kDa alternative translation product of the CCAAT/enhancer binding protein alpha message: transcriptional activator lacking antimitotic activity. *Proc. Natl. Acad. Sci.* 90: 9606-9610

63. Bachmeier M, Loffler G (1997) The effect of platelet-derived growth factor and adipogenic hormones on the expression of CCAAT/enhancer-binding proteins in 3T3-L1 cells in serum-free conditions. *Eur. J. Biochem.* 243: 128-133
64. Ron D, Habener J (1992) CHOP, a novel developmentally regulated nuclear protein that dimerizes with transcription factors C/EBP and LAP and functions as a dominant-negative inhibitor of gene transcription. *Genes. Dev.* 6:439-453
65. Darlington GJ, Ross SE, MacDougald OA (1998) The role of C/EBP genes in adipocyte differentiation. *J. Biol. Chem.* 273: 30057-30060
66. Yeh WC, Cao Z, Classon M, McKnight SL (1995) Cascade regulation of terminal adipocyte differentiation by three members of the C/EBP family of leucine zipper proteins. *Genes Dev* 15: 168-181
67. Chen SS, Chen JF, Johnson PF, Muppala V, Lee YH (2000) C/EBP β , when expressed from the C/ebp α gene locus, can functionally replace C/EBP α in liver but not in adipose tissue. *Mol. Cell Biol.* 20:7292-7299
68. Freytag SO, Paielli DL, Gilbert JD (1994) Ectopic expression of the CCAAT/enhancer binding protein alpha promotes the adipogenic program in a variety of mouse fibroblastic cells. *Genes Dev.* 8: 1654-1663
69. Lin FT, Lane MD (1994) CCAAT/enhancer binding protein alpha is sufficient to initiate the 3T3-L1 adipocyte differentiation program. *Proc. Natl. Acad. Sci. USA* 91: 8757-8761
70. Lin FT, Lane MD (1992) Antisense CCAAT/enhancer-binding protein RAN suppresses coordinate gene expression and triglyceride accumulation during differentiation of 3T3-L1 preadipocytes. *Genes Dev* 6: 533-544

71. Wu Z, Xie Y, Bucher NLR, Farmer SR (1995) Conditional ectopic expression of C/EBP β in NIH-3T3 cells induces PPAR γ and stimulates adipogenesis. *Genes Dev* 9: 2350-2363
72. Tanaka T, Yoshida N, Kishimoto T, Akira S (1997) Defective adipocyte differentiation in mice lacking the C/EBP β and/or C/EBP δ gene. *EMBO J.* 16:7432-7443
73. Zuo Y, Qiang L, Farmer SR (2006) Activation of CCAAT/enhancer-binding protein (C/EBP) α expression by C/EBP β during adipogenesis requires a peroxisome proliferator-activated receptor γ associated repression of HDAC1 at the C/ebp α gene promoter. *J. Biol. Chem* 281: 7960-7967
74. Wu Z, et al. (1999) Cross-regulation of C/EBP α and PPAR γ controls the transcriptional pathway of adipogenesis and insulin sensitivity. *Mol. Cell* 3: 151-158
75. El-Jack AK, Hamm JK, Pilch PF, farmer SR (1999) Reconstitution of insulin-sensitive glucose transport in fibroblasts requires expression of both PPAR γ and C/EBP α . *J. Biol. Chem* 274: 7946-7951
76. Mori T et al. (2005) Role of Kruppel-like factor 15 (KLF15) in transcriptional regulation of adipogenesis. *J. Biol. Chem.* 280: 12867-12875
77. Gray S et al. (2002) The kruppel-like factor KLF15 regulates the insulin-sensitive glucose transporter GLUT4. *J. Biol. Chem.* 277: 34322-34328
78. Oishi Y et al. (2005) Kruppel-like transcription factor KLF5 is a key regulator of adipocyte differentiation. *Cell Metab.* 1: 27-39
79. Li D et al. (2005) Kruppel-like factor-6 promotes preadipocytes differentiation through histone deacetylase 3-dependent repression of DLK1. *J. Biol. Chem.* 280: 26941-26952

80. Wu J, Srinivasan SV, Neumann JC, Lingrel JB (2005) The KLF2 transcription factor does not affect the formation of preadipocytes but inhibits their differentiation into adipocytes. *Biochemistry* 44: 11098-11105
81. Banerjee SS et al. (2003) The kruppel-like factor KLF2 inhibits peroxisome proliferator-activated receptor γ expression and adipogenesis. *J. Biol. Chem.* 278: 2581-2584
82. Kanazawa A et al. (2005) Single nucleotide polymorphisms in the gene encoding Kruppel-like factor 7 are associated with type 2 diabetes. *Diabetol.* 48: 1315-1322
83. Kim JB, Spotts GD, Halvorsen Y, Shih HM, Ellenberger T et al. (1995) Dual DNA binding specificity of ADD1/SREBP1 controlled by a single amino acid in the basic helix-loop-helix domain. *Mol. Cell. Biol.* 15: 2582-2588
84. Tontonoz P, Kim JB, Graves RA, Spiegelman BM (1993) ADD1: a novel helix-loop-helix transcription factor associated with adipocyte determination and differentiation. *Mol. Cell. Biol.* 13: 4753-59
85. Brown MA, Goldstein JL (1997) The SREBP pathway: regulation of cholesterol metabolism by proteolysis of a membrane-bound transcription factor. *Cell* 89: 331-340
86. Kim JB, Sarraf P, Wright M, Yao KM, Mueller E et al. (1998) Nutritional and insulin regulation of fatty acid synthetase and leptin gene expression through ADD1/SREBP1. *J. clin. Invest.* 101: 1-9
87. Kim Jb spiegelman BM (1996) ADD1/SREBP-1 promotes adipocyte differentiation and gene expression linked to fatty acid metabolism. *Genes Dev* 10: 1096-107

88. Zanotti G (1999) Muscle fatty acid-binding protein. *Biochim Biophys Acta* 1441: 94-105
89. Motojima K (2000) Differential effects of PPAR α activators on induction of ectopic expression of tissue-specific fatty acid binding protein genes in the mouse liver. *Int J Biochem Cell Biol* 32: 1085-1092
90. Furuhashi M, Ura N, Murakami H, Hyakukoku M, Yamaguchi K, Higashiura K, Shimamoto K (2002) Fenofibrate improves insulin sensitivity in connection with intramuscular lipid content, muscle fatty acid-binding protein, and β -oxidation in skeletal muscle. *J Endocrinol* 174: 321-329
91. Veerkamp JH, Van Moerkerk HT (1993) Fatty acid-binding protein and its relation to fatty acid oxidation. *Mol Cell Biochem* 123: 101-106
92. Spiegelman BM, Frank M, Green H (1983) Molecular cloning of mRNA from 3T3 adipocytes. Regulation of mRNA content for glycerophosphate dehydrogenase and other differentiation-dependent proteins during adipocyte development. *J Biol Chem* 258:10083-10089
93. Hunt CR, Ro JH, Dobson DE, Min HY, Spidgelman BM (1986) Adipocyte P2 gene: developmental expression and homology of 5'-flanking sequences among fat cell-specific genes. *Proc Natl Acad Sci USA* 83: 3786-3790
94. Furuhashi M, Hotamisligil GS (2008) Fatty acid-binding proteins: role in metabolic diseases and potential as drug targets. *Nature Reviews* 7: 489-503
95. Schachtrup D, Emmler T, Bleck B, Sandqvist A, Spener F (2004) Functional analysis of peroxisome-proliferator-responsive element motif in genes of fatty acid-binding proteins. *Biochem. J.* 382: 239-245

96. Motojima K (2000) Differential effects of PPAR α activators on induction of ectopic expression of tissue-specific fatty acid binding protein genes in the mouse liver. *Int. J Biochem. Cell Biol.* 32: 1085-1092
97. Tan NS et al. (2002) Selective cooperation between fatty acid binding proteins and peroxisome proliferator-activated receptors in regulating transcription. *Mol. Cell Biol.* 22: 5114-5127
98. Wolfrum C, Borrmann CM, Borchers T, Spener F (2001) Fatty acids and hypolipidemic drugs regulate peroxisome proliferator-activated receptors α - and γ -mediated gene expression via liver fatty acid binding protein: a signaling path to the nucleus. *Proc. Natl. Acad. Sci. USA* 98: 2323-2328
99. Ayers SD, Nedrow KL, Gillilan RE, Noy N (2007) Continuous nucleocytoplasmic shuttling underlies transcriptional activation of PPAR γ and FABP4. *Biochemistry* 46: 6744-6752
100. Makowski L, Brittingham KC, Reynolds JM, Suttles J, Hotamisligil GS (2005) The fatty acid-binding protein, aP2, coordinates macrophage cholesterol trafficking and inflammatory activity. Macrophage expression of aP2 impacts peroxisome proliferator-activated receptor γ and I κ B kinase activities. *J. Biol. Chem.* 280: 12888-12895
101. Haunerland NH, Spener F (2004) Fatty acid-binding proteins-insights from genetic manipulations. *Prog. Lipid Res.* 43: 328-349
102. Rolf B et al. (1995) Analysis of the ligand binding properties of recombinant bovine liver-type fatty acid binding protein. *Biochim. Biophys. Acta* 1259: 245-253
103. Kamijo-Ikemori A, Sugaya T, Kimura K (2006) Urinary fatty acid binding protein in renal disease. *Clin. Chim. Acta* 374: 1-7

104. Agellon LB, Toth MJ, Thomson AB (2002) Intracellular lipid binding proteins of the small intestine. *Mol. Cell Biochem* 239: 79-82
105. Vassileva G, Huwyler L, Poirier K, Agellon LB, and Toth MJ (2000) The intestinal fatty acid binding protein is not essential for dietary fat absorption in mice. *FASEB J.* 14: 2040-2046
106. Makowski L, Hotamisligil GS (2005) The role of fatty acid binding proteins in metabolic syndrome and atherosclerosis. *Curr Opin Lipidol* 16: 543-548
107. Binas B, Danneberg H, McWhir J, Mullins L, Clark AJ (1999) Requirement for the heart-type fatty acid binding protein in cardiac fatty acid utilization. *FASEB J.* 13: 805-812
108. Schaap FG, Binas B, Danneberg H, van der Vusse GJ, Glate JF (1999) Impaired long-chain fatty acid utilization by cardiac myocytes isolated from mice lacking the heart-type fatty acid binding protein gene. *Circ res.* 85: 329-337
109. Binas B et al. (2003) A null mutation in D-FABP only partially inhibits skeletal muscle fatty acid metabolism. *Am. J. Physiol Endocrinol. Metab.* 285: E481-E489
110. Hotamisligil GS et al. (1996) Uncoupling of obesity from insulin resistance through a targeted mutation in aP2, the adipocyte fatty acid binding protein. *Science* 274: 1377-1379
111. Uysal KT, Scheja L, Wiesbrock SM, Nonner-Weir S, Hotamisligil GS (2000) Improved glucose and lipid metabolism in genetically obese mice lacking aP2. *Endocrinology* 141: 3388-3396

112. Shen WJ, Sridhar K, Bernlohr DA, Kraemer FB (1999) Interaction of rat hormone-sensitive lipase with adipocyte lipid-binding protein. *Proc. Natl. Acad. Sci. USA* 96: 5528-5532
113. Scheja L et al. (1999) Altered insulin secretion associated with reduced lipolytic efficiency in aP2^{-/-} mice. *Diabetes* 48: 1987-1994
114. Coe NR, Simpson MA, Bernlohr DA (1999) Targeted disruption of the adipocyte lipid-binding protein (aP2 protein) gene impairs fat cell lipolysis and increases cellular fatty acid levels. *J. Lipid Res.* 40: 967-972
115. Makowski L et al. (2001) Lack of macrophage fatty-acid-binding protein aP2 protects mice deficient in apolipoprotein E against atherosclerosis. *Nature Med.* 7: 699-705
116. Pelton PD, Zhou L, demarest KT, Burriss TP (1999) PPAR γ activation induces the expression of the adipocyte fatty acid binding protein gene in human monocyte. *Biochem. Biophys. Res. Commun.* 261: 456-458
117. Fu Y, Luo N, Lopes-Virella MF (2000) Oxidized LDL induces the expression of ALBP/aP2 mRNA and protein in human THP-1 macrophages. *J. Lipid Res.* 41: 2017-2023
118. Fu y, Luo N, Lopes-Virella MF, Garvey WT (2002) The adipocyte lipid binding protein (ALBP/aP2) gene facilitates foam cell formation in human THP-1 macrophages. *Atherosclerosis* 165: 259-269
119. Kazemi MR, McDonald CM, Shigenaga JK, Grunfeld C, Feingold KR (2005) Adipocyte fatty acid-binding protein expression and lipid accumulation are increased during activation of murine macrophages by toll-like receptor agonists. *Arterioscler. Thromb. Vasc. Biol.* 25: 1220-1224

120. Llaverias G et al. (2004) Atorvastatin reduces CD68, FABP4, and HBP expression in oxLDL-treated human macrophages. *Biochem. Biophys. Res. Commun.* 318: 265-274
121. Shum BO et al. (2006) The adipocyte fatty acid-binding protein aP2 is required in allergic airway inflammation. *J. Clin. Invest.* 116: 2183-2192
122. Rolph MS et al. (2006) Regulation of dendritic cell function and T cell priming by the fatty acid-binding protein AP2. *J. Immunol.* 177: 7794-7801
123. Simpson MA, LiCata VJ, Ribarik Coe N, Bernlohr DA (1999) Biochemical and biophysical analysis of the intracellular lipid binding proteins of adipocytes *Mol. Cell Biochem.* 192: 33-40
124. Hertzal AV, Bennaars-Eiden A, Bernlohr DA (2002) Increased lipolysis in transgenic animals overexpressing the epithelial fatty acid binding protein in adipose cells. *J. Lipid Res.* 43: 2105-2111
125. Maeda K et al. (2003) Role of the fatty acid binding protein mal 1 in obesity and insulin resistance. *Diabetes* 52: 300-307
126. Feng L, Hatten ME, Heinta M (1994) Brain lipid-binding protein (BLBP): a novel signaling system in the developing mammalian CNS. *Neuron* 12: 895-908
127. Xu LZ, Sanchez R, Sali A, Heinta N (1996) Ligand specificity of brain lipid-binding protein. *J. Biol. Chem.* 271: 24711-24719
128. Bohmer FD et al. (1987) Identification of a polypeptide growth inhibitor from bovine mammary gland. Sequence homology to fatty acid- and retinoid-binding proteins. *J. Biol. Chem.* 262: 15137-15143

129. Specht B et al. (1996) Mammary derived growth inhibitor is not a distinct protein but a mix of heart-type and adipocyte-type fatty acid-binding protein. *J. Biol. Chem.* 271: 19943-19943
130. Shi YE et al. (1997) Antitumor activity of the novel human breast cancer growth inhibitor, mammary-derived growth inhibitor-related gene, MRC. *Cancer res.* 57: 3084-3091
131. Hohoff C, Spener F, Correspondence RE, Shi YE et al. (1998) Antitumor activity of the novel human breast cancer growth inhibitor, mammary-derived growth inhibitor-related gene, MRC. *Cancer Res.* 57: 3084-3091 (1997), *Cancer Res* 58: 4015-4017
132. Girard J, Perdereau D, Foufelle F, Frip-Buus C, Ferre P (1994) Regulation of lipogenic enzyme gene expression by nutrients and hormones. *FASEB J.* 8: 36-42
133. Kiess W, Gallaher B (1998) Hormonal control of programmed cell death/apoptosis. *Eur. J. Endocrinol.* 138: 482-91
134. Reed BC, Lane MD (1979) Expression of insulin receptors during preadipocyte differentiation. *Adv. Enzyme reg.* 18: 97-117
135. Smith PJ, Wise LS, Berkowitz R, Wan C, Rubin CS (1988) Insulin-like growth factor I is an essential regulator of the differentiation of 3T3-L1 adipocytes. *J. Biol. Chem.* 263: 9402-9408
136. Schmidt W, Poll-Jordan g, Loffler G (1990) Adipose conversion of 3T3-L1 cells in a serum-free culture system depends on epidermal growth factor, insulin-like growth factor I, corticosterone, and cyclic AMP. *J. Biol. Chem.* 265: 15489-15498

137. Wu Z, Bucher NLR, Farm SR (1996) Induction of peroxisome proliferator-activated receptor γ during the conversion of 3T3 fibroblasts into adipocytes is mediated by C/EBP β , C/EBP δ , and glucocorticoids. *Mol. Cell. Biol.* 16: 4128-36
138. Smas CM, Chen L, Sul HS (1997) Cleavage of membrane-associated pref-1 generates a soluble inhibitor of adipocyte differentiation. *Mol. Cell. Biol.* 17: 977-988
139. Catalioto RM, Gaillard D, Ailhaud G, Negrel R (1992) terminal differentiation of mouse preadipocyte cells: the mitogen-adipogenic role of growth hormone is mediated by the protein kinase C signaling pathway. *Growth factors* 6: 255-264
140. Green H, Morikawa M, Nixon T (1985) A dual effector theory of growth-hormone activity. *Differentiation* 29: 195-198
141. Hausman GJ, Martin RJ (1989) The influence of human growth hormone on preadipocyte development in serum-supplemented and serum-free cultures of stromal-vascular cells from pig adipose tissue. *Domest. Anim. Endocrinol.* 6: 331-337
142. Wabitsch M, Hauner H, Heinze E, teller WM (1995) The role of growth hormone/insulin-like growth factors in adipocyte differentiation. *Metabolism* 44: 45-49
143. Gaibi-Chihi J, Grimaldi P, Torresani J, Ailhaud g (1981) Triiodothyronine and adipose conversion of OB17 preadipocytes binding to high affinity sites and effects on fatty acid synthesizing and esterifying enzymes. *J. Recept. Res.* 2: 153-173
144. Safonava I, Darimount C, Amri EZ, Grimaldi P, ailhaud g et al. (1994) Retinoids are positive effectors of adipose cell differentiation. *Mol. Cell. Endocrinol.* 104: 201-11
145. OhsumiJ, Sakakibara S, Yamaguchi J, Miyadai K, Yoshioka S et al. (1994) Troglitazone prevents the inhibitory effects of inflammatory cytokines on insulin-induced adipocyte differentiation in 3T3-L1 cells. *Endocrinology* 135: 2279-2282

146. Petruschke T, Hauner H (1993) Tumor necrosis factor- α prevents the differentiation of human adipocyte precursor cells and causes delipidation of newly developed fat cells. *J. Clin. Endocrinol. Metab.* 76: 742-47
147. Fried SK, zechner R (1989) Cachectin/tumor necrosis factor decrease human adipose tissue lipoprotein lipase mRNA levels, synthesis, and activity. *J. Lipid res.* 30: 1917-1923
148. Hauner H, Rohrig K, Petruschke T (1995) effects of epidermal growth factor (EGF), platelet-derived growth factor (PDGF) and fibroblast growth factor (FGF) on human adipocyte development and function. *Eur. J. Clin. Invest.* 25: 90-96
149. Navre M, Ringold GM (1989) Differential effects of fibroblast growth factor and tumor promoters on the initiation and maintenance of adipocyte differentiation. *J. cell Biol.* 109: 1875-1863
150. Serrero G, Mills D (1991) Physiological role of epidermal growth factor on adipose tissue development in vivo. *Proc. Natl. acad. Sci USA* 88: 3912-3916
151. Adams M, Reginato MJ, shao d, Lazar MA, Chatterhee VK (1997) Transcriptional activation by peroxisome proliferator-activated receptor γ is inhibited by phosphorylation at a consensus mitogen-activated protein kinase site. *J. Biol. Chem.* 272: 5128-5132
152. Camo HS, Tafuri SR (1997) Regulation of peroxisome proliferator-activated receptor γ activity by mitogen-activated protein kinase. *J. Biol. Chem.* 272: 10811-10816
153. Camo HS, Tafuri SR, Leff (1999) c-Jun N-terminal kinase phosphorylates peroxisome proliferator-activated receptor γ a and negatively regulates its transcriptional activity. *Endocrinology* 140: 392-397

154. Font de Mora J, Porras A, Ahn N, Santos E (1997) Mitogen-activated protein kinase activation is not necessary for, but antagonizes 3T3-L1 adipocyte differentiation. *Mol. Cell. Biol.* 17: 6068-6075
155. Hu E, Kim JB, Sarraf P, Spiegelman BM (1996) Inhibition of adipogenesis through MAP kinase-mediated phosphorylation of PPAR γ . *Science* 274: 2100-2103
156. Solomon C, White JH, Kremer R (1999) Mitogen-activated protein kinase inhibits 1,25-dihydroxyvitamin D₃-dependent signal transduction by phosphorylating human retinoid C receptor α . *J. Clin. Invest.* 103:1729-1735
157. Smas CM, Sul HS (1993) Pref-1, a protein containing EGF-like repeats, inhibits adipocyte differentiation. *Cell* 73: 725-734
158. Smas CM, Chen L, Sul HS (1997) Cleavage of membrane-associated pref-1 generates a soluble inhibitor of adipocyte differentiation. *Mol. Cell. Biol.* 17:977-988
159. Brown AJ, Dusso A, Slatopolsky E (1999) Vitamin D. *Am J. Physiol.* 277: F157-F175
160. Sutton ALM, MacDonald PN (2003) Vitamin D: More than a "bone-a-fide" hormone. *Molecular Endocrinology* 17: 777-791
161. Van Leeuwen JP, van der Lijde M, van den Berd GJ, Pols HA (2001) Vitamin D control of osteoblast function and bone extracellular matrix mineralization. *Crit. Rev. Eukaryot Gene Expr* 11: 199-226
162. Martini LA, Wood RJ (2006) Vitamin D status and the metabolic syndrome. *Nutrition Reviews* 64: 479-486
163. Wood RJ. Vitamin D and adipogenesis: new molecular insights. 2007. *Nutr Rev.* 66 (1): 40-46

164. Hida Y, Kawada T, Kayahashi S, et al. Counteraction of retinoic acid and 1, 25 - dihydroxyvitamin D3 on up-regulation of adipocyte differentiation with PPAR γ ligand, an antidiabetic thiazolidinedione, in 3T3-L1 cells. 1998. *Life Sci.* 62: 205-211
165. Blumberg JM, Tzamei I, Astapova I, et al. Complex role of the vitamin D receptor and its ligand in adipogenesis in 3T3-L1 cells. 2006. *J. Biol. Chem.* 281 (16): 11205-11213
166. Rochford JJ, Semple RK, Laudes M, et al. ETO/MTG8 is an inhibitor of C/EBP β activity and a regulator of early adipogenesis. 2004. *Mol. Cell. Biol.* 24: 9863-9872
167. Kong J and Li YC. Molecular mechanism of 1, 25 - dihydroxyvitamin D3 inhibition of adipogenesis in 3T3-L1 cells. 2006. *Am J Physiol Endocrinol Metab.* 290: 916-924
168. Hidioglou M, Proulx JG, Roubos D. 1979. 1, 25 - hydroxyvitamin D in plasma of cattle. *J. Dairy Sci.* 62: 1076
169. Bonet ML, Felipe RF, and Palou A. 2002. Vitamin A and the regulation of fat reserves. *Cell. Mol. Life Sci.* 60:1311-1321
170. Kojima R, Fujimori T, Kiyota N, et al. In vivo isomerization of retinoic acids: rapid isomer exchange and gene expression. 1994. *J. Biol. Chem.* 269: 32700-32707
171. Magelsdorf DJ, Umesono K, Evans RM (1994) The retinoid receptors. In: *The retinoids. Biology, Chemistry and medicine*, 2nd edn, pp 319-349, Sporn MB, Roberts AB, Goodman DS (eds), Raven Press, New York
172. Chambon P (1996) A decade of molecular biology of retinoic acid receptors. *FASEB J.* 10: 940-954
173. Kuri-Harcuch W. Differentiation of 3T3 F442A cells into adipocytes is inhibited by retinoic acid. 1982. *Differentiation.* 23: 164-169

174. Kawada T, Kamei Y, and Sugimoto E. The possibility of active form of vitamin A and D as suppressors on adipocyte development via ligand-dependent transcriptional regulators. 1996. *Int. J. Obes. Relat. Metab. Disord.* 20: S52-S57
175. Schwarz EJ, Reginato MJ, Shao D, et al. Retinoic acid blocks adipogenesis by inhibiting C/EBP β -mediated transcription. 1997. *Mol. Cell. Biol.* 17: 1552-1561
176. Kamei Y, Kawada T, Kazuki R, et al. Retinoic acid receptor gamma 2 gene expression is up-regulated by retinoic acid in 3T3-L1 preadipocytes. 1993. *Biochem. J.* 293: 807-812
177. Kawada T, Kamei Y, Fujita A, et al. Carotenoids and retinoids as suppressors on adipocyte differentiation via nuclear receptors. 2000. *Biofactors.* 13: 103-109
178. Ziouzenkoca O, Orasanu G, Sharlach Molly, et al. Retinaldehyde represses adipogenesis and diet-induced obesity. 2007. *Nature medicine.* 13 (6): 695-702
179. Safonova I, Darimont C, Armi EZ, et al. Retinoids are positive effectors of adipose cell differentiation. 1994. *Mol. Cell. Endocrinol.* 104: 201-211
180. Puigserver P, Vazquez F, Bonet ML, Pico C, Palou A (1996) In vitro and in vivo induction of brown adipocyte uncoupling protein (thermogenin) by retinoic acid. *Biochem. J.* 317: 827-833
181. Bonet ML, Oliver J, Pico C, Felipe F, Ribot J, Cinti s et al. (2000) Opposite effects of vitamin A deficient diet-feeding and retinoic acid treatment on brown adipose tissue UCP1, UCP2 and leptin expression. *J. endocrinol.* 166: 511-517
182. Bibot J, Felipe f, Bonet ML, Palou A (2001) Changes of adiposity in response to vitamin A status correlate with changes of PPAR gamma 2 expression. *Obes. Res.* 9: 500-509

183. Daniel MC, Astruc, D (2004) Gold nanoparticles: assembly, supramolecular chemistry, quantum-size-related properties, and applications toward biology, catalysis, and nanotechnology. *Chem Rev* 104, 293-346
184. Porta F, Speranza G, Krpetic Z, Santo VD, Francescato P, Scari G (2007) Gold nanoparticles capped by peptides. *Materials Science and Engineering B-Solid State Materials for Advanced Technology* 140, 187-194
185. Levy R, Thanh NTK, Doty RC, Hussain I, Nichols RJ, Schiffrin DJ, Brust M, Fernig DG (2004) Rational and combinatorial design of peptide capping Ligands for gold nanoparticles. *Journal of the American Chemical Society* 126, 10076-10084
186. Nativo P, Prior IA, Brust M (2008) Uptake and intracellular fate of surface-modified gold nanoparticles. *ACS Nano* 2, 1639-1644
187. de la Fuente JM, Berry CC (2005) Tat peptide as an efficient molecule to translocate gold nanoparticles into the cell nucleus. *Bioconjug Chem* 16, 1176-1180
188. Wang G, Papasani, MR, Cheguru P, Hrdlicka PJ, Hill RA Gold-peptide nanoconjugate cellular uptake is modulated by serum proteins. *Nanomedicine: NBM* (2011)
189. Rosi NL, Giljohann DA, Thaxton CS, Lytton-Jean AKR, Han MS, Kirkin CA (2006) Oligonucleotide-modified gold nanoparticles for intracellular gene regulation. *Science* 312, 1027-1030
190. Giljohann DA, Seferos DS, Patel PC, Milstone JE, Rosi NL, Mirkin CA (2007) Oligonucleotide loading determines cellular uptake of DNA-modified gold nanoparticles. *Nano Lett* 7, 3818-3821

191. El-Sayed IH, Huang X, El-Sayed MA (2005) Surface plasmon resonance scattering and absorption of anti-EGFR antibody conjugated gold nanoparticles in cancer diagnostics: applications in oral cancer. *Nano Lett* 5, 829-834
192. Nam JM, Jang KJ, Groves JT (2007) Detection of proteins using a colorimetric bio-barcode assay. *Nat Protoc* 2, 1438-1444
193. Tkachenko AG, Xie H, Liu Y, Coleman D, Ryan J, Glomm WR, Shipton MK, Granzen S, Feldheim DL (2004) Cellular trajectories of peptide-modified gold particle complexes: Comparison of nuclear localization signals and peptide transduction domains. *Bioconjugate Chemistry* 15, 482-490
194. Liu Y, Franzen S (2008) Factors determining the efficacy of nuclear delivery of antisense oligonucleotides by gold nanoparticles. *Bioconjug Chem* 19, 1009-1016
195. Patel PC, Giljohann DA, Seferos DS, Mirkin CA (2008) Peptide antisense nanoparticles. *Proc Natl Acad Sci U S A* 105, 17222-17226
196. Sandhu KK, McIntosh CM, Simard JM, Smith SW, Rotello VM (2002) Gold nanoparticle-mediated transfection of mammalian cells. *Bioconjug Chem* 13, 3-6
197. Liu Y, Shipton MK, Ryan J, Kaufman ED, Franzen S, Feldheim DL (2007) Synthesis, stability, and cellular internalization of gold nanoparticles containing mixed peptide-poly(ethylene glycol) monolayers. *Anal Chem* 79, 2221-2229
198. Seferos DS, Prigodich AE, Giljohann DA, Patel PC, Mirkin CA (2009) Polyvalent DNA nanoparticle conjugates stabilize nucleic acids. *Nano Lett* 9, 308-311
199. Lee SH, Bae KH, Kim SH, Lee KR, Park TG (2008) Amine-functionalized gold nanoparticles as non-cytotoxic and efficient intracellular siRNA delivery carriers. *Int J Pharm* 364, 94-101

200. Oishi M, Nakaogami J, Ishii T, Nagasaki Y (2006) Smart PEGylated gold nanoparticles for the cytoplasmic delivery of siRNA to induce enhanced gene silencing. *Chemistry Letters* 35, 1046-1047
201. Elbakry A, Zaky A, Liebl R, Rachel R, Goepferch A, Breunig M (2009) Layer-by-layer assembled gold nanoparticles for siRNA delivery. *Nano Lett* 9, 2059-2064
202. Guo S, Huang Y, Jiang Q, Sun Y, Deng L, Liang Z, Du Q, Xing J, Zhao Y, Wang PC, Dong A, Liang X (2010) Enhanced gene delivery and siRNA silencing by gold nanoparticles coated with charge-reversal polyelectrolyte. *ACS Nano* 4, 5505-5511
203. Song WJ, Du JZ, Sun TM, Zhang PZ, Wang J (2010) Gold nanoparticles capped with polyethyleneimine for enhanced siRNA delivery. *Small* 6, 239-246
204. Giljohann DA, Seferos DS, Prigodich AE, Patel PC, Mirkin CA (2009) Gene Regulation with Polyvalent siRNA-Nanoparticle Conjugates. *Journal of the American Chemical Society* 131, 2072-+
205. Berry CC, de la Fuente JM, Mullin M, Chu SW, Curtis AS (2007) Nuclear localization of HIV-1 tat functionalized gold nanoparticles. *IEEE Trans Nanobioscience* 6, 262-269
206. Munro S, Pelham HRB (1986) An Hsp70-Like Protein in the Er - Identity with the 78 Kd Glucose-Regulated Protein and Immunoglobulin Heavy-Chain Binding-Protein. *Cell* 46, 291-300
207. Munro S, Pelham HRB (1987) A C-Terminal Signal Prevents Secretion of Luminal Er Proteins. *Cell* 48, 899-907
208. Hsu VW, Shah N, Klausner RD (1992) A Brefeldin-a-Like Phenotype Is Induced by the Overexpression of a Human Erd-2-Like Protein, Elp-1. *Cell* 69, 625-635

209. Lewis MJ, Pelham HRB (1992) Ligand-Induced Redistribution of a Human Kdel Receptor from the Golgi-Complex to the Endoplasmic-Reticulum. *Cell* 68, 353-364
210. Tang BL, Wong SH, Qi XL, Low SH, Hong WJ (1993) Molecular-Cloning, Characterization, Subcellular-Localization and Dynamics of P23, the Mammalian Kdel Receptor. *Journal of Cell Biology* 120, 325-338
211. Sonnichsen B, Fullekrug J, Nguyen Van P, Diekmann W, Robinson DG, Mieskes G (1994) Retention and Retrieval - Both Mechanisms Cooperate to Maintain Calreticulin in the Endoplasmic-Reticulum. *Journal of Cell Science* 107, 2705-2717
212. Griffiths G, Ericsson M, Krijnse-Locker J, Nilsson T, Goud B, Soling HD, tang BL, Wong SH, Hong W (1991) Localization of the Lys, Asp, Glu, Leu Tetrapeptide Receptor to the Golgi-Complex and the Intermediate Compartment in Mammalian-Cells. *Journal of Cell Biology* 127, 1557-1574
213. Pelham HR (1991) Recycling of proteins between the endoplasmic reticulum and Golgi complex. *Curr Opin Cell Biol* 3, 585-591
214. Sonnichsen B, Watson R, Clausen H, Misteli T, Warren G (1996) Sorting by COP I-coated vesicles under interphase and mitotic conditions. *Journal of Cell Biology* 134, 1411-1425
215. Majoul IV, Bastiaens PIH, Soling HD (1996) Transport of an external Lys-Asp-Glu-Leu (KDEL) protein from the plasma membrane to the endoplasmic reticulum: Studies with cholera toxin in Vero cells. *Journal of Cell Biology* 133, 777-789
216. Acharya S, Hill RA (2013) High efficacy gold-KDEL peptide-siRNA nanoconstruct-mediated transfection in C2C12 myoblasts and myotubes. *Nanomedicine: NBM* 10: 329-337

217. Wang J, Lu Z, Wientjes MG, Au JL (2010) Delivery of siRNA therapeutics: barriers and carriers. *AAPS J* 12, 492-503 (2010)
218. Rand TA, Ginalski K, Grishin N, Wang X (2004) Biochemical identification of Argonaute 2 as the sole protein required for RNA-induced silencing complex activity. *Proc Natl Acad Sci U S A* 101, 14385-14389
219. Matranga C, Tomari Y, Shin C, Bartel DP, Zamore PD (2005) Passenger-strand cleavage facilitates assembly of siRNA into Ago2-containing RNAi enzyme complexes. *Cell* 123, 607-620
220. Ameres SL, Martinez J, Schroeder R (2007) Molecular basis for target RNA recognition and cleavage by human RISC. *Cell* 130, 101-112
221. Hutvagner G, Zamore PD (2002) A microRNA in a multiple-turnover RNAi enzyme complex. *Science* 297, 2056-2060
222. Bartlett DW, Davis ME (2006) Insights into the kinetics of siRNA-mediated gene silencing from live-cell and live-animal bioluminescent imaging. *Nucleic Acids Res* 34, 322-333
223. Unnamalai N, Kang BG, Lee WS (2004) Cationic oligopeptide-mediated delivery of dsRNA for post-transcriptional gene silencing in plant cells. *FEBS Lett* 566, 307-310
224. Endoh T, Ohtsuki T (2009) Cellular siRNA delivery using cell-penetrating peptides modified for endosomal escape. *Adv Drug Deliv Rev* 61, 704-709
225. Muratovska A, Eccles MR (2004) Conjugate for efficient delivery of short interfering RNA (siRNA) into mammalian cells. *FEBS Lett* 558, 63-68
226. Davidson TJ, Harel S, Arboleda VA, Prunell GF, Shelanski ML, Vreene LA, Troy CM (2004) Highly efficient small interfering RNA delivery to primary mammalian

neurons induces MicroRNA-like effects before mRNA degradation. *J Neurosci* 24, 10040-10046

227. Agarwal A, Unfer R, Mallapragada SK (2005) Novel cationic pentablock copolymers as non-viral vectors for gene therapy. *J Control Release* 103, 245-258

228. Werth S, Urban-Klein B, Dal L, Hobel S, Grzelinski M, Bakowsky U, Czubayko F, Aigner A (2006) A low molecular weight fraction of polyethylenimine (PEI) displays increased transfection efficiency of DNA and siRNA in fresh or lyophilized complexes. *J Control Release* 112, 257-270

229. Nguyen J, Steele TW, Merkel O, Reul R, Kissel T (2008) Fast degrading polyesters as siRNA nano-carriers for pulmonary gene therapy. *J Control Release* 132, 243-251

230. Katas H, Cevher E, Alpar HO (2009) Preparation of polyethyleneimine incorporated poly(D,L-lactide-co-glycolide) nanoparticles by spontaneous emulsion diffusion method for small interfering RNA delivery. *Int J Pharm* 369, 144-154

231. Halder J, Kamat AA, Landen Jr CN, Han LY, Lutgendor SK, Lin YG, Merritt WM, Jennings NB, Chavez-Reyes A, Coleman RL, Gershenson DM, Schmandt R, Cole SW, Lopez-Berestain G, Sood AK (2006) Focal adhesion kinase targeting using in vivo short interfering RNA delivery in neutral liposomes for ovarian carcinoma therapy. *Clin Cancer Res* 12, 4916-4924

232. Santel A, Aleku M, Keil O, Endruschat J, Esche V, Fisch G, Dames S, Loffler K, Fechtner M, Arnold W, Giese K, Klippel A, Kaufmann J (2006) A novel siRNA-lipoplex technology for RNA interference in the mouse vascular endothelium. *Gene Ther* 13, 1222-1234

233. Li SD, Chen YC, Hackett MJ, Huang L (2008) Tumor-targeted delivery of siRNA by self-assembled nanoparticles. *Mol Ther* 16, 163-169
234. Tseng YC, Mozumdar S, Huang L (2009) Lipid-based systemic delivery of siRNA. *Adv Drug Deliv Rev* 61, 721-731
235. Chen AM, Zhang M, Wei D, Stueber D, Taratula O, Minko Tamara, He H (2009) Co-delivery of doxorubicin and Bcl-2 siRNA by mesoporous silica nanoparticles enhances the efficacy of chemotherapy in multidrug-resistant cancer cells. *Small* 5, 2673-2677
236. Xia T, Kovoichich M, Liong M, Meng H, Kabehie S, Gorge S, Zink JI, Nel AE (2009) Polyethyleneimine coating enhances the cellular uptake of mesoporous silica nanoparticles and allows safe delivery of siRNA and DNA constructs. *ACS Nano* 3, 3273-3286
237. Meng H, Liong M, Xia T, Li Z, Ji Z, Zink JI, Nel AE (2010) Engineered design of mesoporous silica nanoparticles to deliver doxorubicin and P-glycoprotein siRNA to overcome drug resistance in a cancer cell line. *ACS Nano* 4, 4539-4550
238. Cheong S, Lee C, Kim S, Jeong H, Jim, E, Park E, Kim DW, Lim ST, Sohn M (2009) Superparamagnetic iron oxide nanoparticles-loaded chitosan-linoleic acid nanoparticles as an effective hepatocyte-targeted gene delivery system. *Int J Pharm* 372, 169-176
239. Bae KH, Lee K, Kim C, Park TG (2011) Surface functionalized hollow manganese oxide nanoparticles for cancer targeted siRNA delivery and magnetic resonance imaging. *Biomaterials* 32, 176-184
240. Lytton-Jean AK, Langer R, Anderson DG (2011) Five years of siRNA delivery: spotlight on gold nanoparticles. *Small* 7, 1932-1937

241. Chen AA, Derfus AM, Khetani SR, Bhatia SN (2005) Quantum dots to monitor RNAi delivery and improve gene silencing. *Nucleic Acids Res* 33, e190
242. Derfus AM, Chen AA, Min DH, Ruoslahti E, Bhatia SN (2007) Targeted quantum dot conjugates for siRNA delivery. *Bioconjug Chem* 18, 1391-1396
243. Tan WB, Jiang S, Zhang Y (2007) Quantum-dot based nanoparticles for targeted silencing of HER2/neu gene via RNA interference. *Biomaterials* 28, 1565-1571
244. Qi L, Gao X (2008) Quantum dot-amphipol nanocomplex for intracellular delivery and real-time imaging of siRNA. *ACS Nano* 2, 1403-1410

CHAPTER II

REGULATION OF ADIPOGENESIS AND KEY ADIPOGENIC GENE EXPRESSION BY 1, 25-DIHYDROXYVITAMIN D IN 3T3-L1 CELLS

This chapter is accepted for publication in PLoS One, as citation, Shuhan Ji, Matthew E. Doumit, and Rodney A. Hill, 2015, Regulation of adipogenesis and key adipogenic gene expression by 1,25-dihydroxyvitamin D in 3T3-L1 cells, journal doi: 10.1371/journal.pone.0126142

Abstract

The functions of 1, 25-dihydroxyvitamin D (1, 25-(OH)₂D₃) in regulating adipogenesis, adipocyte differentiation and key adipogenic gene expression were studied in 3T3-L1 preadipocytes. Five concentrations (0.01, 0.1, 1, 10, 100 nM) of 1, 25-(OH)₂D₃ were studied and lipid accumulation measured by Oil Red O staining and expression of adipogenic genes quantified using quantitative real-time PCR. Adipogenic responses to 1, 25-(OH)₂D₃ were determined on 6, and 12 h, and days 1-10 after induction of adipogenesis by a hormonal cocktail (insulin, 3-Isobutyl-1-methylxanthine, and dexamethasone) with or without 1, 25-(OH)₂D₃. In response to 1, 25-(OH)₂D₃ (1, 10, and 100 nM), lipid accumulation and the expression of *PPAR*γ, *C/EBP*α, *FABP4* and *SCD-1* were inhibited

through day 10, and VDR expression was inhibited in the early time points. The greatest inhibitory effect was upon expression of *FABP4*. Expression of *SREBP-1c* was only affected on day 2. The lowest concentrations of 1, 25-(OH)₂D₃ tested did not affect adipocyte differentiation or adipogenic gene expression. The *C/EBPα* promoter activity response to 1, 25-(OH)₂D₃ was also tested, with no effect detected. These results indicate that 1, 25-(OH)₂D₃ inhibited adipogenesis via suppressing adipogenic-specific genes, and is invoked either during PPAR γ activation or immediately up-stream thereof. Gene expression down-stream of PPAR γ especially *FABP4* was strongly inhibited, and we suggest that the role of 1, 25-(OH)₂D₃ in regulating adipogenesis will be informed by further studies of adipogenic-specific gene promoter activity.

Introduction

Growth of adipose tissue mass involves two distinct processes: hypertrophy (because of lipid synthesis and the subsequent increase in the size of adipocytes) and hyperplasia (because of proliferation, when preadipocyte and adipocyte numbers increase) [1]. Adipogenesis is the process of preadipocyte differentiation to form mature adipocytes, and during this process lipid accumulation occurs. The transcriptional control of adipocyte differentiation requires a sequential series of gene expression events and activation of a number of key signaling pathways [2]. This cascade starts with the induction of CCAAT/enhancer – binding protein β and δ (*C/EBP β* and *C/EBP δ*). These two proteins then induce the expression of nuclear receptor peroxisome proliferator – activated receptor γ (PPAR γ), which in turn induces *C/EBP α* expression [3]. Once expressed, *C/EBP α* activity positively feeds back on PPAR γ activity. These two factors enhance each other's

expression and maintain the differentiated state [4]. Sterol-regulatory element binding protein 1c (*SREBP-1c*) is another notable key adipogenic gene [5]. *SREBP-1c* was independently discovered by two different research groups, and was named as ADD1 and SREBP-1c [6] [7]. This gene is induced during adipogenesis and is further regulated by insulin in cultured adipocytes [8,9]. In addition, SREBP-1c can modulate a variety of genes linked to fatty acid and triglyceride metabolism, and can also regulate adipogenesis [3] via induction of PPAR γ gene expression through E box motifs present in the PPAR γ promoter [10]. Increased expression of *SREBP-1c* leads to activation of PPAR γ by inducing its expression and by increasing the production of an endogenous PPAR γ ligand. All these transcriptional factors are necessary for the terminally differentiated phenotype.

Moreover, in humans, obesity is characterized by an increase in lipid accumulation and is the leading risk-factor for the development of Type 2 diabetes [11]. Understanding the biological process of adipogenesis is important for the development of novel targets for obesity therapy. Increasing evidence suggests there is a potential link between obesity and vitamin D insufficiency [12]. The bioactive metabolite of vitamin D is 1, 25 - (OH) $_2$ D $_3$, which acts as a steroid hormone and a high-affinity ligand for the vitamin D receptor (VDR). The 1, 25 - (OH) $_2$ D $_3$ activated VDR can form a heterodimer with the retinoid X receptor (RXR), which can bind to vitamin D response elements in various genes [13]. This VDR-RXR heterodimer may be competitive, inhibiting [14] the expression of PPAR γ , which is a key regulator of adipogenesis, and thus also inhibit adipocyte maturation [13]. Therefore, 1, 25 - (OH) $_2$ D $_3$ and VDR may play important roles in regulating adipogenesis. The vitamin D receptor is expressed very early in adipogenesis in 3T3-L1 cells. The VDR

expression levels reach a maximum during the first 6 h after induction of differentiation, then decline to background levels after 2 days [15]. This creates a short window of opportunity for 1, 25 - (OH)₂D₃ to influence the differentiation process in forming mature adipocytes. Previous work has indicated that 1, 25 - (OH)₂D₃ is an inhibitor of adipogenesis in the 3T3-L1 cells [16,17]. In 1998, work performed by Kelly and Gimble [18] have established that 1, 25 - (OH)₂D₃ inhibits adipocyte differentiation in murine bone marrow cells. However, the specific mechanisms of the inhibitory actions of 1, 25 - (OH)₂D₃ in adipogenesis have not been described.

In the present study, we have determined the inhibitory effect of different concentrations of 1, 25 - (OH)₂D₃ in 3T3-L1 preadipocyte differentiation. We also studied the inhibitory activity of different concentrations of 1, 25 - (OH)₂D₃ on expression levels of key adipogenic genes (*C/EBPs* and *PPARγ*). As an important transcriptional factor during adipocyte differentiation, *C/EBPα* was a focus of the present study. We sought to determine whether there is a relationship between the inhibitory effect of 1, 25 - (OH)₂D₃ and the promoter activity of *C/EBPα*. Our study provides an experimental basis to better understand the function of 1, 25 - (OH)₂D₃ in regulation of adipogenesis, and the interactions between 1, 25 - (OH)₂D₃ and key adipogenic genes.

Materials and Methods

Materials

Mouse embryonic fibroblast cells (3T3-L1) were obtained from the American Type Culture Collection (ATCC). Dulbecco's Modified Eagle's Medium (DMEM), fetal bovine serum (FBS) and penicillin/streptomycin were from Gibco, Life Technologies (Grand Island, NY). Trizol, DNase I kit, high capacity cDNA reverse transcription kit (Cat # 4368814), and Taqman Master Mix were obtained from Life Technologies (Grand Island, NY). The Dual Reporter Luciferase Assay System was purchased from Promega Corporation, (Madison, WI). Oil Red O (ORO) powder, dexamethasone (D8893), insulin from bovine pancreas (I6634), 3-isobutyl-1-methylxanthine (IBMX) (I7018), and 1 α ,25-Dihydroxyvitamin D₃ (D1530) were purchased from Sigma-Aldrich (St. Louis, MO). Mouse-specific anti-PPAR γ (sc-7196) rabbit polyclonal antibody was purchased from Santa Cruz Biotechnology (Dallas, Texas). Mouse-specific anti-C/EBP α (ab139731) rabbit polyclonal antibody, and anti- β -actin mouse-monoclonal (ab8226) were purchased from Abcam (Cambridge, MA). AlexaFluor 680 anti-rabbit IgG was from life Technologies (Grand Island, NY) and IRDye800 anti-mouse IgG was from Li-Cor (Lincoln, NE).

Cell culture

Mouse 3T3-L1 preadipocytes were cultured at 37 °C with 5% CO₂ enriched air in DMEM with 10 % FBS, 100 I.U. /ml penicillin, 100 μ g/ml streptomycin (basal growth medium). Cells were seeded in 6-well plates and 24-well plates with glass cover slips in basal growth

medium and cultured until confluent. On day 0 (two days post confluence), 1, 25-dihydroxyvitamin D was added to the differentiation medium at the following final concentrations: 100, 10, 1, 0.1, and 0.01 nM, and cultures were incubated for 48 h. Cells grown in basal growth medium without 1, 25-dihydroxyvitamin D served, as a negative control. Cells grown in medium containing basal growth medium with dexamethasone (1 μ M), IBMX (500 μ M) and insulin (1.7 mM) (standard hormonal differentiation medium, DM) served, as a positive control. For the DMI treatment, insulin, dexamethasone and IBMX were provided for the first 48 h followed by only insulin in basal growth medium throughout the remaining time points. Media were changed every 2 days for all treatments. Cells were harvested on 0, 6, and 12 h, and days 1, 2, 4, 6, 8 and 10 for RNA extraction, or protein extraction. Parallel cultures were stained with ORO and representative images of ORO stained cells on day 10 were quantified using MetaMorph Image analysis software (Nashville, TN).

Cells and transfection

For each cell culture well, 3.5×10^5 3T3-L1 cells were plated and allowed to reach 80% confluence. Cells were then co-transfected with 2 μ g [pGL4.10 (luc2/-500 C/EBP α)] and 0.2 μ g of internal transfection control vector [pGL4.74 (hRluc/TK)], and transferred to growth medium. Cells were incubated 24 h, and allowed to reach 100% confluence. Two days post confluence cells (0 h) were treated with 100 nM of 1, 25(OH) $_2$ D $_3$ plus differentiation medium, differentiation medium only, or growth medium only. Cells were harvested on 0, 12, 24, and 24 h, and assayed for firefly luciferase and renilla luciferase activities using the Dual Reporter Luciferase Assay System (Promega, Madison, WI) and

a Wallac 1420 Multi Label Counter. Firefly luciferase activity units were normalized to units of renilla luciferase activity to correct for transfection efficiency.

Oil Red O (ORO) and Hematoxylin staining

Accumulation of lipids was observed using ORO staining [19]. Oil Red O in isopropanol stock solution (3.5 mg/ml) was prepared, stirred overnight and filtered. Cells grown on cover slips in 24-well plates were used for lipid staining. On the day of the time point, culture medium was removed and cells were gently rinsed once with phosphate buffer saline (PBS). Cells were fixed in 10 % formaldehyde in PBS for 1 hr at RT. After fixation, cells were rinsed with PBS and then 60 % isopropanol. Oil Red O solution (6:4 v/v of stock solution and water) was added and incubated for 10 min at RT. Finally, cells were washed with distilled water, three times. Hematoxylin counter staining was done according to the manufacturer's instructions. Briefly, cells were incubated with filtered hematoxylin for two minutes and rinsed twice with tap water. Differentiation solution (0.25 % HCl in 70 % alcohol) was added and cells were rinsed again with tap water. The glass cover slips were then removed from the wells and inverted on to a glass slide with mounting medium (Vecta Shield, Vector Labs, Burlingame, CA).

RNA extraction and cDNA synthesis

Total RNA was extracted using Trizol according to the manufacturer's instructions. The RNA pellet was resuspended in nuclease-free water and stored at -80°C until further use. RNA was quantified using a Nanodrop ND-1000 UV-Vis Spectrophotometer (Nanodrop

Technologies, Wilmington, DE). The quality of RNA was verified on 1% agarose gels. Two μg of RNA from each treatment was DNase treated. Synthesis of cDNA was conducted using a high capacity cDNA reverse transcription kit and random hexamers as primers according to the manufacturer's instructions. To ensure availability of cDNA sufficient to perform all real-time PCR reactions, cDNA synthesized from 2 μg of RNA was pooled for each sample. Pooled cDNA was diluted 1:10 using nuclease-free water for real-time PCR.

Real-time PCR

Quantitative real-time PCR was performed using Taqman MGB primer/probe sets with an ABI 7500 Fast Real Time PCR system (Applied Biosystems, Foster City, CA). Primers and probes for all genes were designed using Applied Biosystems Primer Express 3.0 software. Primers (Integrated DNA Technologies, Coralville, IA) and probes (Life Technologies, Grand Island, NY) were designed to have a T_m of 58-60 °C and 69-70 °C, respectively. Primer-probe sets that span exon-junctions (trans-intronic positions) were chosen for real-time PCR, to prevent binding to genomic DNA (Table 1). Eukaryotic translation elongation factor 2 (*EEF2*) was used as an endogenous control for gene expression. Probes were labeled with 6-FAM or VIC for all target genes or control (*EEF2*), respectively. Real-time PCR assays for each sample were conducted in duplicate wells with all genes including endogenous control on the same plate. Reactions contained Taqman Universal Fast PCR Master Mix, No AmpErase UNG (Applied Biosystems, Foster City, CA) (1X), forward primer (0.5 μM), reverse primer (0.5 μM), Taqman probe (0.125 μM) and cDNA template made up to a final volume of 15 μl in nuclease-free water. Real-time

PCR cycle conditions included a holding time of 90 °C for 20 sec, followed by 40 cycles of 90 °C for 3 sec and 60 °C for 30 sec of melting and extension temperatures, respectively.

Data were analyzed using the relative C_T ($\Delta\Delta C_t$) method [20]. Average C_t values of endogenous control (*EEF2*) were subtracted from target gene average C_t values of each gene, to obtain ΔC_t values of each gene for each sample. For each gene, ΔC_t values in the control treatment at each time point were used to normalize ΔC_t values of corresponding time points of each treatment to obtain $\Delta\Delta C_t$ and mRNA fold expression values [$2^{(-\Delta\Delta C_t)}$].

Table 1: Primer-probe sets for real-time PCR. Primers and probe sequences used in real-time PCR listed 5' to 3': Forward primer (FP), reverse primer (RP) and Taqman probes for the following genes were designed from the corresponding GenBank accession numbers.

Accession No.	Gene name	Sequences
NM_007907.1	<i>Eukaryotic translation elongation factor 2 (Eef2)</i>	FP: CTGCCTGTCAATGAGTCCTTG RP: GCCGCCGGTGTGGAT Probe: CTCACCGCTGATCTG
NM_011146.2	<i>Peroxisome proliferator activated receptor gamma (PPARγ)</i>	FP: GCTTCCACTATGGAGTTCATGCT RP: AATCGGATGGTCTTCGGAAA Probe: TGAAGGATGCAAGGGTT

NM_007678.3	<i>CCAAT/enhancer binding protein alpha (C/EBPα)</i>	<i>FP: CGCAAGAGCCGAGATAAAGC</i> <i>RP: GTCAACTCCAGCACCTTCTGTTG</i> <i>Probe: AACGCAACGTGGAGAC</i>
NM_009504.4	<i>Vitamin D receptor (VDR)</i>	<i>FP: GGCTTCCACTTCAACGCTATG</i> <i>RP: TGCTCCGCCTGAAGAAACC</i> <i>Probe: CCTGTGAAGGCTGCAA</i>
NM_009883.3	<i>CCAAT/enhancer binding protein beta (C/EBPβ)</i>	<i>FP: GCGCACCGGGTTTCG</i> <i>RP: GCGCTCAGCCACGTTTG</i> <i>Probe: ACTTGATGCAATCCGGA</i>
NM_007679.4	<i>CCAAT/enhancer binding protein delta (C/EBPδ)</i>	<i>FP: CTGTGCCACGACGAACTCTTC</i> <i>RP: GCCGGCCGCTTTGTG</i> <i>Probe: CGACCTCTTCAACAGC</i>
NM_024406.1	<i>Fatty acid binding protein 4 (FABP4)</i>	<i>FP: CCGCAGACGACAGGAAGGT</i> <i>RP: AGGGCCCCGCCATCT</i> <i>Probe: AAGAGCATCATAACCC</i>
NM_010052.3	<i>Preadipocyte factor-1 (Pref-1)</i>	<i>FP: AATAGACGTTCTGGGCTTGCA</i> <i>RP: GGTCACGCAAGTTCCATTG</i> <i>Probe: CTCAACCCCCTGCGC</i>
NM_011480.3	<i>Sterol regulatory element binding transcription factor 1 (Srebf1)</i>	<i>FP: GCGGTTGGCACAGAGCTT</i> <i>RP: CTGTGGCCTCATGTAGGAATACC</i> <i>Probe: CGGCCTGCTATGAGG</i>
NM_009127.4	<i>Stearoyl-Coenzyme A desaturase 1 (Scd1)</i>	<i>FP: CAACACCATGGCGTTCCA</i> <i>RP: TGGCGCGGTGATCTC</i> <i>Probe: AATGACGTGTACGAATGG</i>

Western Blot

Protein extraction from 3T3-L1 preadipocytes and adipocytes was performed using cell lysis buffer with addition of phosphatase and protease inhibitors (Cell Signaling Technologies, Danvers, MA). The supernatant was extracted by centrifugation and protein concentration was determined by BCA protein assay according to manufacturer's protocol (Thermo Scientific, Rockford, IL). Ten μg of whole cell lysate was resolved on SDS-PAGE (4-10% precise gels) and then transferred to PVDF membrane. Membranes were blocked with 5% non-fat milk in 1X TBST for 1h at room temperature. Membranes were incubated with anti-PPAR γ , anti-C/EBP α and anti- β -actin at 4 °C overnight, then washed with 1X TBST and incubated with AlexaFluor 680 conjugated anti-rabbit IgG and IRDye 800 conjugated anti-mouse IgG for 1 h at room temperature. After thorough washing, blots were scanned and quantified using an Odyssey Dual Infrared Imaging System (Li-Cor).

Microscopy

Images were obtained using a Nikon 80i phase-contrast microscope, using a 20X objective lens. Image quantification was performed using MetaMorph Image analysis software (Nashville, TN). Area fractions were collected for each image. Images were collected in six to eight replicates from each culture well. Average area fractions of each of the six to eight replicates were used to calculate average area fraction of each treatment sample. Further, average area fraction values of each treatment were normalized to average area fraction values of corresponding controls.

Statistical analysis

Statistical analysis software (SAS) 9.3 was used to perform all data analysis. Data were analyzed using a one-way analysis of variance (ANOVA) for each time point. Tukey's test was used to find the significant differences among the different means. Differences, when $p < 0.05$, were considered statistically significant. Gene expression data were analyzed by comparing log (base 2) transformed values of mRNA fold expression across treatments within each time-point. All data are reported as mean \pm SE (n = 3).

Results

1, 25 - (OH)₂D₃ inhibits lipid accumulation

Cultures of 3T3-L1 cells were incubated in standard hormonal differentiation medium, in the presence or absence of 1, 25 - (OH)₂D₃. DMI medium served as a positive control treatment. Basal growth medium served as a negative control. Lipid accumulation was observed through ORO staining on days 0, 2, 4, 6, 8 (data not shown) and 10 (Fig. 2.1A-G). Image quantification analysis shows that lipid accumulation at higher concentrations of 1, 25 - (OH)₂D₃ (100, 10, 1 nM) treated cells was similar to that in negative control cells, and significantly lower than the positive control (Figure 2.1H). The lowest concentration of 1, 25 - (OH)₂D₃ treated cells showed higher lipid accumulation than negative control and other 1, 25 - (OH)₂D₃ treated cells, however, lipid accumulation was still significantly lower when compared to the positive control (Fig. 2.1H). This suggests that 1, 25 - (OH)₂D₃ treatment inhibited lipid accumulation and adipogenesis in a dose dependent manner.

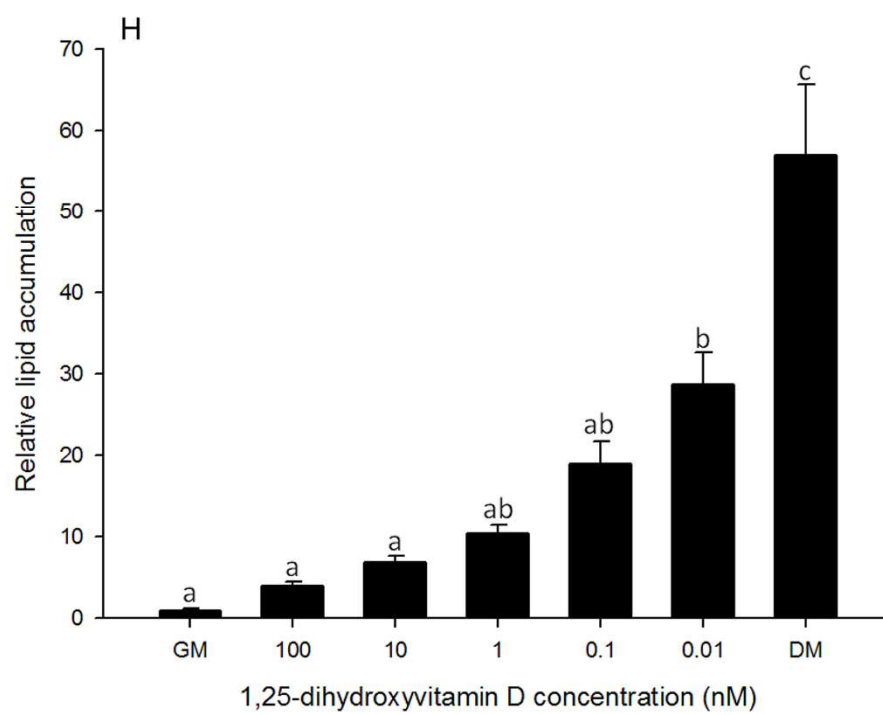
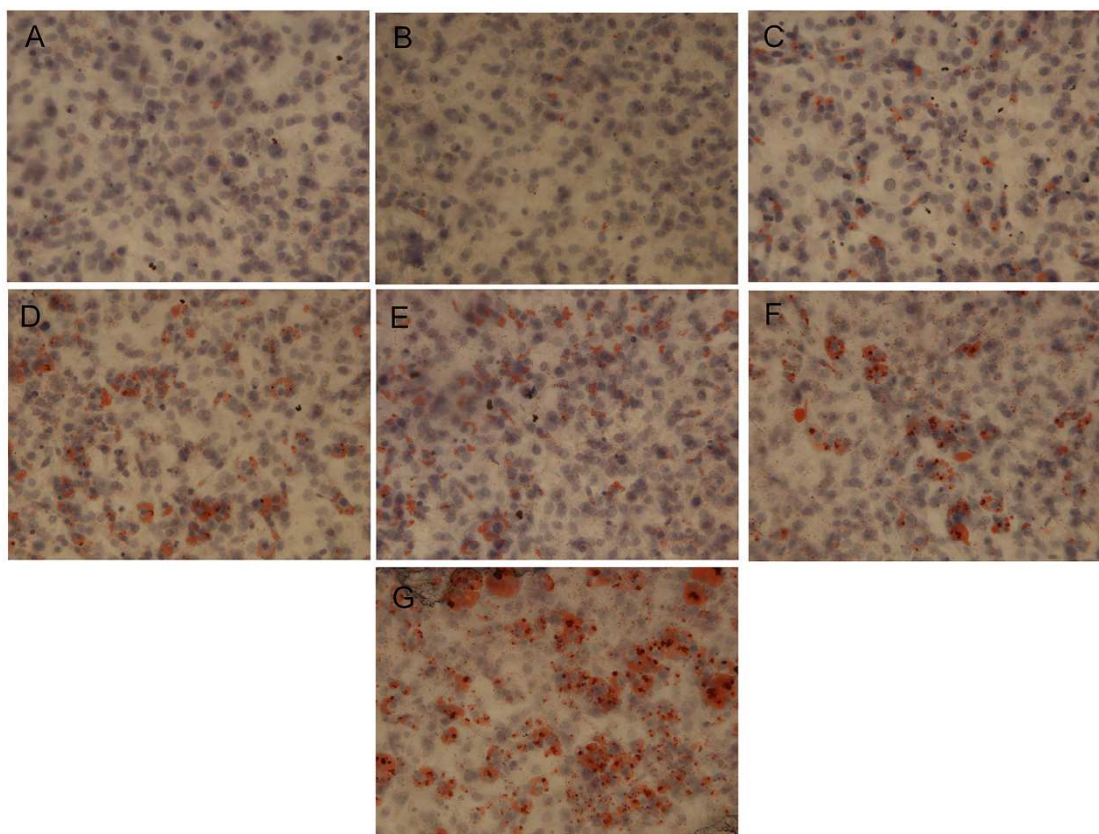


Figure 2.1 Oil Red O staining in 3T3-L1 cells

Cells were treated with basal growth medium (GM) (A) or differentiation medium plus different concentrations of 1, 25 - (OH)₂D₃, 100 nM (B), 10 nM (C), 1 nM (D), 0.1 nM (E) or 0.01 nM (F) or differentiation medium (DM) (G). Oil Red O staining was performed on days 2, 4, 6, 8 and 10. Representative day 10 images are shown. Images were collected at 400x magnification. (H): Quantification of lipid accumulation in 3T3-L1 cells. Lipid accumulation was quantified using MetaMorph Image analysis software. Area fractions were collected for each treatment and normalized to control of corresponding time point. Data are means ± SE (n = 3). Different letters represent treatment effects that were significantly different ($P < 0.05$). The dose-response effect of 1, 25 - (OH)₂D₃ treatment on lipid accumulation is illustrated.

High concentrations of 1, 25 - (OH)₂D₃ inhibit PPAR γ expression

To better understand the expression pattern of PPAR γ during the process of adipocyte differentiation, RNA extracts and protein extracts from 3T3-L1 cells treated with DM only were obtained for real-time PCR and Western blots tests. Gene expression levels of PPAR γ began to increase after day 2, and reached a maximum on day 8 (Fig. 2.2A). Protein levels of PPAR γ were consistent with gene expression levels, increasing on day 2, and reaching the highest level on day 10 (Fig. 2.2B). This suggests PPAR γ expression level increased concurrent with adipocyte differentiation, and consistent with increasing lipid accumulation.

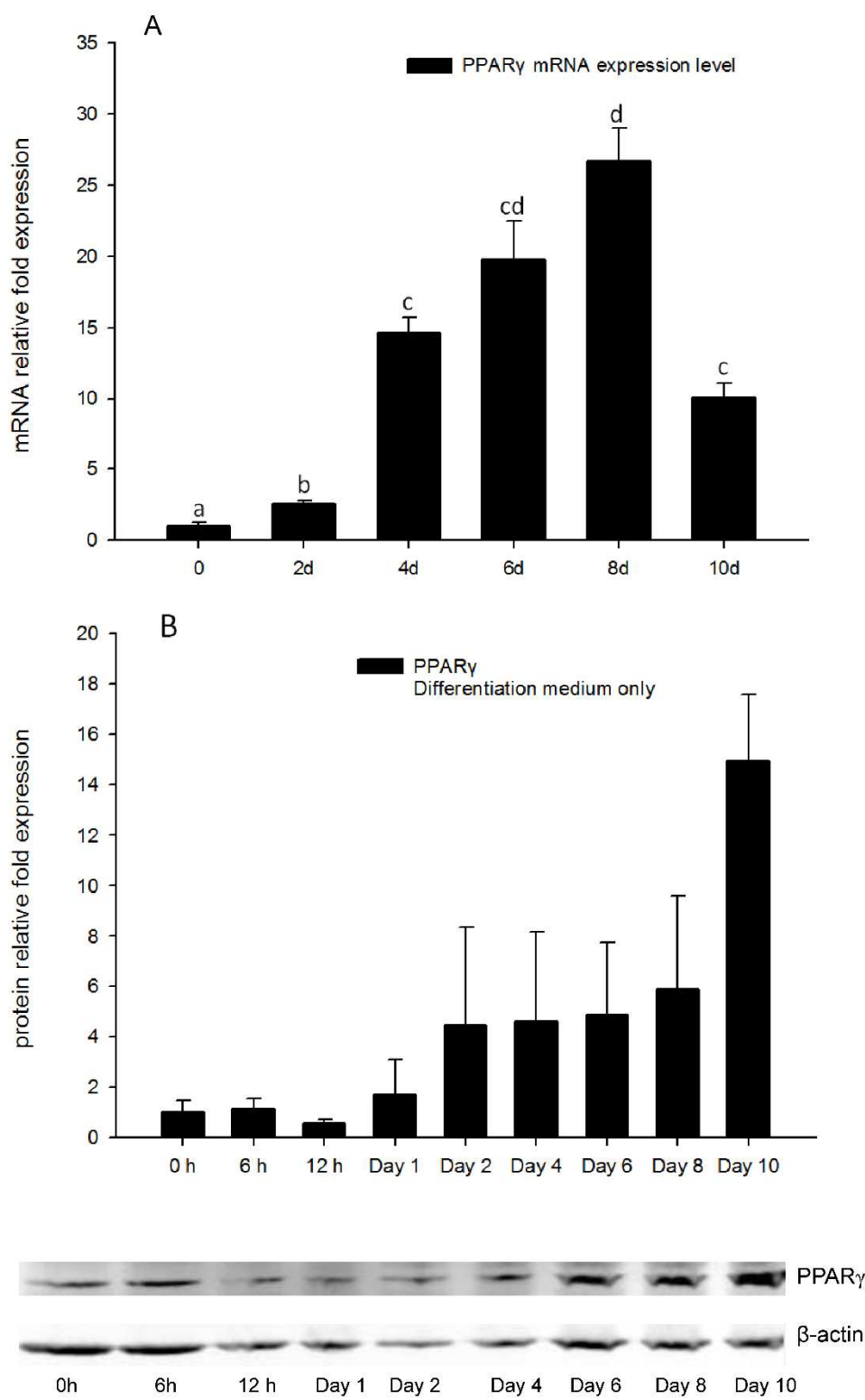


Figure 2.2 (A) Real-time PCR quantification of *PPAR γ* gene expression in DM treatment of 3T3-L1 cells on days 0, 2, 4, 6, 8, and 10 with *EEF2* used as endogenous control (Δ Ct). Data were normalized to *PPAR γ* gene expression of the day 0 group ($\Delta\Delta$ Ct). **(B) Image showing Western blot analysis** (Odyssey® Dual Infrared Imaging System (Li-Cor)) of *PPAR γ* on 0, 6, and 12 h, days 1, 2, 4, 6, 8 and 10. β -actin was used as an internal protein loading control. Quantification of *PPAR γ* normalized to β -actin is shown. Data are means \pm SE (n = 3). Different letters represent treatment effects that were significantly different ($P < 0.05$).

Gene expression levels of *PPAR γ* in 3T3-L1 cells treated with high concentrations (100, 10, and 1 nM) of 1, 25 - (OH)₂D₃ were significantly inhibited compared to the positive control (Fig. 2.3A-E) at all time-points measured. In addition, for all time-points, 3T3-L1 cultures treated with low concentrations (0.1 and 0.01 nM) of 1, 25 - (OH)₂D₃ showed no significant differences in *PPAR γ* gene expression levels as compared to positive control cultures (Fig. 2.3A-E). On days 2, 4 and 10, the highest concentration (100 nM) of 1, 25 - (OH)₂D₃ had the greatest inhibitory effect on *PPAR γ* mRNA expression levels. This suggests that *PPAR γ* gene expression levels were inhibited by 1, 25 - (OH)₂D₃, and 1, 25 - (OH)₂D₃ had greater efficacy in inhibiting *PPAR γ* gene expression at higher concentrations.

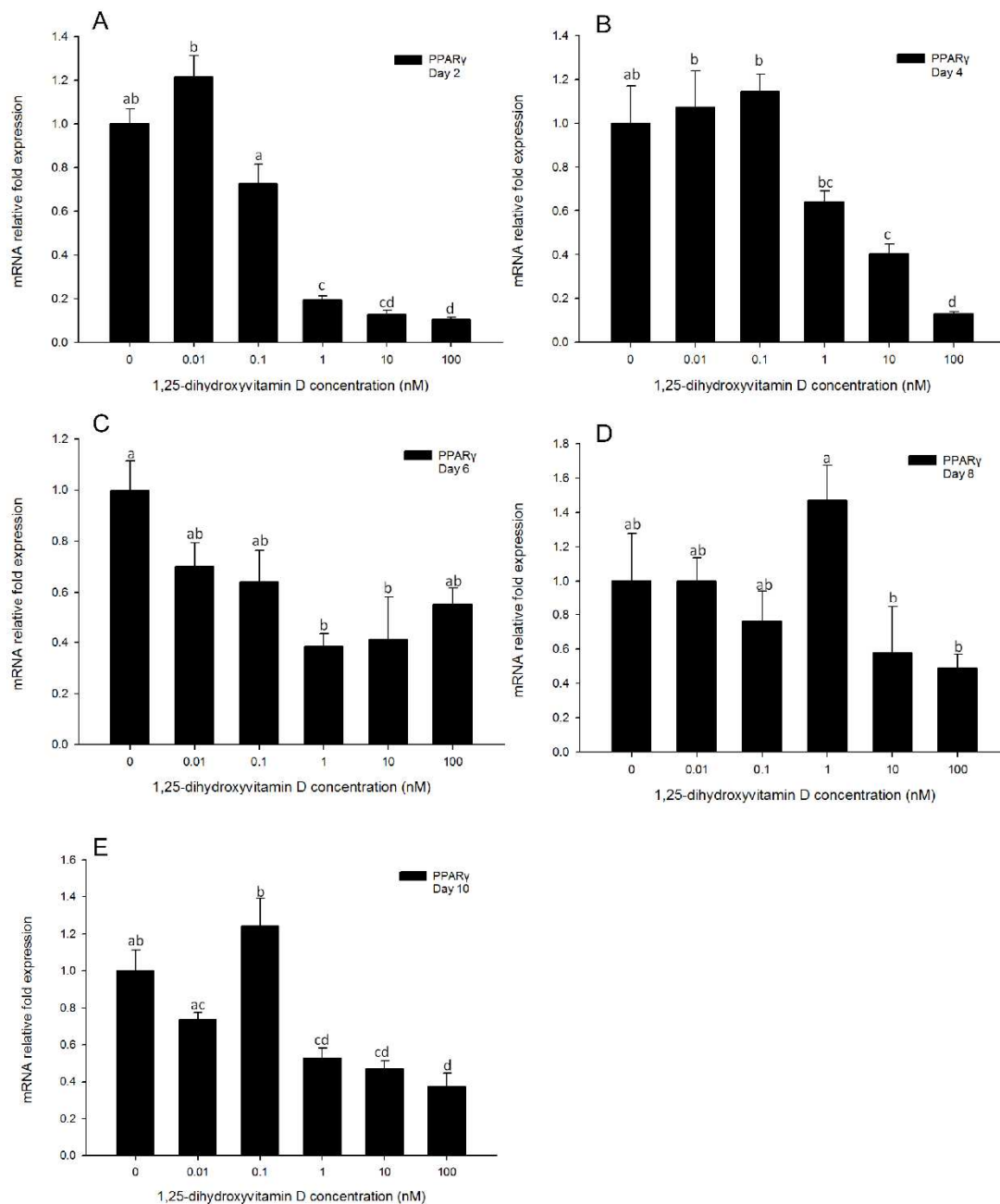


Figure 2.3 Real-time PCR quantification of PPAR γ gene expression in 3T3-L1 cells on days 2 (A), 4 (B), 6 (C), 8 (D) and 10 (E). Cells were treated with DM in the presence or absence of 0.01, 0.1, 1, 10, and 100 nM 1, 25 - (OH) $_2$ D $_3$ and *EEF2* was used as endogenous control (Δ Ct). Data were normalized to PPAR γ gene expression of the positive control (DM)

at the corresponding time point ($\Delta\Delta\text{Ct}$). Data are means \pm SE ($n = 3$). Different letters represent treatment effects that were significantly different ($P < 0.05$).

To confirm the real-time PCR results, Western blots also were performed on whole cell lysates following treatment with 100 or 1 nM of 1, 25 - (OH)₂D₃ at all the time points. Basal growth medium (GM) and differentiation medium (DM) served as negative and positive controls, respectively. PPAR γ protein levels were inhibited by 1, 25 - (OH)₂D₃ at 6 h (S2.1A Fig.), but thereafter the PPAR γ protein levels were high in the 100 nM 1, 25 - (OH)₂D₃ treated groups, but remained low in DM only groups from 12 h to day 4 (S2.1B-E Fig.). On day 8, both the 1, 25 - (OH)₂D₃ treated groups and DM only group had high PPAR γ protein level (S2.1G Fig.), and on day 10, PPAR γ protein levels in both 100 and 1 nM of 1, 25 - (OH)₂D₃ treatment groups decreased to levels similar to the GM only treatment. However, in the DM only group, PPAR γ protein level still remained relatively high (S2.1H Fig.). This suggests that 1, 25 - (OH)₂D₃ treatments inhibit PPAR γ protein levels only at the early time point, 6 h, and again at the late time point, day 10. At the other time points, since the whole cell lysates were used for Western blots measurement, and the 1, 25 - (OH)₂D₃ treated group had higher PPAR γ protein level than the DM only group, suggesting that the inhibitory efficacy of 1, 25 - (OH)₂D₃ on adipogenesis may function at the level of blocking PPAR γ protein trafficking to nucleus.

Gene expression of C/EBP α is inhibited by high concentrations of 1, 25 - (OH) $_2$ D $_3$

Both C/EBP α mRNA expression and protein level were measured in DM only treatments as a reference to help understand regulation of this gene in adipocyte differentiation (Fig. 2.4). Gene expression of C/EBP α was increased from days 2 to 10, and reached the maximum at day 8 (Fig. 2.4A), however, total cell protein levels of C/EBP α did not change significantly from 0 h to day 10 (Fig. 2.4B), and appeared to remain at relatively high levels throughout the test period.

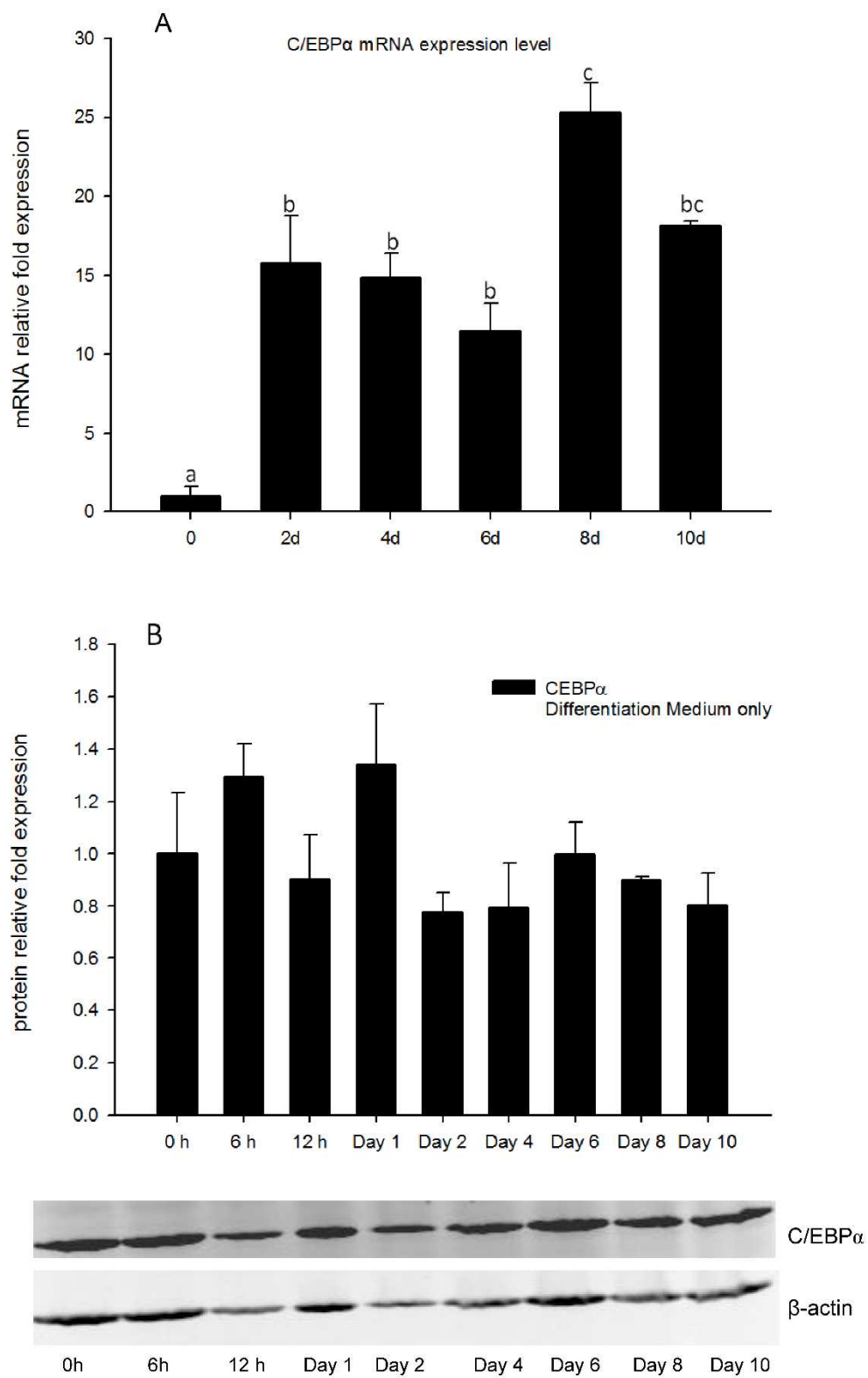


Figure 2.4 (A) Real-time PCR quantification of *C/EBP α* gene expression in DM treatment of 3T3-L1 cells on days 0, 2, 4, 6, 8, and 10 with *EEF2* used as endogenous control (Δ Ct). Data were normalized to *C/EBP α* gene expression of the day 0 group ($\Delta\Delta$ Ct). **(B) Image showing Western blot analysis** (Odyssey® Dual Infrared Imaging System (Li-Cor)) of *C/EBP α* on 0, 6, and 12 h, days 1, 2, 4, 6, 8 and 10. β -actin was used as an internal protein loading control. Quantification of *C/EBP α* was normalized to β -actin. Data are means \pm SE (n = 3). Different letters represent treatment effects that were significantly different ($P < 0.05$).

Similarly to *PPAR γ* , no significant changes in *C/EBP α* gene expression levels were observed in the cells treated with low concentrations (0.01 and 0.1 nM) of 1, 25 - (OH)₂D₃ as compared to the positive control cells at all time-points measured. (Fig. 2.5). Cells treated with high concentrations (100, 10, and 1 nM) of 1, 25 - (OH)₂D₃ showed significant inhibition of *C/EBP α* expression as compared to the positive control for days 2 and 4 (Fig. 2.5A-B). Similarly to *PPAR γ* expression, *C/EBP α* gene expression levels showed no significant difference between treatments groups on day 6 (Fig. 2.5C). The inhibitory efficacy of 1, 25 - (OH)₂D₃ was significant on days 8 and 10 in 1, 25 - (OH)₂D₃ treatment groups compared to DM only group (Fig. 2.5D-E). This suggests that similarly to regulation of *PPAR γ* expression, that 1, 25 - (OH)₂D₃ treatments had significant inhibitory effects on *C/EBP α* gene transcription, and this efficacy lasted until day 10.

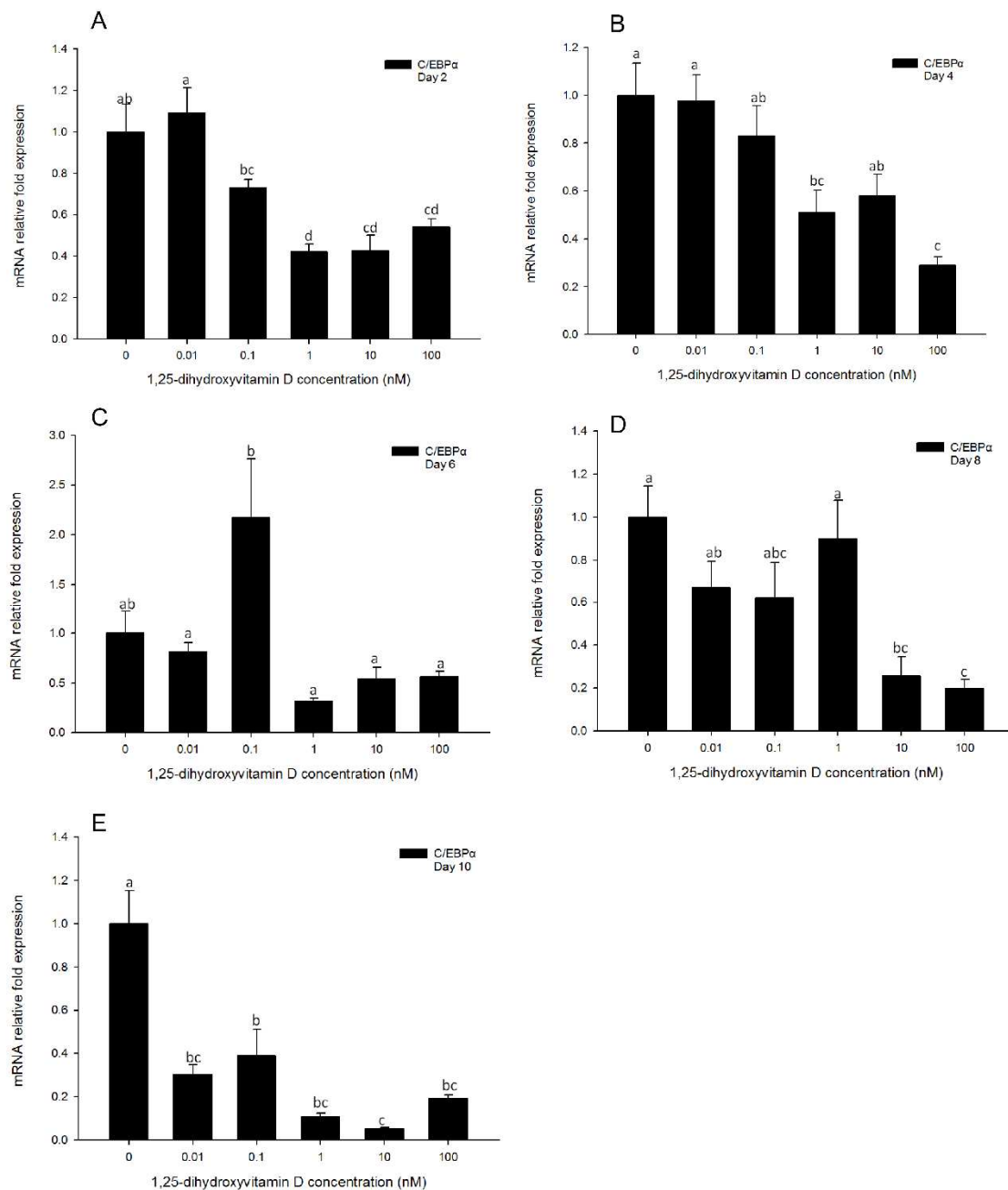


Figure 2.5 Real-time PCR quantification of *C/EBP α* gene expression in 3T3-L1 cells on days 2 (A), 4 (B), 6 (C), 8 (D) and 10 (E). Cells were treated with DM in the presence or absence of 0.01, 0.1, 1, 10, and 100 nM 1, 25 - (OH) $_2$ D $_3$ and *EEF2* was used as endogenous control (Δ Ct). Data were normalized to *C/EBP α* gene expression of positive control (DM)

at the corresponding time point ($\Delta\Delta C_t$). Data are means \pm SE ($n = 3$). Different letters represent treatment effects that were significantly different ($P < 0.05$).

Total cell protein levels of C/EBP α were also determined (S2.2 Fig.). In the early time points (6 and 12 h), C/EBP α protein levels were not changed in the 1, 25 - (OH) $_2$ D $_3$ treatment groups and DM only group compared to negative control (S2.2A-B Fig.). Furthermore, there were no significant differences in C/EBP α protein levels compared to DM only group to 1, 25 - (OH) $_2$ D $_3$ treated groups at all the time points, suggesting that total cellular C/EBP α protein levels were not influenced by 1, 25 - (OH) $_2$ D $_3$ treatment.

In the early time points, Vitamin D receptor gene expression is inhibited by high concentrations of 1, 25 - (OH) $_2$ D $_3$

To better understand the expression pattern of vitamin D receptor, VDR mRNA expression were quantified from 0 h to day 10 in DM only treatments (Fig. 2.6A). Gene expression of *VDR* increased from 6 h, and reached the maximum at 12 h, and then decreased after 24 h. This results showed that VDR was induced in the early time points of adipocyte differentiation process, suggesting it may play an important role in inhibition of adipocyte differentiation by 1, 25 - (OH) $_2$ D $_3$.

VDR gene expression was also determined with 1, 25 - (OH) $_2$ D $_3$ treatments on 6, 12 h, and day 1, 2, 4, 6, 8, 10. On 6 and 12 h (Fig. 2.6B-C), *VDR* gene expression was only inhibited in cells treated with the highest concentration (100 nM) of 1, 25 - (OH) $_2$ D $_3$. Significant changes in *VDR* gene expression levels were observed in the cells treated with high concentrations (100, 10 and 1 nM) of 1, 25 - (OH) $_2$ D $_3$ as compared to the positive control

cells at day1, 2, and 4. (Fig. 2.6D-F). Cells treated with low concentrations of 1, 25 - (OH)₂D₃ showed no significant inhibition of *VDR* expression as compared to DM only group at all the time points except day 10 (Fig. 2.6B-I). On day 10, *VDR* expression was inhibited by 1, 25 - (OH)₂D₃ treatments in all the concentrations (Fig. 2.6I). These results suggests that similarly to regulation of *PPARγ* and *C/EBPα* expression, 1, 25 - (OH)₂D₃ treatments had significant inhibitory effects on *VDR* gene transcription, especially in the early time process (day1 and 2) of adipocyte differentiation.

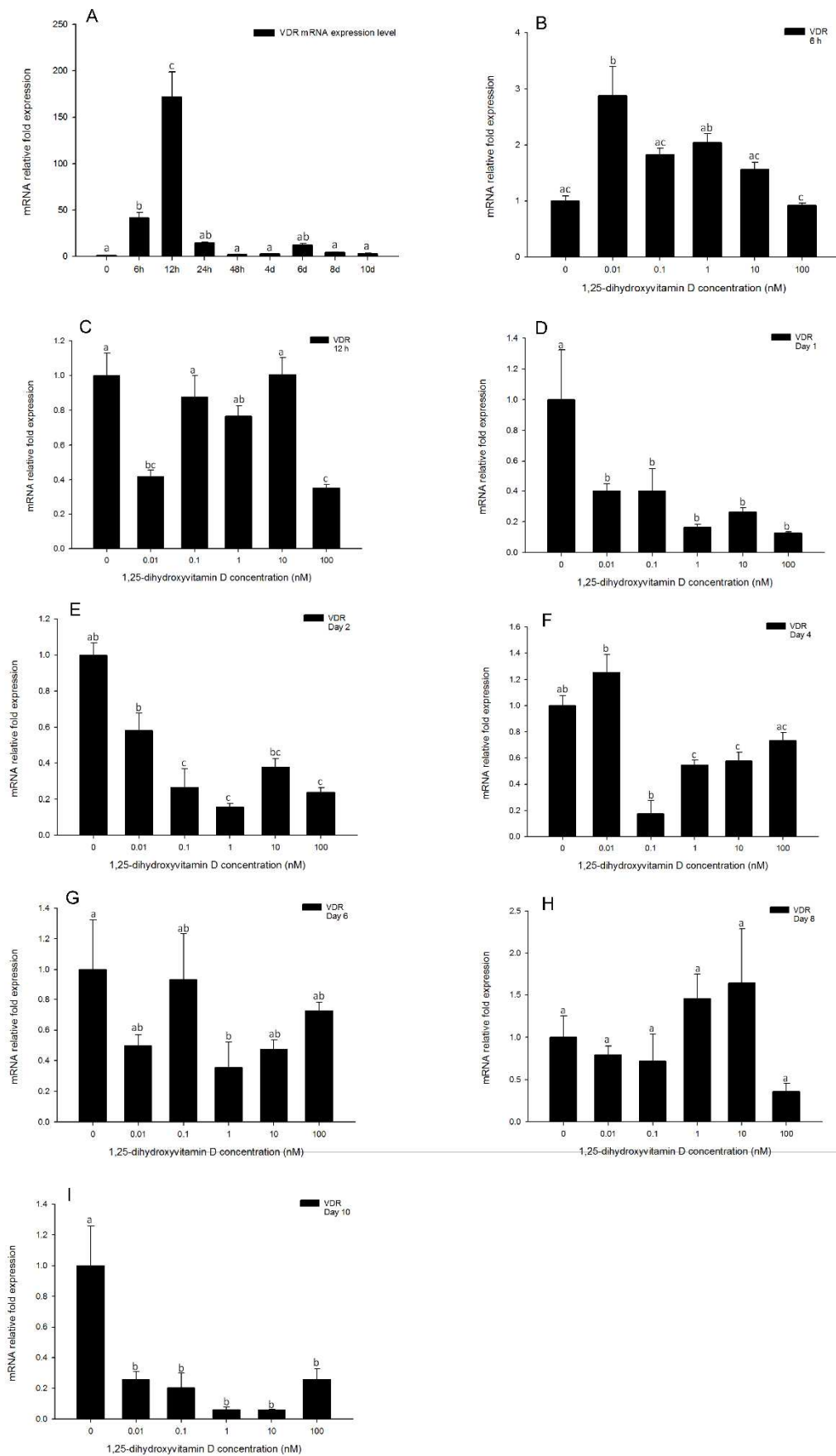


Figure 2.6 Real-time PCR quantification of VDR gene expression in 3T3-L1 cells (A): in the positive control treatment (DM) at 0, 6, and 12 h, and days 1, 2, 4, 6, 8, and 10. (B to I). Cells were treated with DM in the presence or absence of 0.01, 0.1, 1, 10, and 100 nM 1, 25 - (OH)₂D₃ and *EEF2* was used as endogenous control (Δ Ct). Data were normalized to *VDR* gene expression of the positive control (DM) at the corresponding time point ($\Delta\Delta$ Ct). (B) 6 h, (C) 12 h, (D) day 1, (E) day 2, (F) day 4 (G) day 6, (H) day 8 and (I) day 10. Data are means \pm SE (n = 3). Different letters represent treatment effects that were significantly different ($P < 0.05$).

There is no effect of 1, 25-Dihydroxyvitamin D treatment on C/EBP β gene expression levels

Gene expression levels of *C/EBP β* in the positive control (Fig. 2.7A) were increased after 6 h, and reached the highest expression level at 12 h, then decreased after day 2. Gene expression of *C/EBP β* was determined at 6, 12, 24 h and days 2, 4, 6, 8 10 by real-time PCR. Unlike *PPAR γ* and *C/EBP α* , *C/EBP β* gene expression level was not impacted by 1, 25 - (OH)₂D₃ compared to DM only group at any time points tested, up to day 10 (Fig. 2.7B-H), suggesting that 1, 25 - (OH)₂D₃ has no effect on *C/EBP β* gene expression levels. However, at day 10, the high concentrations (100, 10, and 1 nM) of 1, 25 - (OH)₂D₃ showed inhibitory effects on *C/EBP β* gene expression (Fig. 2.7I). On day 10, the expression level of *C/EBP β* was very low (Fig. 2.7A). Despite its low expression level, 1, 25 - (OH)₂D₃ had a suppressive effect on *C/EBP β* expression at this time point.

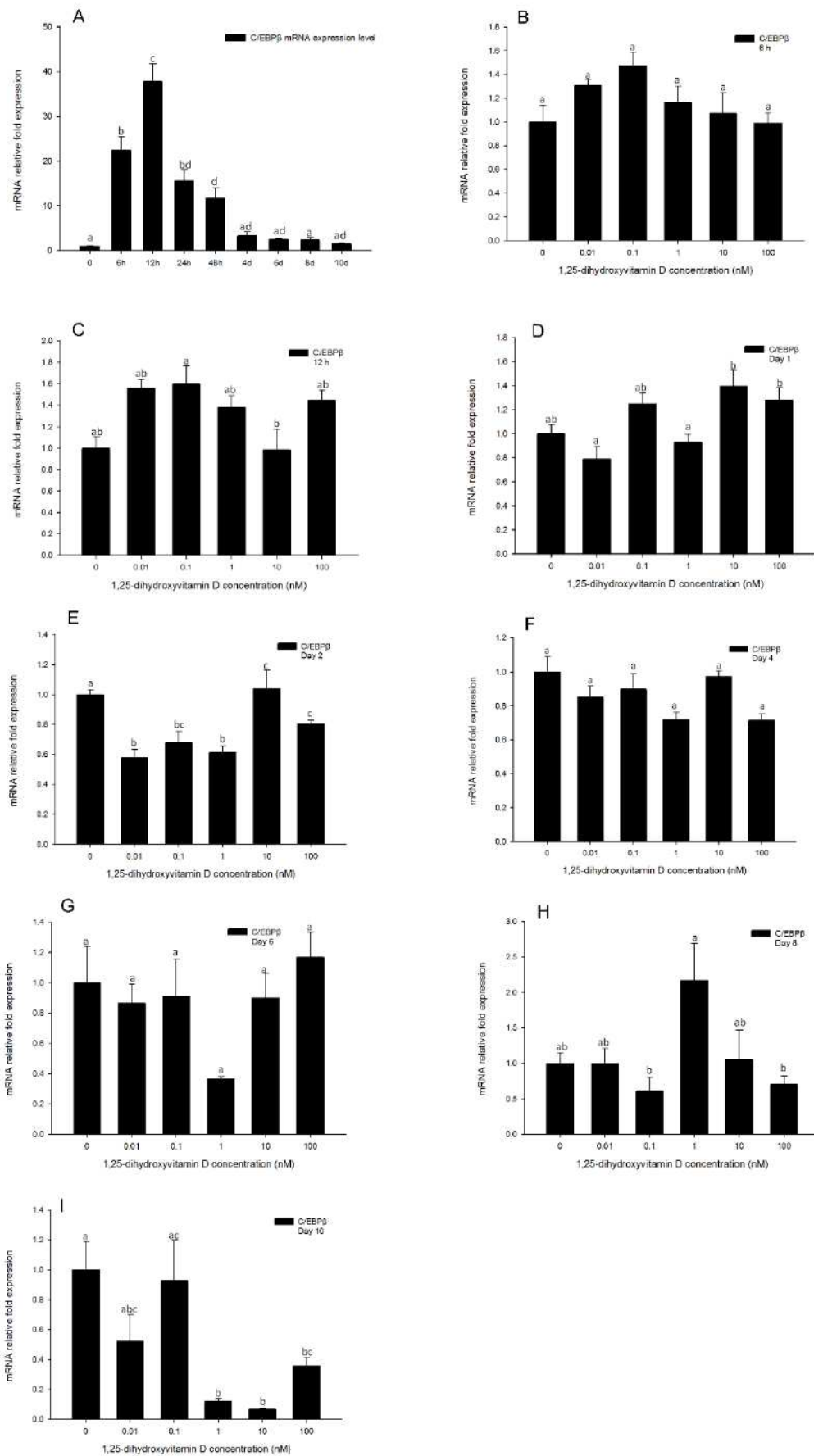


Figure 2.7 Real-time PCR quantification of *C/EBP β* gene expression in 3T3-L1 cells (A): in the positive control treatment (DM) at 0, 6, and 12 h, and days 1, 2, 4, 6, 8, and 10. (B to I). Cells were treated with DM in the presence or absence of 0.01, 0.1, 1, 10, and 100 nM 1, 25 - (OH)₂D₃ and *EEF2* was used as endogenous control (Δ Ct). Data were normalized to *C/EBP β* gene expression of the positive control (DM) at the corresponding time point ($\Delta\Delta$ Ct). (B) 6 h, (C) 12 h, (D) day 1, (E) day 2, (F) day 4 (G) day 6, (H) day 8 and (I) day 10. Data are means \pm SE (n = 3). Different letters represent treatment effects that were significantly different ($P < 0.05$).

***C/EBP δ* gene expression was not changed in response to 1, 25 - (OH)₂D₃ treatments**

This member of the C/EBP family of transcription factors is induced in the early process of adipogenesis. Thus we quantified its gene expression levels at 6, 12, and 24 h, and continued to monitor its expression through days 2, 4, 6, 8, and 10. Similarly to *C/EBP β* , *C/EBP δ* gene expression levels of 1, 25 - (OH)₂D₃ treated cells were generally not inhibited compared to the DM only treated group (Fig. 2.8B-I), even at the highest concentration of 1, 25 - (OH)₂D₃. This suggests that the inhibitory efficacy of 1, 25 - (OH)₂D₃ in adipogenesis does not impact the expression of *C/EBP δ* . Analysis of *C/EBP δ* gene expression in the positive control during adipocyte differentiation indicated that it is increased after 6 h, reaching the highest point at 12 h, and then decreases after 24 h (Figure 8A). Interestingly, the expression level of *C/EBP δ* was again increased after day 8, and reached a similar high expression level compared to 12 h on day 10 (Fig. 2.8A). This suggests that the *C/EBP δ* gene may not only be induced and have a role in the early process of adipogenesis, but may also have a role in the latter stages of adipogenesis.

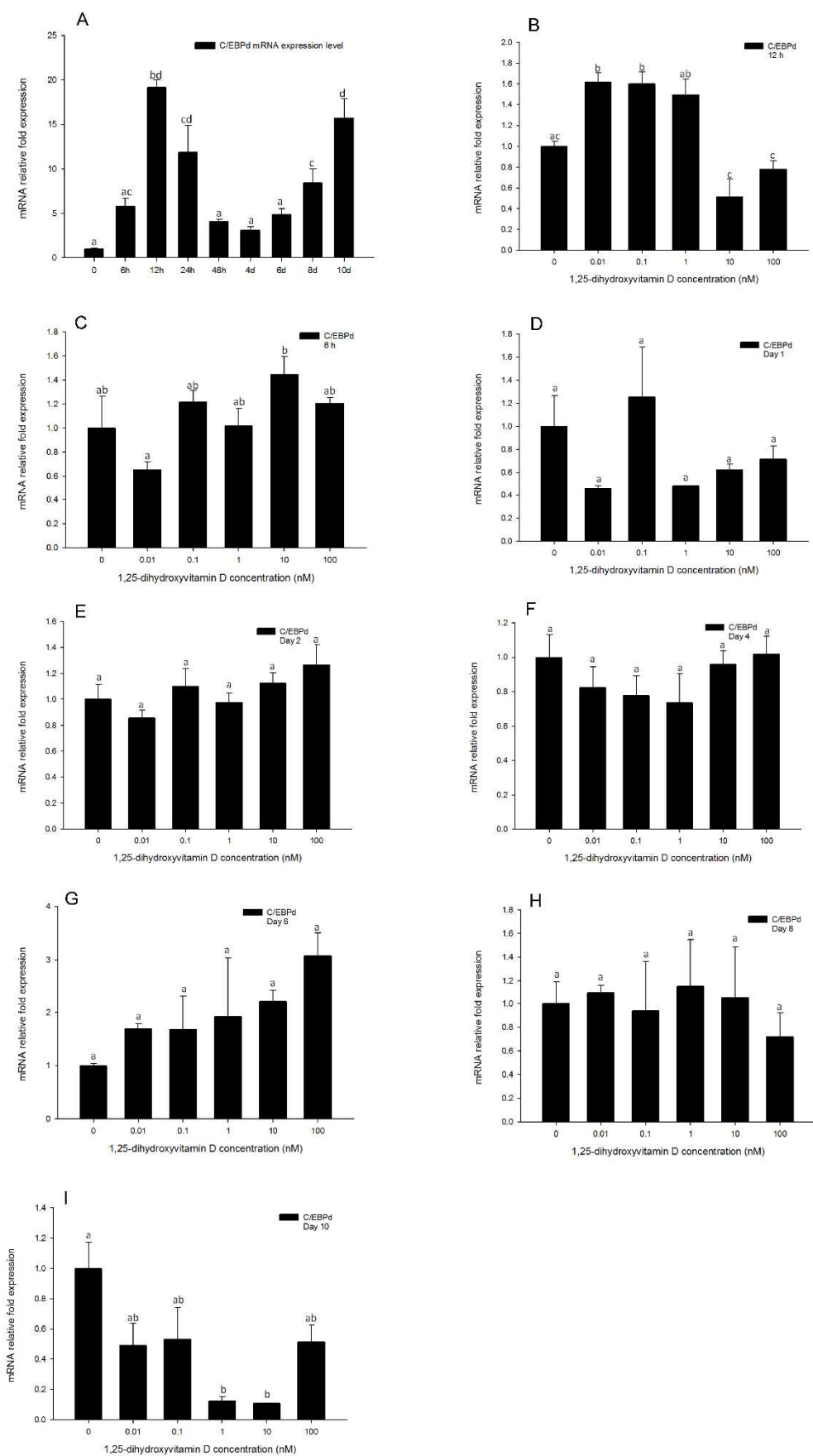


Figure 2.8 Real-time PCR quantification of *C/EBP δ* gene expression in 3T3-L1 cells (A): in the positive control treatment (DM) at 0, 6, and 12 h, and days 1, 2, 4, 6, 8, and 10. (B to I). Cells were treated with DM in the presence or absence of 0.01, 0.1, 1, 10, and 100 nM 1, 25 - (OH)₂D₃ and *EEF2* was used as endogenous control (Δ Ct). Data were normalized to *C/EBP δ* gene expression of the positive control (DM) at the corresponding time point ($\Delta\Delta$ Ct). (B) 6 h, (C) 12 h, (D) day 1, (E) day 2, (F) day 4 (G) day 6, (H) day 8 and (I) day 10. Data are means \pm SE (n = 3). Different letters represent treatment effects that were significantly different ($P < 0.05$).

Gene expression of FABP4 is highly responsive to 1, 25 - (OH)₂D₃ treatments

In the positive control treatments, the expression pattern of *FABP4* was similar to that of *PPAR γ* , increasing after day 2, and reaching the highest expression levels on day 8 but declining to similar levels to day 6 by day 10 (Fig. 2.9F). Gene expression of *FABP4* was strongly inhibited by high concentrations (100, 10, and 1 nM) of 1, 25 - (OH)₂D₃ treatments at all the time points (Fig. 2.9). Moreover, unlike *PPAR γ* and *C/EBP α* expression levels, *FABP4* gene expression levels in response to 0.1 nM 1, 25 - (OH)₂D₃ were also significantly inhibited compared to the positive control at all time-points (Fig. 2.9). The lowest concentration of 1, 25 - (OH)₂D₃ (0.01nM) treatments had no effect on *FABP4* gene expression on days 2 and 4 compared to the DM only group (Fig. 2.9B-C). However, on day 6, even the lowest concentration of 1, 25 - (OH)₂D₃ showed an inhibitory effect on *FABP4* gene expression (Fig. 2.9D). These effects were attenuated on days 8 and 10 (Fig. 2.9E-F).

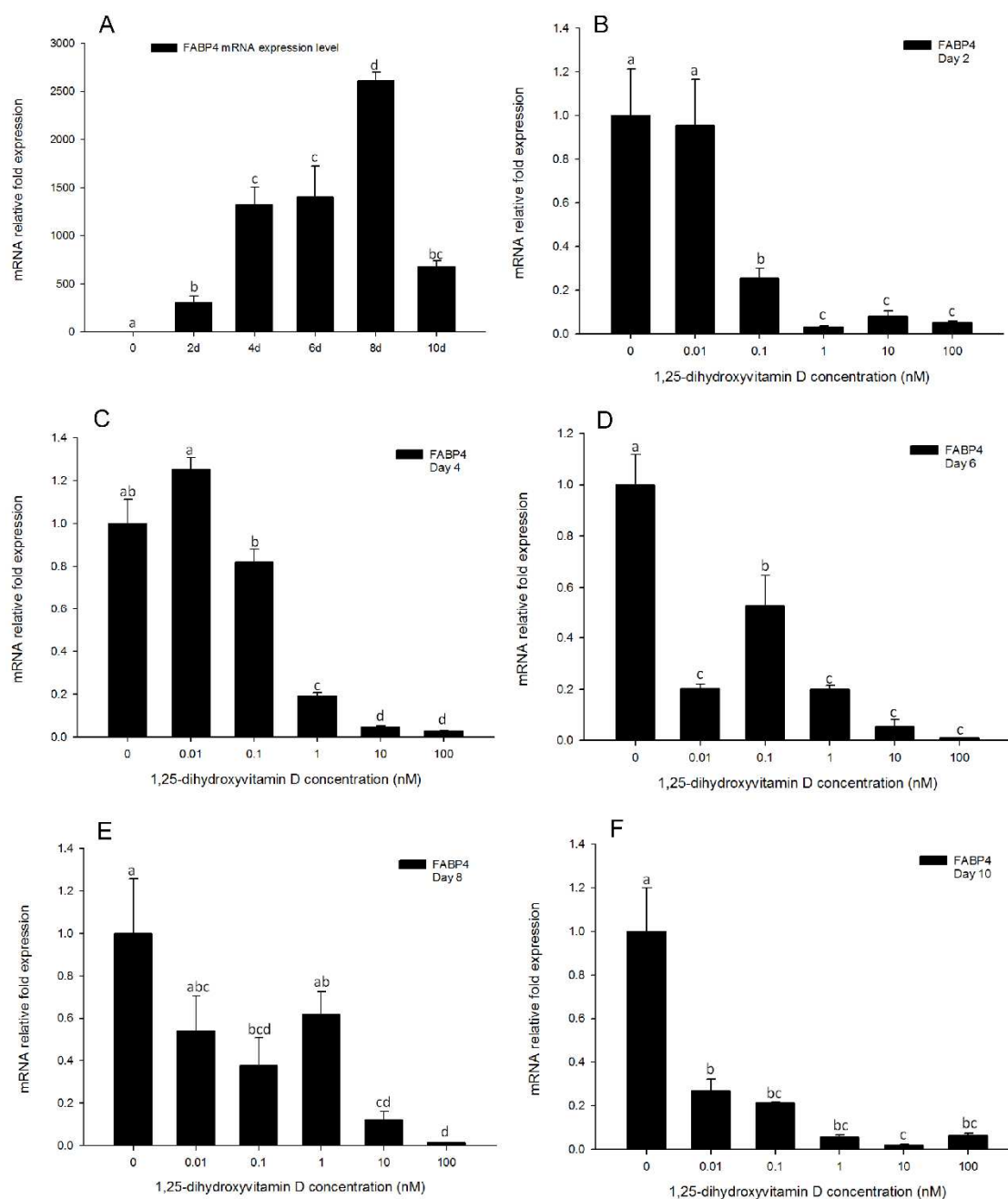


Figure 2.9 Real-time PCR quantification of FABP4 gene expression in 3T3-L1 cells (A): in the positive control treatment (DM) on days 0, 1, 2, 4, 6, 8, and 10 (B to F). Cells were treated with DM in the presence or absence of 0.01, 0.1, 1, 10, and 100 nM 1, 25 - (OH)₂D₃ and *EEF2* was used as endogenous control (Δ Ct). Data were normalized to *FABP4* gene

expression of the positive control (DM) at the corresponding time point ($\Delta\Delta\text{Ct}$). (B) day 2, (C) day 4 (D) day 6, (E) day 8 and (F) day 10. Data are means \pm SE (n = 3). Different letters represent treatment effects that were significantly different ($P < 0.05$).

Patterns of SREBP-1c expression resembled those of C/EBP β and C/EBP δ expression, but was fleetingly inhibited on day 2

The expression pattern of *SREBP-1c* in adipocyte differentiation showed that it was induced to the maximum expression level on day 2, and then decreased quickly from days 4 to 10 (Fig. 2.10A). Interestingly, on day 2, cells treated with 1, 25 - (OH) $_2$ D $_3$ (all concentrations tested, 100, 10, 1, 0.1 and 0.01 nM) showed significant inhibition of *SREBP-1c* gene expression as compared to the positive control (Fig. 2.10B). However, this effect was rapidly attenuated. Similarly to *C/EBP β* and *C/EBP δ* , *SREBP-1c* gene expression levels of 1, 25 - (OH) $_2$ D $_3$ treated cells were generally not different from the positive control from days 4 to 10 (Fig. 2.10C-F). The inhibitory effect of 1, 25 - (OH) $_2$ D $_3$ on day 2 coincides with the time point of maximum *SREBP-1c* expression (Fig. 2.10A), suggesting that 1, 25 - (OH) $_2$ D $_3$ only has an effect when *SREBP-1c* reached a high expression level. These results suggest that *SREBP-1c* may also play an important role in the 1, 25 - (OH) $_2$ D $_3$ modulation pathway, and may have interaction with 1, 25 - (OH) $_2$ D $_3$ during the early stages of adipogenesis.

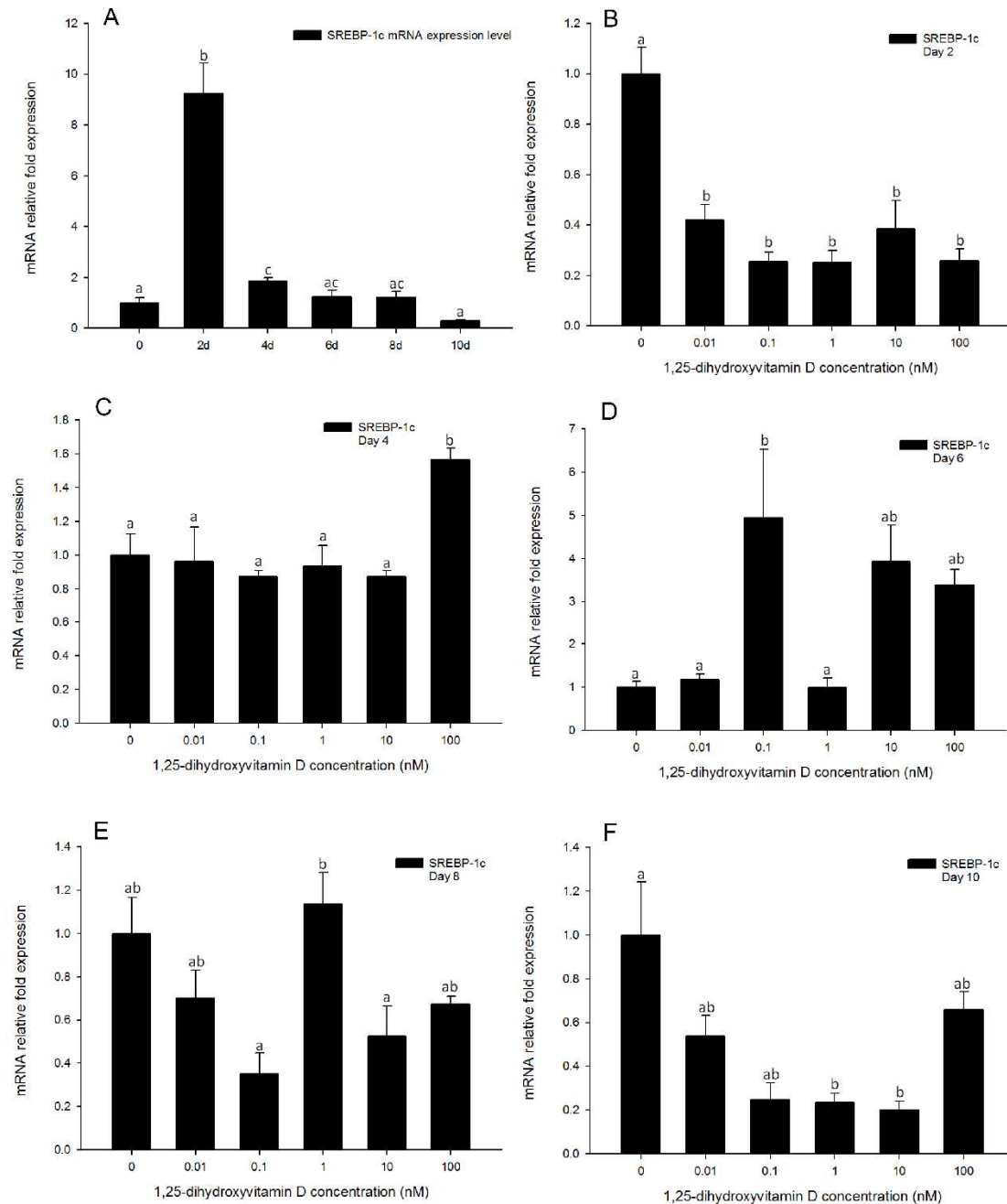


Figure 2.10 Real-time PCR quantification of SREBP-1c gene expression in 3T3-L1 cells

(A): in the positive control treatment (DM) on days 0, 1, 2, 4, 6, 8, and 10 (B to F). Cells were treated with DM in the presence or absence of 0.01, 0.1, 1, 10, and 100 nM 1, 25 - (OH)₂D₃ and *EEF2* was used as endogenous control (Δ Ct). Data were normalized to

SREBP-1c gene expression of the positive control (DM) at the corresponding time point ($\Delta\Delta Ct$). (B) day 2, (C) day 4 (D) day 6, (E) day 8 and (F) day 10. Data are means \pm SE (n = 3). Different letters represent treatment effects that were significantly different ($P < 0.05$).

The inhibitory effect of 1, 25 - (OH)₂D₃ on SCD-1 gene expression levels was more gradual compared to PPAR γ , C/EBP α or FABP4 expression

For the positive control, the expression pattern of *SCD-1* in adipocyte differentiation process was similar to that of *PPAR γ* and *C/EBP α* . Expression of *SCD-1* was increased on day 2, and reached a maximum expression level on day 8, remaining relatively high on day 10 (Fig. 2.11A). The inhibition of *SCD-1* gene expression was induced by all concentrations of 1, 25 - (OH)₂D₃ on day 2 (Fig. 2.11B). However, its inhibitory effect at latter time points was more pronounced (Fig. 2.11C-F). Expression of *SCD-1* was inhibited by high concentrations (100, 10 and 1 nM) of 1, 25 - (OH)₂D₃ on day 4 (Fig. 2.11C), showing a 70% inhibition effect at this time point. This continued to day 6 (Fig. 2.11D), and reached a inhibition effect greater than 90% of the positive control, in all of the three high concentrations of 1, 25 - (OH)₂D₃ treatments. The efficacy of 1, 25 - (OH)₂D₃ was stronger after day 6, and all the five concentrations of 1, 25 - (OH)₂D₃ showed significant inhibition on days 8 and 10 (Fig. 2.11E-F). This suggests *SCD-1* is strongly responsive to 1, 25 - (OH)₂D₃, and may play an important role in the pathway of 1, 25 - (OH)₂D₃ regulation of adipogenesis.

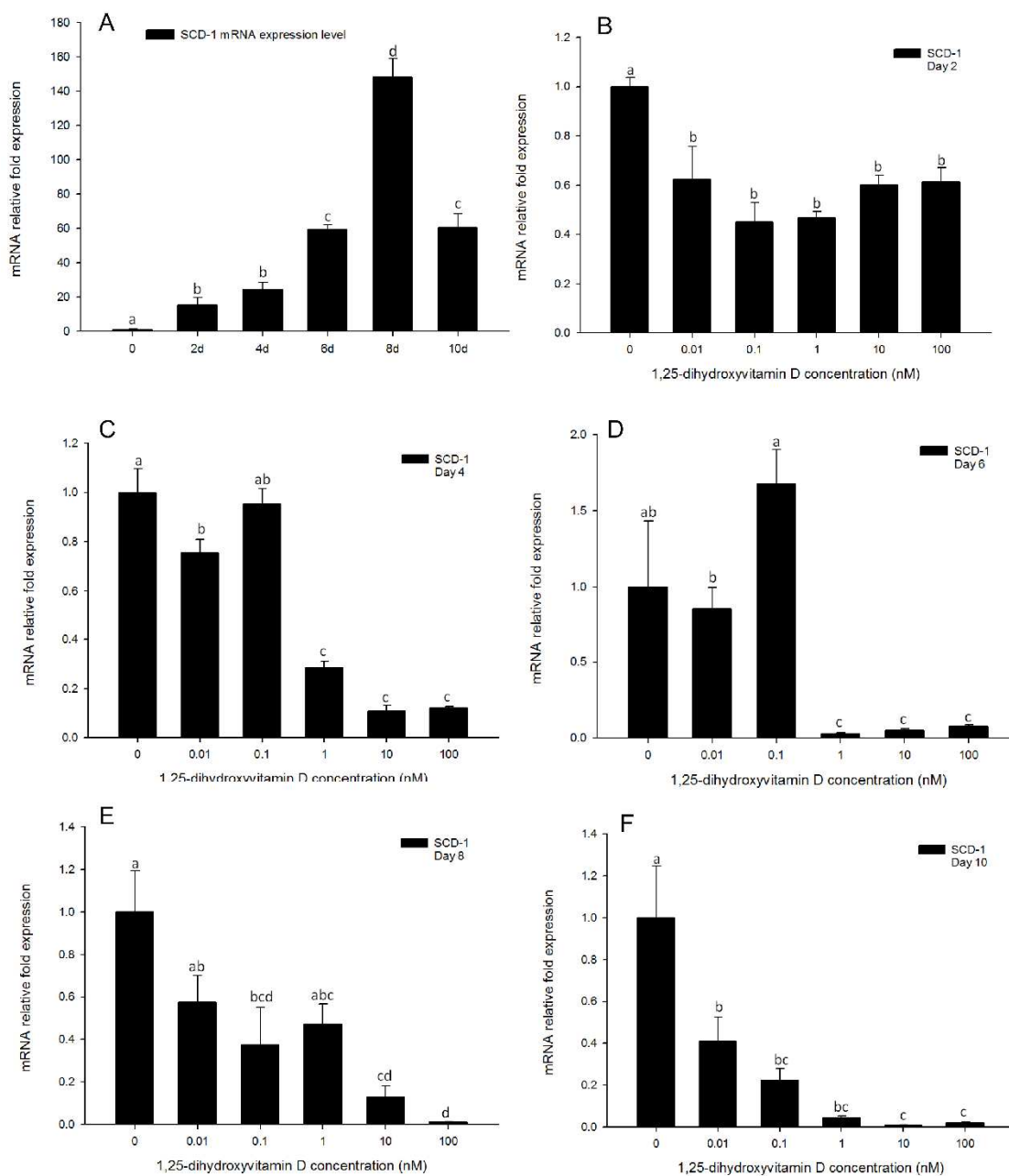


Figure 2.11 Real-time PCR quantification of SCD-1 gene expression in 3T3-L1 cells (A): in the positive control treatment (DM) on days 0, 1, 2, 4, 6, 8, and 10 (B to F). Cells were treated with DM in the presence or absence of 0.01, 0.1, 1, 10, and 100 nM 1,25-(OH)₂D₃ and *EEF2* was used as endogenous control (ΔCt). Data were normalized to SCD-

I gene expression of the positive control (DM) at the corresponding time point ($\Delta\Delta\text{Ct}$). (B) day 2, (C) day 4 (D) day 6, (E) day 8 and (F) day 10. Data are means \pm SE (n = 3). Different letters represent treatment effects that were significantly different ($P < 0.05$).

Gene expression of Pref-1 was altered in early time-points in response to high concentrations of 1, 25 - (OH)₂D₃

In the positive control, the expression pattern of *Pref-1* as expected was decreased by day 2, and remained so through until day 10 (Fig. 2.12A). Expression levels of *Pref-1* were not altered in any of the 1, 25 - (OH)₂D₃ treated cells on day 2 (Fig. 2.12B), values being similar to the positive control. Cells treated with high concentrations of 1, 25 - (OH)₂D₃ (100, 10, and 1 nM) showed a significant increase in *Pref-1* gene expression levels from days 4 to 6 (Fig. 2.12C-D), suggesting greater retention of the preadipocyte phenotype. By day 8, all effects from 1, 25 - (OH)₂D₃ treatments appeared to be attenuated, although the inhibitory effect was at least partially regenerated on day 10 (Fig. 2.12E-F). This results suggest that *Pref-1* expression responds to 1, 25 - (OH)₂D₃ in the latter stages of adipocyte differentiation, and may also plays a role in the pathways of 1, 25 - (OH)₂D₃ inhibited adipogenesis.

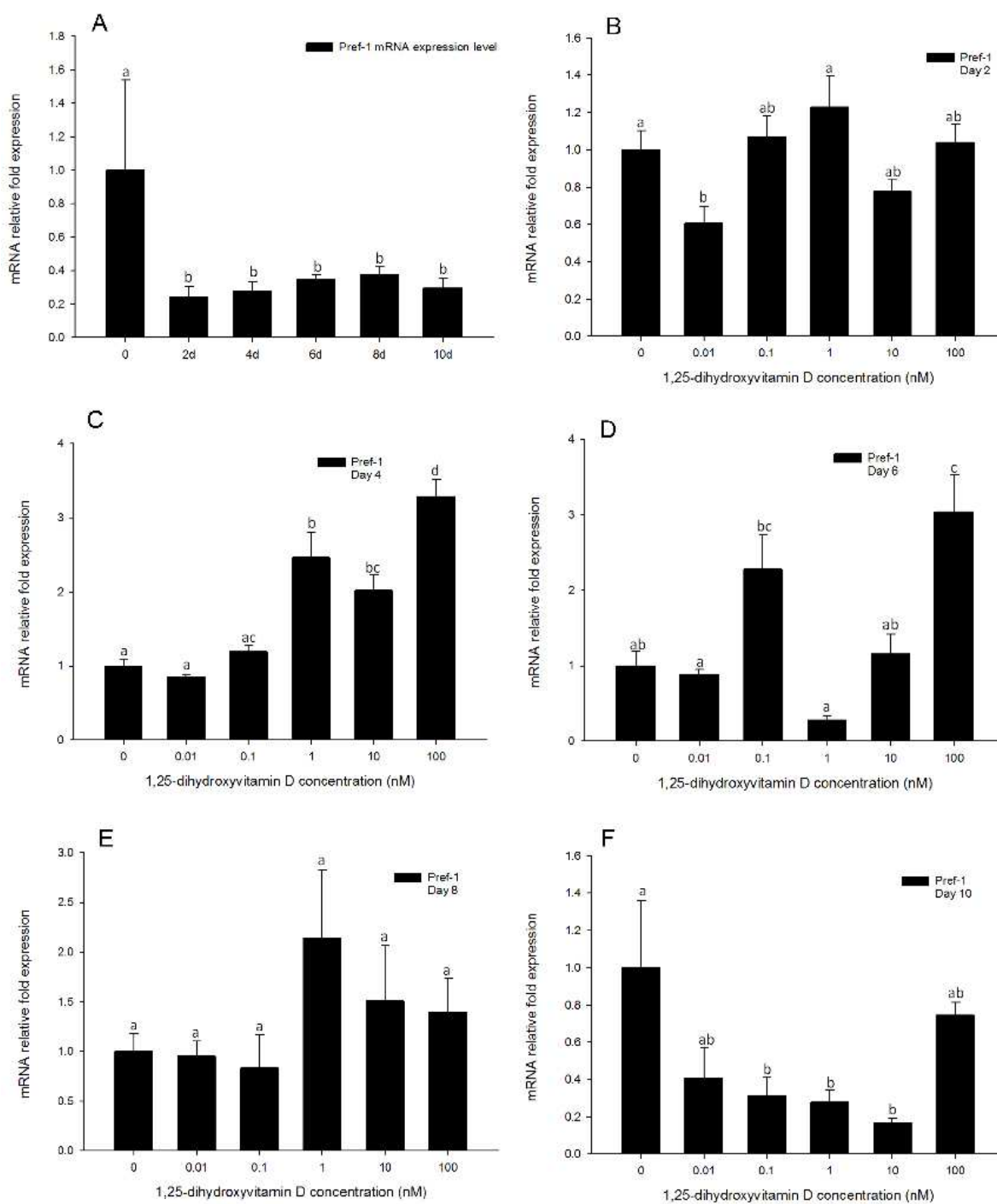


Figure 2.12 Real-time PCR quantification of Pref-1 gene expression in 3T3-L1 cells (A): in the positive control treatment (DM) on days 0, 1, 2, 4, 6, 8, and 10 (B to F). Cells were treated with DM in the presence or absence of 0.01, 0.1, 1, 10, and 100 nM 1, 25 - (OH)₂D₃

and *EEF2* was used as endogenous control (ΔCt). Data were normalized to *Pref-1* gene expression of the positive control (DM) at the corresponding time point ($\Delta\Delta\text{Ct}$). (B) day 2, (C) day 4 (D) day 6, (E) day 8 and (F) day 10. Data are means \pm SE (n = 3). Different letters represent treatment effects that were significantly different ($P < 0.05$).

Relative luciferase activity of C/EBP α promoter activity was not affected by 1, 25 - (OH)₂D₃ treatment

This study was conducted to investigate *C/EBP α* promoter activity in response to transient exposure of cells for 0, 12, 24 and 48 h to 100 nM 1, 25 - (OH)₂D₃ plus differentiation medium, differentiation medium only, and growth medium only. The data obtained with 1, 25 - (OH)₂D₃ treatment indicated no change *C/EBP α* promoter activity at any time points, 12, 24 and 48 h, compared to differentiation medium, suggesting no effects of 1, 25 - (OH)₂D₃ on *C/EBP α* promoter activity (Fig. 2.13) . The promoter activities of *C/EBP α* from cells treated with both differentiation medium and differentiation medium plus 1, 25 - (OH)₂D₃ were significantly higher than growth medium alone (Fig. 2.13), suggesting that the *C/EBP α* promoter is stimulated within the first 48 h of adipocyte differentiation.

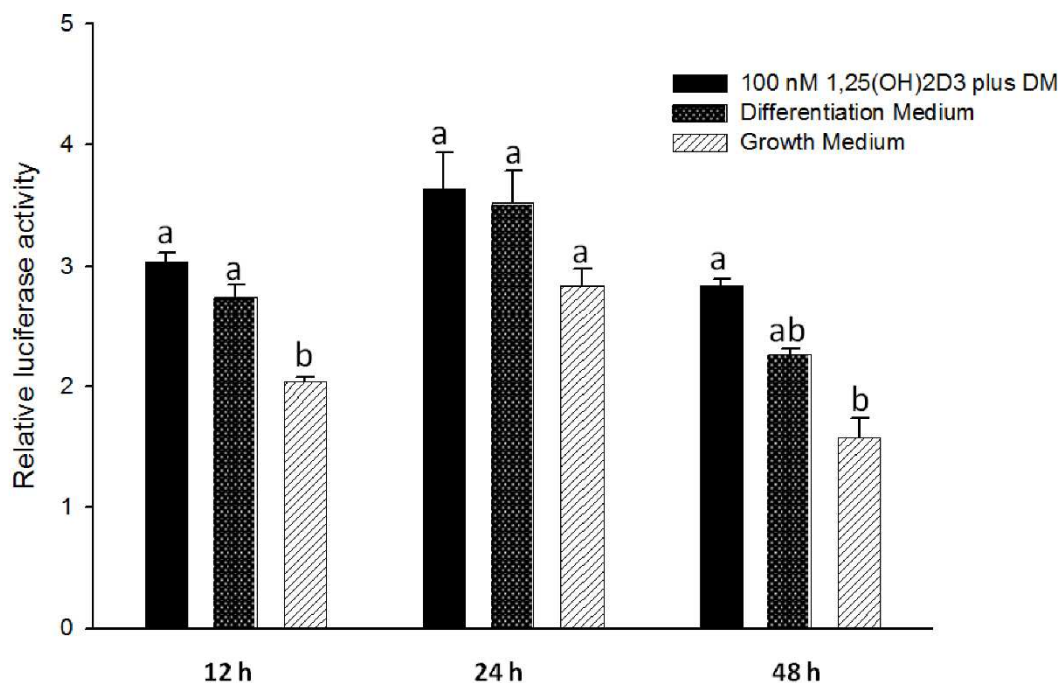


Figure 2.13 Mouse 3T3-L1 cells were transfected with pGL4.10 (*luc2/-500CEBPa*) in triplicate. Following incubation with differentiation medium only, growth medium only, or differentiation medium with 1, 25(OH)₂D₃ (100nM). Fire-fly and Renilla luciferase activity units were measured at 0, 12, 24 and 48 h. The firefly luciferase activity units were normalized to Renilla luciferase activity units. Data are normalized as fold activation relative to 0 h and shown as means ± SE (n = 3). Different letters represent treatment effects that were significantly different ($P < 0.05$) within each time-point.

Discussion

Although the inhibitory effect of 1, 25 - (OH)₂D₃ in adipogenesis has been reported for more than a decade, the molecular mechanisms underlying this inhibition remains unclear. To explore this important question, we have performed a systematic

investigation aimed at studying the molecular events during the adipocyte differentiation response to 1, 25 - (OH)₂D₃. The 3T3-L1 cell line is a major model used in developing understanding of adipocyte differentiation and key adipogenic gene expression. Our strategy was to take advantage of this well-defined adipogenic model and identify the molecular changes at each stage that resulted from 1, 25 - (OH)₂D₃ treatments. We report here that lipid accumulation and expression levels of adipogenic specific genes were inhibited in vitro by high concentrations (1, 10 and 100 nM) of 1, 25 - (OH)₂D₃ but not by lower concentrations (0.1 and 0.01 nM). As discussed in greater detail below, lipid accumulation was inhibited by the high concentrations of 1, 25 - (OH)₂D₃, at levels comparable to the negative control, by day 10. The lower concentrations of 1, 25 - (OH)₂D₃ have slight inhibitory effects on lipid accumulation compared to the positive control. Gene expression levels of *PPAR* γ , *C/EBP* α , *VDR*, *FABP4* and *SCD-1* were inhibited by the high concentrations of 1, 25 - (OH)₂D₃ throughout the experimental period to day 10. However, the lower concentrations of 1, 25 - (OH)₂D₃ had no inhibitory effect. Gene expression levels of *C/EBP* β and *C/EBP* δ were not affected by 1, 25 - (OH)₂D₃ treatments, at any of the concentrations tested. We also studied the effects of 1, 25 - (OH)₂D₃ on *C/EBP* α promoter activity. There appeared to be no inhibitory effect of 1, 25 - (OH)₂D₃ on the activity of the *C/EBP* α promoter. The present study has also provided a detailed temporal analysis of key adipogenic gene expression across time points from days 0 to 10 during the adipocyte differentiation process. These data demonstrate at least three important observations: 1) high concentrations of 1, 25 - (OH)₂D₃ have strongly inhibitory effects on adipogenesis, and this effects persist through day10, 2) not all of the key adipogenic

genes (e.g. *C/EBPβ* and *C/EBPδ*) interact with 1, 25 - (OH)₂D₃, and 3) the pathway of 1, 25 - (OH)₂D₃ mediated inhibition of adipogenesis does not appear to involve the *C/EBPα* promoter.

1, 25-Dihydroxyvitamin D₃ is an endocrine hormone that plays multiple physiological roles [21]. This secosteroid hormone is known to be critical for immune system function [22] and calcium and phosphate homeostasis [23,24]. 1, 25-Dihydroxyvitamin D₃ is also known to affect adipocyte differentiation and metabolism [25]. 1, 25-Dihydroxyvitamin D₃ is also the ligand of VDR, hence, VDR may play an important part in the inhibitory pathway of 1, 25 - (OH)₂D₃ in adipogenesis. The VDR has previously been reported to play an important role in the vitamin D signaling pathway in health and disease [25]. Kong and Li [26] found that VDR protein expression was very low in mouse 3T3-L1 preadipocytes, however, VDR expression increases dramatically by 4 h following treatment with adipogenic differentiation medium, and returns to baseline levels by day 2. 1, 25-Dihydroxyvitamin D₃ treatment was able to stabilize VDR expression for at least another day. The mechanism of VDR stabilization by 1, 25 - (OH)₂D₃ is currently not known. However, the observation of VDR expression in the early time points of adipogenesis may provide a short window for 1, 25 - (OH)₂D₃ to inhibit adipogenesis [13]. The role of the VDR in pre-adipocyte differentiation in 3T3-L1 cells was also studied by Blumberg et al [15]. Their studies reported that the mRNA levels of VDR increased to a maximum by 6 h following initiation of adipocyte differentiation, and the protein levels of VDR reached a maximum by 12 h in the nucleus, and then declined to baseline level by day 2. These

similar reports suggest that the inhibition of adipogenesis by 1, 25 - (OH)₂D₃ binding VDR may occur in the early time points (before day 2) during adipogenesis, however, the specific mechanism still remains unknown. In our studies, *VDR* gene expression pattern in adipocyte differentiation was measured from 0 h to day 10. The expression of *VDR* was induced after adipocyte differentiation initiated 6 h, and reached the maximum expression level at 12 h, then declined after 24 h, which is consistent with previous literature reports. *VDR* gene expression was also inhibited by 1, 25 - (OH)₂D₃ treatments in early time points. This suggests that *VDR* plays an important role in the inhibitory pathway of 1, 25 - (OH)₂D₃ regulating adipocyte differentiation.

The *C/EBP* family is a class of basic-leucine zipper transcription factors, and does not form homo-or hetero dimers. Furthermore, their tissue distribution is not limited to adipose tissue [27]. The gene expression of several *C/EBP* family members is known to be regulated during adipogenesis, and they have been shown to be regulators of adipocyte differentiation. Both *C/EBPβ* and *C/EBPδ* mRNA and protein levels were reported to rise early and transiently in preadipocytes which have been induced to differentiate [28-30]. In the present study, real-time PCR results confirmed that during adipogenesis, *C/EBPβ* mRNA expression levels began to rise by 6 h, and reached a maximum by 12 h following induction, then declined to baseline level after 24 h (Figure 2.7A). The mRNA expression levels of *C/EBPδ* also increased by 6 h, and reached the highest level at 12 h, then decreased after 24 h (Fig. 2.8A). These results are consistent with previous reports, and the timing of expression of these two genes was similar to VDR, suggesting that there may be an interaction between 1, 25 -

(OH)₂D₃ through VDR binding, inhibiting adipogenesis and *C/EBPβ* or *C/EBPδ* expression during early adipogenesis. Blumberg et al [15] reported that 1, 25 - (OH)₂D₃ treatment inhibited *C/EBPβ* mRNA expression level, however, *C/EBPδ* gene expression did not change in response to 1, 25 - (OH)₂D₃. Their studies indicate that after binding with VDR, 1, 25 - (OH)₂D₃ inhibits adipogenesis via inhibiting *C/EBPβ* gene expression but not *C/EBPδ*. In contrast, Kong and Li [26] reported that 1, 25 - (OH)₂D₃ treatments did not influence the gene expression of either *C/EBPβ* or *C/EBPδ* [27]. In the present study, we quantified gene expression levels of both *C/EBPβ* and *C/EBPδ* in response to 1, 25 - (OH)₂D₃ treatment, and our results are similar to those reported by Kong and Li [26]. From 6 h to 24 h, and days 2 to 10, gene expression levels of *C/EBPβ* and *C/EBPδ* were not changed by 1, 25 - (OH)₂D₃ treatments. These data demonstrate that even though the gene expression of these C/EBP family members is stimulated in early adipogenesis, corresponding to the maximum expression time of VDR, these two factors are not included in the pathway of 1, 25 - (OH)₂D₃ inhibited adipogenesis.

The *PPAR* family is a group of transcriptional factors belonging to the nuclear hormone receptor superfamily. These transcriptional factors heterodimerize with another nuclear hormone receptor, retinoid X receptor (RXR), bind to the response elements of target gene promoters and function as active transcriptional factors [31]. When PPARs are heterodimerized with RXR, the complex is activated and transported to the nucleus to bind to specific sequences in promoter regions (termed as *PPAR* response elements, PPREs) of downstream target genes, activating their transcription [6,32-33].

There are three major isoforms: *PPAR α* , *PPAR δ* , and *PPAR γ* [34]. The three isoforms have specific roles in lipid metabolism. Importantly, *PPAR γ* plays an important role in triglyceride synthesis and adipocyte differentiation [33]. Activation of *PPAR γ* expression occurs downstream of *C/EBP β* and *C/EBP δ* transcription during the cascade of adipogenesis, and upstream of *C/EBP α* . In the present study, gene expression of *PPAR γ* was highly inhibited by 1, 25 - (OH)₂D₃, from day 2 until day 10 (Fig. 3). Moreover, the cellular response of *C/EBP α* to 1, 25 - (OH)₂D₃ was similar to that of *PPAR γ* . The inhibition of 1, 25 - (OH)₂D₃ was persistent until day 10 (Figure 2.5). These data indicate that the 1, 25 - (OH)₂D₃ induced inhibition of adipogenesis in 3T3-L1 cells was associated with an inhibition of *PPAR γ* and *C/EBP α* gene expression.

To confirm these results, the protein levels of both *PPAR γ* and *C/EBP α* were measured using Western blot. Interestingly, the whole cell lysate from 1, 25 - (OH)₂D₃ plus DM treated cells had the highest *PPAR γ* protein level from 6 h to day 4, and the whole cell lysate from DM only treated cells had lower *PPAR γ* levels than the 1, 25 - (OH)₂D₃ treated cells, but comparable to growth medium treated cells. By day 6, the 1, 25 - (OH)₂D₃ plus DM treated cells and DM only treated cells had similar levels of *PPAR γ* protein, however, by day 10, DM only treated cells had the highest *PPAR γ* protein level, and *PPAR γ* protein level from 1, 25 - (OH)₂D₃ plus DM treated cells was decreased to the same level as growth medium only treated cells (S2.1 Fig.). Protein levels of *C/EBP α* in the whole cell lysate were not changed in response to 1, 25 - (OH)₂D₃ treatments on any of the time points in comparison to DM only treated cells (S2.2 Fig.), suggesting that *C/EBP α* protein was not influenced by 1, 25 - (OH)₂D₃

treatments. In previous studies by Blumberg et al [15], they reported the protein level of PPAR γ and C/EBP α was inhibited by 1, 25 - (OH) $_2$ D $_3$ treatments. However, these authors used the nuclear extracts to measure the protein level of these two transcriptional factors. In the present study, we used the whole cell lysate to measure the protein levels. These observations together suggest that regulation of PPAR γ effects are not directly mediated at transcriptional or translational levels. Rather, mediation occurs via regulation of PPAR γ activation and transport to the nucleus. Thus, we hypothesize that 1, 25 - (OH) $_2$ D $_3$ treatments block the trafficking of PPAR γ from the cytoplasm to the nucleus. Thus, PPAR γ protein is not transferred into nucleus preventing activation of downstream target genes in adipogenesis. In contrast, without 1, 25 - (OH) $_2$ D $_3$ treatment, the PPAR γ protein in the DM only treated cells was readily transported into the nucleus, and functioned as transcriptional factor, inducing the downstream genes (e.g. C/EBP α , FABP4). Therefore, the protein level of PPAR γ in DM only treated cells was lower compared to 1, 25 - (OH) $_2$ D $_3$ treated cells. The protein levels of PPAR γ and C/EBP α in DM only treated cells were measured from 0, 6, and 12 h to days 1, 2, 4, 6, 8, and 10. The protein levels of PPAR γ were consistent with mRNA expression levels quantified by real-time PCR. Interestingly, unlike PPAR γ , the protein levels of C/EBP α were only slightly changed throughout the experimental time points. We hypothesize that this may be because the C/EBP α protein has longer half-life than PPAR γ or is accumulated in the cytoplasm before adipogenesis is initiated. The activity of the C/EBP α promoter was also measured using the Dual Reporter Luciferase Assay System (Promega, Madison, WI). Relative luciferase activity data showed that the activity of C/EBP α promoter appeared to be unchanged

in response to 1, 25 - (OH)₂D₃ treatments. These intriguing data demonstrate that 1, 25 - (OH)₂D₃ treatments inhibit adipogenesis via inhibiting *PPAR* γ and *C/EBP* α gene expression, and that *PPAR* γ may play a more important role in this pathway in comparison to *C/EBP* α . Further studies are needed to explore the mechanism of *PPAR* γ interaction with 1, 25 - (OH)₂D₃ in its inhibition of adipogenesis.

In the present study, *SREBP-1c* gene expression was only inhibited by 1, 25 - (OH)₂D₃ treatments on day 2, coinciding with its maximum expression level in the positive control treatment. Both the high (100, 10, and 1 nM) and low (0.1 and 0.01 nM) concentrations of 1, 25 - (OH)₂D₃ inhibited *SREBP-1c* gene expression on day 2 (Fig. 2.10B). However, from days 4 to 10, the inhibitory effects were ameliorated, and the expression of *SREBP-1c* was not changed in response to 1, 25 - (OH)₂D₃ treatments, at any of the concentrations tested (Fig. 2.10C-F). These data indicate that the inhibition of *SREBP-1c* gene expression by 1, 25 - (OH)₂D₃ treatment was transient and corresponded with the d 2 time point, in which its expression rose, 10-fold in the positive control in comparison to the time-point at d 0. Thus, it is not clear whether *SREBP-1c* may be involved in the 1, 25 - (OH)₂D₃ signaling pathway that inhibits adipogenesis, showing a similar gene expression profile to *C/EBP* β and also reflecting the profile observed for *C/EBP* δ at time-points up to d 6. These three genes are upstream of *PPAR* γ in the transcriptional activation of adipogenesis, hence, the inhibition of adipogenesis caused by 1, 25 - (OH)₂D₃ may be unrelated to mechanisms involving the transcriptional factors that are expressed in the early stages of adipogenesis.

In addition to *PPAR* γ and *C/EBP* α , gene expression levels of *FABP4* and *SCD-1* were strongly inhibited by 1, 25 - (OH) $_2$ D $_3$ treatments. Gene expression of *FABP4* was strongly inhibited by the high concentrations (100, 10 and 1 nM) of 1, 25 - (OH) $_2$ D $_3$ treatments from days 2 to 4 (Fig. 2.9B-C). Moreover, from days 6 to 10, all the concentrations of 1, 25 - (OH) $_2$ D $_3$ had significant inhibitory effects on *FABP4* gene expression (Fig. 2.9D-F). The inhibitory effects of 1, 25 - (OH) $_2$ D $_3$ treatments on *SCD-1* gene expression were gradual in comparison to effects on *FABP4* expression. Inhibition by high concentrations of 1, 25 - (OH) $_2$ D $_3$ began by day 4 (Fig. 2.10C), and remained until day 8 (Fig. 2.11D-E). However, by day 10, gene expression of *SCD-1* was inhibited by all concentrations of 1, 25 - (OH) $_2$ D $_3$ tested (Fig. 2.11F), and comparable to effects on *FABP4*. In previous reports, *FABP4* has been shown to have a *PPAR* γ response element (PPRE) in its promoter region and *PPAR* γ regulates gene expression of *FABP4* [32,35]. In 1, 25 - (OH) $_2$ D $_3$ treated cells, *PPAR* γ expression was significantly inhibited, and this effect also appeared to cause a negative action on gene expression of *FABP4*. Similarly to *FABP4*, *SCD-1* also plays an important role in adipogenesis. Its functions include incorporation of double bonds in fatty acids and synthesis of long chain fatty acids in adipocytes [36]. In the present study, *SCD-1* expression was gradually increased from days 2 to 10 with DM treatment, and significantly inhibited by 1, 25 - (OH) $_2$ D $_3$ treatments, suggesting that *SCD-1* may play a role in the pathway of 1, 25 - (OH) $_2$ D $_3$ inhibited adipogenesis. Mechanisms of *FABP4* and *SCD-1* gene expression in response to 1, 25 - (OH) $_2$ D $_3$ still need to be explored further.

Preadipocyte factor 1 is a marker protein of preadipocytes and is not expressed in mature adipocytes [37]. During initiation of adipogenesis, the gene expression of *Pref-1* decreases and the expression of key adipogenic genes increases [38]. We hypothesized that gene expression of *Pref-1* would decrease in treatments with differentiation medium, and would remain at higher levels in treatments with 1, 25 - (OH)₂D₃ when compared to in DM treated cells. In the present study, *Pref-1* gene expression was significantly lower compared to that of day 4, DM only treated cells, and remained at low levels through day 10 (Fig. 2.12A). In the cells treated with 1, 25 - (OH)₂D₃, *Pref-1* gene expression was significantly higher than in DM only treated cells by day 6 (Fig. 2.12B-F), and declined to similar levels to the DM only group from days 8 to 10 (Fig. 2.12E-F). These data support our hypothesis, and in the 1, 25 - (OH)₂D₃ treatments where *PPAR*γ, *C/EBP*α, *FABP4* and *SCD-1* gene expression levels were inhibited, the expression of *Pref-1* gene correspondingly remained significantly higher than in DM only treatments.

In conclusion, lipid accumulation and the expression of key adipogenic key genes, *PPAR*γ, *C/EBP*α, *FABP4*, and *SCD-1* were significantly inhibited by 1, 25 - (OH)₂D₃ treatments until day 10. Gene expression of *SREBP-1c* was transiently inhibited by 1, 25 - (OH)₂D₃ on day 2, and then rebounded back to levels similar to the low levels observed in DM treatment by days 4, 6, 8, and 10. In contrast, *C/EBP* β and *C/EBP* δ expression were not changed in response to 1, 25 - (OH)₂D₃ treatments. Our study has demonstrated that 1, 25 - (OH)₂D₃ represses adipogenesis via inhibition of the expression of *PPAR*γ, but not *C/EBP* β or *C/EBP* δ, and hence, the adipogenic-specific

genes (*C/EBP α* , *FABP4*, and *SCD-1*) downstream of *PPAR γ* during the transcriptional cascade of adipogenesis, were also inhibited. In future, studies are needed to explore the mechanisms by which 1, 25 - (OH)₂D₃ interacts with *PPAR γ* and regulates adipogenesis.

Acknowledgments

We thank Ann Norton of the Optical Imaging Center at the University of Idaho for assistance with the ORO image capture and analysis.

References

1. Hirsch J, Batchelor B (1976) Adipose tissue cellularity in human obesity. *Clin Endocrinol Metab* 5: 299-311.
2. Cheguru P, Chapalamadugu KC, Doumit ME, Murdoch GK, Hill RA (2012) Adipocyte differentiation-specific gene transcriptional response to C18 unsaturated fatty acids plus insulin. *Pflugers Archiv-European Journal of Physiology* 463: 429-447.
3. Rosen ED, Spiegelman BM (2000) Molecular regulation of adipogenesis. *Annu Rev Cell Dev Biol* 16: 145-171.
4. Rosen ED, Hsu CH, Wang X, Sakai S, Freeman MW, Gonzalez FJ, et al. (2002) C/EBPalpha induces adipogenesis through PPARgamma: a unified pathway. *Genes Dev* 16: 22-26.
5. Gregoire FM, Smas CM, Sul HS (1998) Understanding adipocyte differentiation. *Physiol Rev* 78: 783-809.
6. Rosen ED, Walkey CJ, Puigserver P, Spiegelman BM (2000) Transcriptional regulation of adipogenesis. *Genes Dev* 14: 1293-1307.
7. Brown MS, Goldstein JL (1997) The SREBP pathway: regulation of cholesterol metabolism by proteolysis of a membrane-bound transcription factor. *Cell* 89: 331-340.
8. Kim JB, Sarraf P, Wright M, Yao KM, Mueller E, Solanes G, et al. (1998) Nutritional and Insulin Regulation of Fatty Acid Synthetase and Leptin Gene Expression through ADD1/SREBP1. *J Clin Invest* 101: 1-9.

9. Kim JB, Spiegelman BM (1996) ADD1/SREBP1 promotes adipocyte differentiation and gene expression linked to fatty acid metabolism. *Genes Dev* 10: 1096-1107.
10. Fajas L, Schoonjans K, Gelman L, Kim JB, Najib J, Martin G, et al. (1999) Regulation of peroxisome proliferator-activated receptor gamma expression by adipocyte differentiation and determination factor 1/sterol regulatory element binding protein 1: implications for adipocyte differentiation and metabolism. *Mol Cell Biol* 19: 5495-5503.
11. Matsuo T, Matsuo M, Kasai M, Takeuchi H (2001) Effects of a liquid diet supplement containing structured medium- and long-chain triacylglycerols on bodyfat accumulation in healthy young subjects. *Asia Pac J Clin Nutr* 10: 46-50.
12. Martini LA, Wood RJ (2006) Vitamin D status and the metabolic syndrome. *Nutr Rev* 64: 479-486.
13. Wood RJ (2008) Vitamin D and adipogenesis: new molecular insights. *Nutr Rev* 66: 40-46.
14. Hida Y, Kawada T, Kayahashi S, Ishihara T, Fushiki T (1998) Counteraction of retinoic acid and 1,25-dihydroxyvitamin D₃ on up-regulation of adipocyte differentiation with PPARgamma ligand, an antidiabetic thiazolidinedione, in 3T3-L1 cells. *Life Sci* 62: PL205-211.
15. Blumberg JM, Tzamelis I, Astapova I, Lam FS, Flier JS, et al. (2006) Complex role of the vitamin D receptor and its ligand in adipogenesis in 3T3-L1 cells. *J Biol Chem* 281: 11205-11213.

16. Sato M, Hiragun A (1988) Demonstration of 1 alpha,25-dihydroxyvitamin D3 receptor-like molecule in ST 13 and 3T3 L1 preadipocytes and its inhibitory effects on preadipocyte differentiation. *J Cell Physiol* 135: 545-550.
17. Kamei Y, Kawada T, Kazuki R, Ono T, Kato S, Sugimoto E (1993) Vitamin D receptor gene expression is up-regulated by 1, 25-dihydroxyvitamin D3 in 3T3-L1 preadipocytes. *Biochem Biophys Res Commun* 193: 948-955.
18. Kelly KA, Gimble JM (1998) 1,25-Dihydroxy vitamin D3 inhibits adipocyte differentiation and gene expression in murine bone marrow stromal cell clones and primary cultures. *Endocrinology* 139: 2622-2628.
19. Ramirezzacarias JL, Castromunozledo F, Kuriharcuch W (1992) Quantitation of Adipose Conversion and Triglycerides by Staining Intracytoplasmic Lipids with Oil Red-O. *Histochemistry* 97: 493-497.
20. Pfaffl MW (2001) A new mathematical model for relative quantification in real-time RT-PCR. *Nucleic Acids Research* 29: e45.
21. Sutton AL, MacDonald PN (2003) Vitamin D: more than a "bone-a-fide" hormone. *Mol Endocrinol* 17: 777-791.
22. Van Etten E, Decallonne B, Verlinden L, Verstuyf A, Bouillon R, Mathieu C (2003) Analogs of 1alpha,25-dihydroxyvitamin D3 as pluripotent immunomodulators. *J Cell Biochem* 88: 223-226.
23. Li YC, Pirro AE, Amling M, Delling G, Baron R, Bronson R, et al. (1997) Targeted ablation of the vitamin D receptor: an animal model of vitamin D-dependent rickets type II with alopecia. *Proc Natl Acad Sci U S A* 94: 9831-9835.

24. Yoshizawa T, Handa Y, Uematsu Y, Takeda S, Sekine K, Yoshihara Y, et al. (1997) Mice lacking the vitamin D receptor exhibit impaired bone formation, uterine hypoplasia and growth retardation after weaning. *Nat Genet* 16: 391-396.
25. Jones G, Strugnell SA, DeLuca HF (1998) Current understanding of the molecular actions of vitamin D. *Physiol Rev* 78: 1193-1231.
26. Kong J, Li YC (2006) Molecular mechanism of 1,25-dihydroxyvitamin D₃ inhibition of adipogenesis in 3T3-L1 cells. *Am J Physiol Endocrinol Metab* 290: E916-924.
27. Lekstrom-Himes J, Xanthopoulos KG (1998) Biological role of the CCAAT/enhancer-binding protein family of transcription factors. *J Biol Chem* 273: 28545-28548.
28. Cao Z, Umek RM, McKnight SL (1991) Regulated expression of three C/EBP isoforms during adipose conversion of 3T3-L1 cells. *Genes Dev* 5: 1538-1552.
29. Darlington GJ, Ross SE, MacDougald OA (1998) The role of C/EBP genes in adipocyte differentiation. *J Biol Chem* 273: 30057-30060.
30. Yeh WC, Cao Z, Classon M, McKnight SL (1995) Cascade regulation of terminal adipocyte differentiation by three members of the C/EBP family of leucine zipper proteins. *Genes Dev* 9: 168-181.
31. Laudet V, Hanni C, Coll J, Catzeflis F, Stehelin D (1992) Evolution of the nuclear receptor gene superfamily. *EMBO J* 11: 1003-1013.
32. Berger J, Moller DE (2002) The mechanisms of action of PPARs. *Annu Rev Med* 53: 409-435.
33. Rosen ED, Spiegelman BM (2001) PPAR γ : a nuclear regulator of metabolism, differentiation, and cell growth. *J Biol Chem* 276: 37731-37734.

34. Desvergne B, Michalik, L. and Wahli, W. (2006) Transcriptional Regulation of Metabolism. *Physiol Rev* 86: 465-514.
35. Tontonoz P, Hu E, Graves RA, Budavari AI, Spiegelman BM (1994) mPPAR gamma 2: tissue-specific regulator of an adipocyte enhancer. *Genes Dev* 8: 1224-1234.
36. Enoch HG, Strittmatter P (1978) Role of tyrosyl and arginyl residues in rat liver microsomal stearylcoenzyme A desaturase. *Biochemistry* 17: 4927-4932.
37. Sul HS (2009) Minireview: Pref-1: role in adipogenesis and mesenchymal cell fate. *Mol Endocrinol* 23: 1717-1725.
38. Macdougald OA, Lane MD (1995) Transcriptional Regulation of Gene-Expression During Adipocyte Differentiation. *Annual Review of Biochemistry* 64: 345-373.

Supplementary Information

Regulation of adipogenesis and key adipogenic gene expression by 1, 25-dihydroxyvitamin D in 3T3-L1 cells

Shuhan Ji *et al.* PLOS ONE, 2015

Fig S2.1: Western Blot quantification of PPAR γ protein expression.

Representative images showing Western blot analysis (Odyssey® Dual Infrared Imaging System (Li-Cor)) of PPAR γ on 6 h (A), 12 h (B), days 1 (C), 2 (D), 4 (E), 6 (F), 8 (G) and 10 (H). Cells were treated with differentiation medium in the presence or absence of 100 and 1 nM 1, 25 - (OH) $_2$ D $_3$, and basal growth medium. β -actin was used as an internal protein loading control. Quantification of PPAR γ normalized to β -actin. Comparisons are with blank within day. Data are means \pm SE (n = 3).

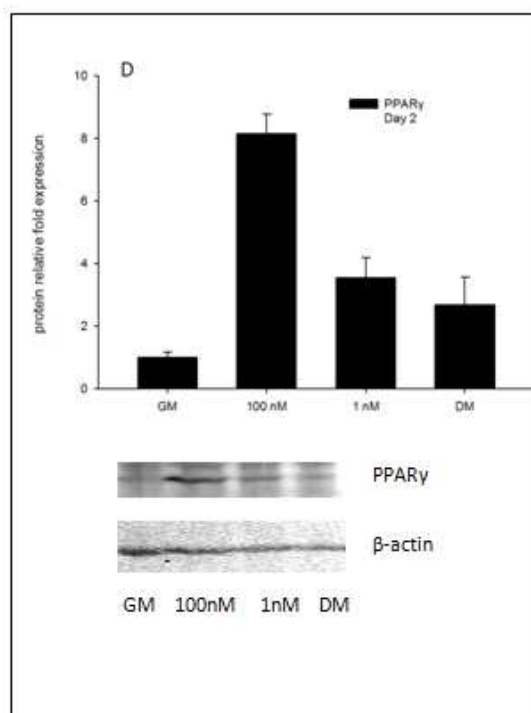
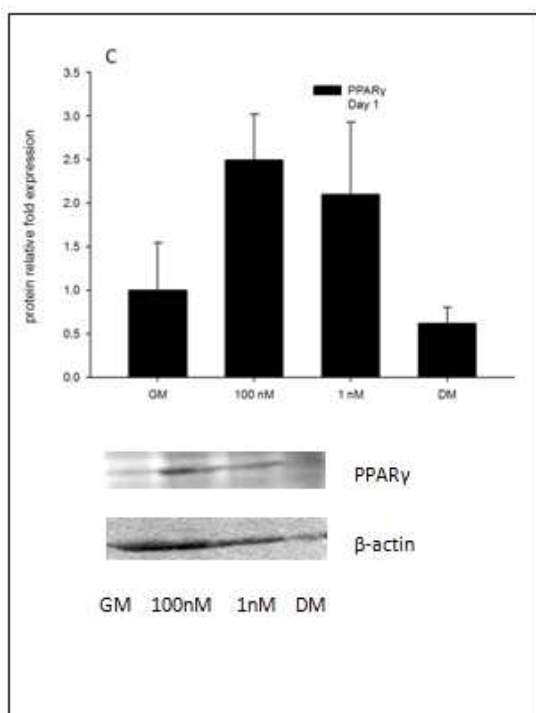
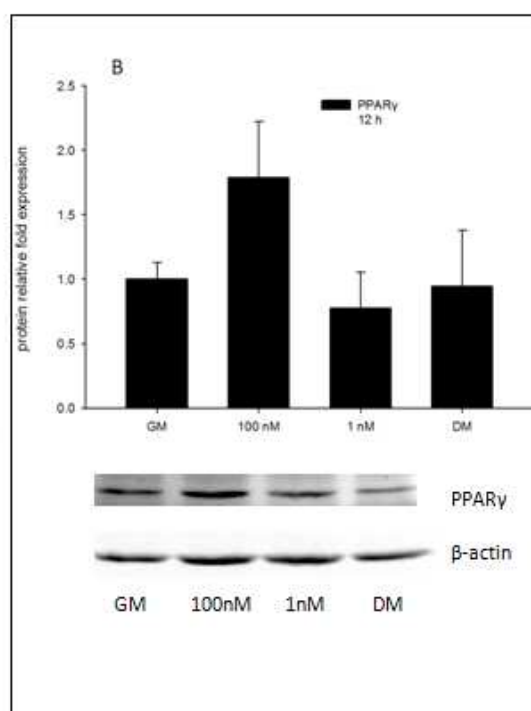
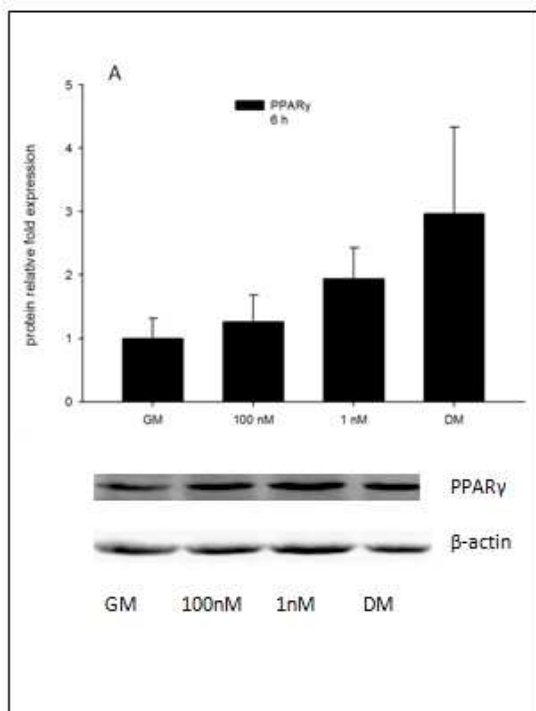


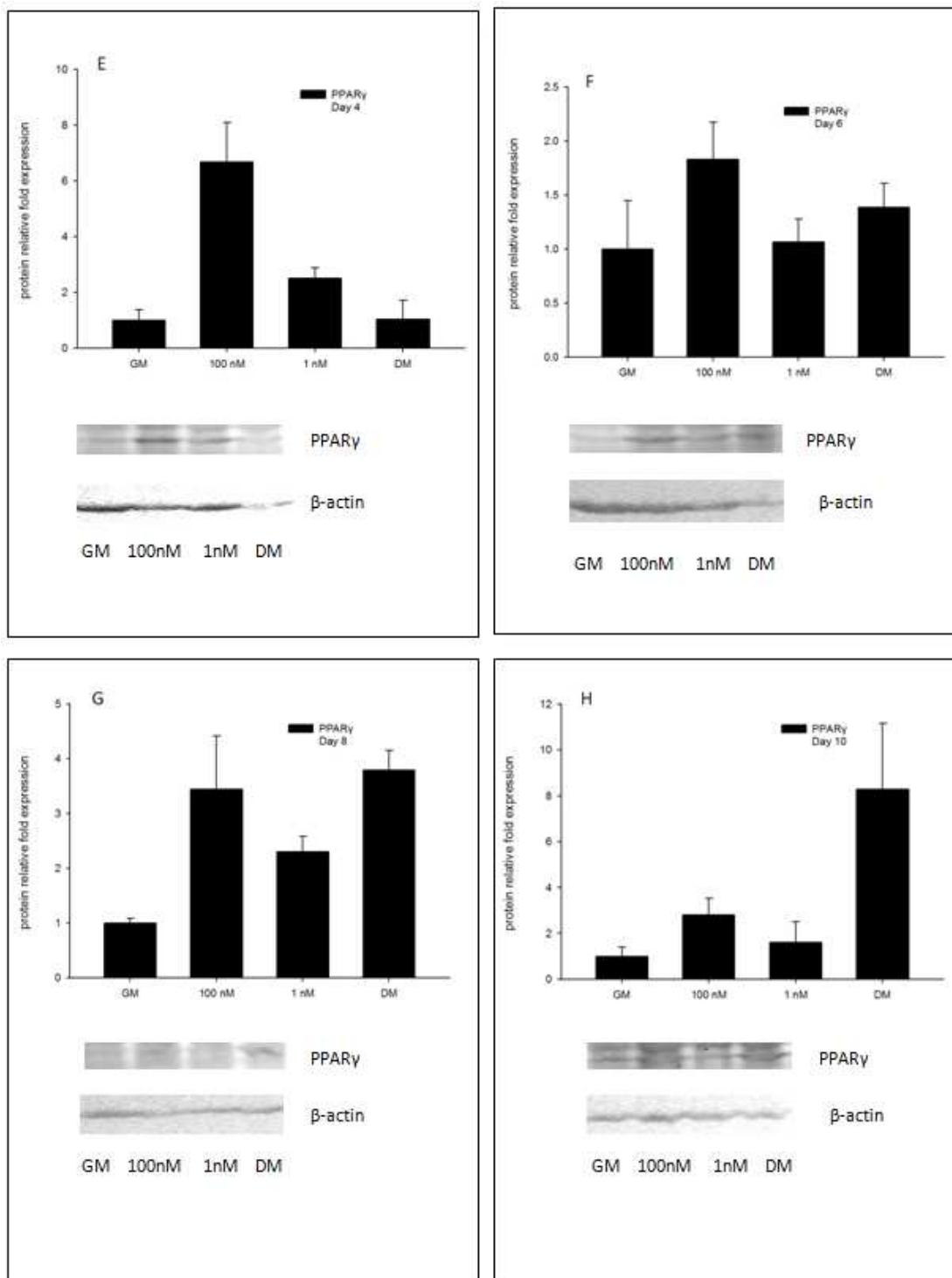
Fig S1 (Cont.): Western Blot quantification of PPAR γ protein expression

Fig S2.2: Western Blot quantification of C/EBP α protein expression.

Representative images showing Western blot analysis (Odyssey® Dual Infrared Imaging System (Li-Cor)) of C/EBP α on 6 h (A), 12 h (B), days 1 (C), 2 (D), 4 (E), 6 (F), 8 (G) and 10 (H). Cells were treated with differentiation medium in the presence or absence of 100 and 1 nM 1, 25 - (OH) $_2$ D $_3$, and basal growth medium. β -actin was used as an internal protein loading control. Quantification of PPAR γ normalized to β -actin. Comparisons are with blank within day. Data are means \pm SE (n = 3).

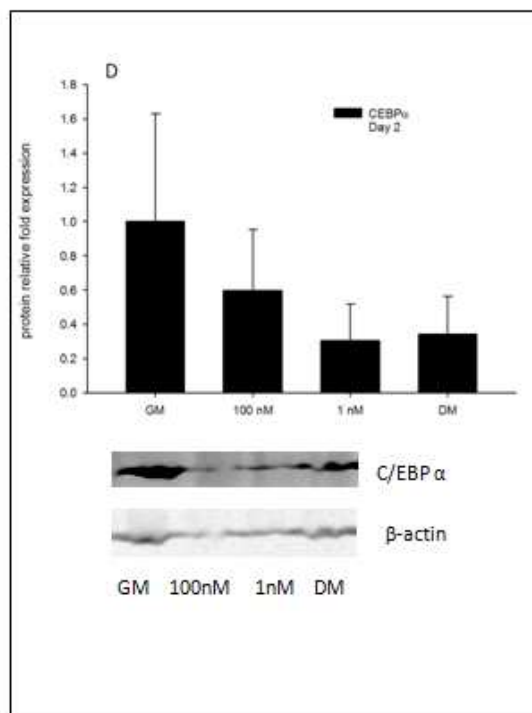
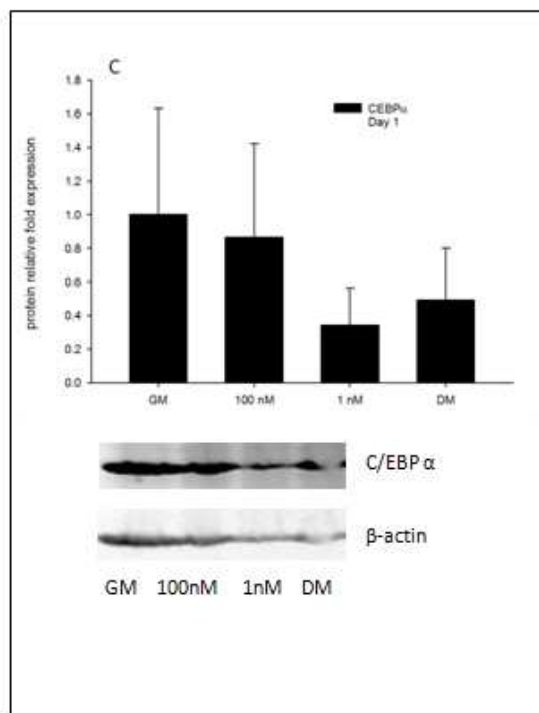
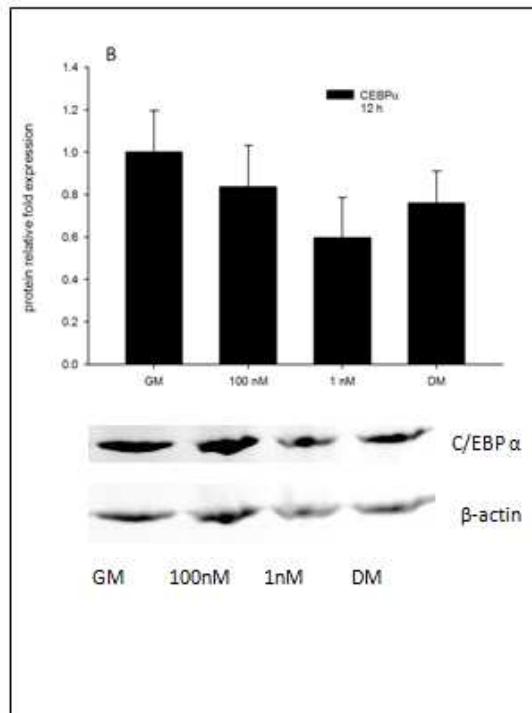
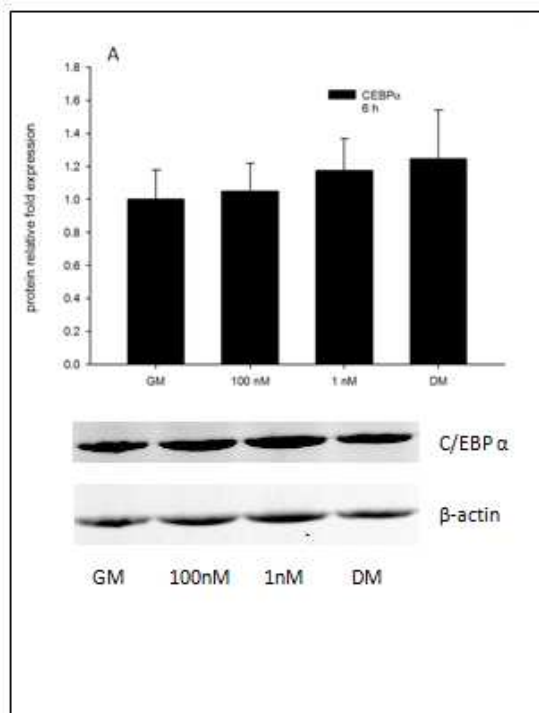
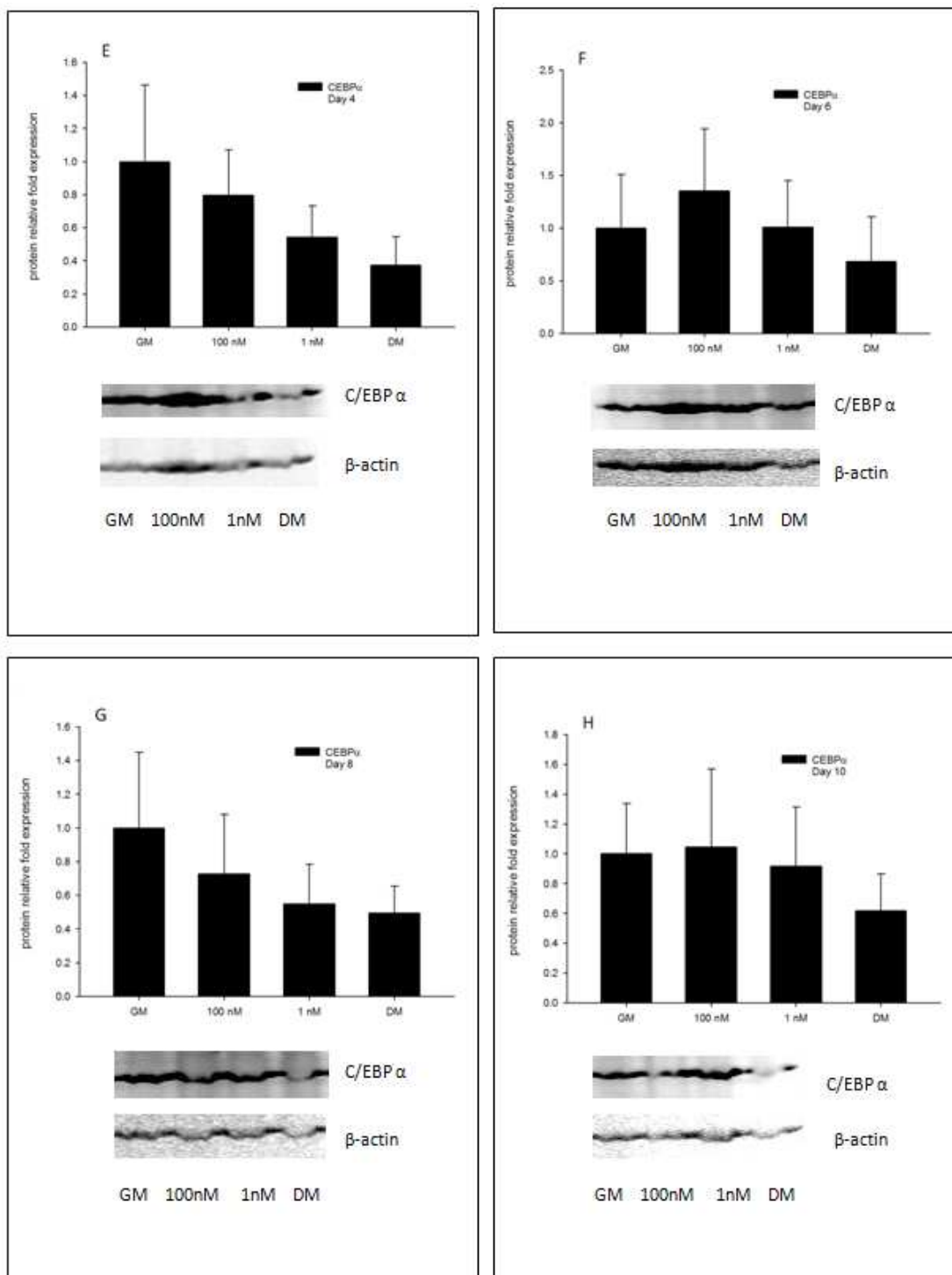


Fig S2 (Cont.): Western Blot quantification of C/EBP α protein expression

CHAPTER III

ADIPOGENESIS AND KEY ADIPOGENIC GENE EXPRESSION RESPONSE TO RETINOIC ACID IN 3T3-L1 CELLS

This chapter will be submitted to International Journal of Obesity, as citation, Shuhan Ji, Min Du, Rodney A. Hill, 2015, Adipogenesis and key adipogenic gene expression response to retinoic acid in 3T3-L1 cells.

Abstract

Background and objective: Adipogenesis plays an important role in metabolic homeostasis and nutrient pathways. The transcriptional control of adipogenesis requires a sequential series of gene expression events and activation of a number of key signaling pathways. Retinoic acid has been considered a potent inhibitor of adipogenesis for decades, and understanding the mechanism of retinoic acid regulation of adipogenesis is potentially useful in developing therapeutic interventions to control body fat. To investigate the function of retinoic acid in regulation of adipogenesis adipocyte differentiation and key adipogenic gene expression, dose-response and time-course studies of retinoic acid effects were studied in 3T3-L1 preadipocytes.

Methods: Lipid accumulation was measured by Oil Red O staining and expression of key adipogenic genes was quantified using quantitative real-time PCR. Adipogenic responses

to different concentrations of retinoic acid were determined on day 2, 4, 6, 8, 10 after stimulation of adipogenesis with the traditional hormonal cocktail (dexamethasone, isobutyl-1-methylxanthine and insulin) in the absence or presence of retinoic acid.

Results: In response to high concentrations (1000 and 100 nM) of retinoic acid, lipid accumulation and the expression of *PPAR γ* , *C/EBP α* , *C/EBP β* , *FABP4*, *SREBP-1c* and *SCD-1* were inhibited through day 8, but on day 10, lipid accumulation and the expression levels of these genes rebounded to levels comparable to the control. Interestingly, the greatest effects of retinoic acid treatments were upon expression of *FABP4*. However, expression of *C/EBP δ* was not affected. The lowest retinoic acid concentration (0.1 nM) did not affect adipocyte differentiation or expression of adipogenic genes.

Conclusions: These results indicate that retinoic acid inhibited adipogenesis via suppressing adipogenic specific genes, especially *FABP4*. Our data indicate that a deeper understanding of the roles of retinoic acid in regulating adipogenesis will be informed by further study of adipogenic specific gene promoter activity.

Introduction

Adipocyte differentiation is a complex process involving a cascade of molecular events triggered by an adipogenic stimulus [1]. During this process, lipid accumulation occurs and preadipocytes differentiate to form mature adipocytes. It is important to the improvement of human health that the positive and negative regulation for the proliferation and differentiation of adipocytes be well defined [2]. The transcriptional control of adipocyte differentiation requires a sequential series of gene expression events and activation of a number of key signaling pathways [3, 4]. There are two classes of transcription factors,

nuclear receptor peroxisome proliferator-activated receptor γ (PPAR γ) [5] and CCAAT/enhancer – binding protein α (C/EBP α) [6, 7, 8, 9] that are key regulators in the process of adipogenesis.

At the beginning of the cascade of changes in expression of adipogenic genes, another two members from the C/EBP family, C/EBP β and C/EBP δ , are initially expressed. These two proteins then induce the expression of PPAR γ , which in turn induces C/EBP α expression [10]. The activation of C/EBP α has positive feedback on PPAR γ activity. With the enhancement by each other's inducing, these two transcriptional factors maintain the differentiated state [11]. Upstream of PPAR γ in the process of adipogenesis, there is another notable factor, sterol-regulatory element binding protein 1c (*SREBP-1c*) [12]. The discovery of *SREBP-1c* was reported by two different research groups, and was named as *ADD1* and *SREBP-1c* [13, 14]. SREBP-1c is a member of the basic helix-loop-helix (bHLH) family of transcription factors [13], and plays a crucial role in adipogenesis [15]. The expression of *SREBP-1c* is further regulated by insulin in cultured adipocytes [16]. Moreover, SREBP-1c inducing the expression of PPAR γ in adipogenesis is via binding E box motifs present in the PPAR γ promoter [17]. SREBP-1c also has influence in regulation of a variety of genes involved in fatty acid and triglyceride metabolism [10]. All these transcriptional factors are necessary for maintaining the terminally differentiated phenotype.

Retinoic acid (RA) is the most studied metabolite in the vitamin A pathway. It regulates a broad range of biological effects in large part by controlling gene expression [18]. In particular, it was reported that as an active form of retinoids and carotenoids, RA inhibited the differentiation of adipocytes in culture [19, 20]. In the present study, we have determined the inhibitory effect of different concentrations of RA in 3T3-L1 preadipocyte differentiation. We also studied the inhibitory activity of different concentrations of RA on expression levels of key adipogenic genes (*C/EBPs* and *PPAR γ*). As important transcriptional factors during adipocyte differentiation, *FABP4* and *SREBP-1c* were also a focus of the present study. Our study provides an experimental basis to better understand the function of RA in regulation of adipogenesis, and the interactions between RA and key adipogenic genes.

Materials and Methods

Materials

Mouse embryonic fibroblast cells (3T3-L1) were obtained from the American Type Culture Collection (ATCC). Dulbecco's Modified Eagle's Medium (DMEM), fetal bovine serum (FBS) and penicillin/streptomycin were from Gibco, Life Technologies (Grand Island, NY). Trizol, DNase I kit, high capacity cDNA reverse transcription kit (Cat # 4368814), and Taqman Master Mix were obtained from Life Technologies (Grand Island, NY). The Dual Reporter Luciferase Assay System was purchased from Promega Corporation, (Madison, WI). Oil Red O (ORO) powder, dexamethasone (D8893), insulin from bovine pancreas (I6634), 3-isobutyl-1-methylxanthine (IBMX) (I7018), and 1 α ,25-Dihydroxyvitamin D₃ (D1530) were purchased from Sigma-Aldrich (St. Louis, MO).

Mouse-specific anti-PPAR γ (sc-7196) rabbit polyclonal antibody was purchased from Santa Cruz Biotechnology (Dallas, Texas). Mouse-specific anti-C/EBP α (ab139731) rabbit polyclonal antibody, and anti- β -actin mouse-monoclonal (ab8226) were purchased from Abcam (Cambridge, MA). AlexaFluor 680 anti-rabbit IgG was from life Technologies (Grand Island, NY) and IRDye800 anti-mouse IgG was from Li-Cor (Lincoln, NE).

Cell culture.

Mouse 3T3-L1 preadipocytes were cultured at 37 °C with 5% CO₂ enriched air in DMEM with 10 % FBS, 100 I.U. /ml penicillin, 100 μ g/ml streptomycin (basal growth medium). Cells were seeded in 6-well plates and 24-well plates with glass cover slips in basal growth medium and cultured until confluent. On day 0 (two days post confluence), retinoic acid was added to the differentiation medium at the following final concentrations: 1000, 100, 10, 1, and 0.1 nM, and cultures were incubated for 48 h. Cells grown in basal growth medium without retinoic acid served, as a negative control. Cells grown in medium containing basal growth medium with dexamethasone (1 μ M), IBMX (500 μ M) and insulin (1.7 mM) (standard hormonal differentiation medium, DMI) served, as a positive control. For the DMI treatment, insulin, dexamethasone and IBMX were provided for the first 48 h followed by only insulin in basal growth medium throughout the remaining time points. Media were changed every 2 days for all treatments. Cells were harvested on 0, 6, and 12 h, and days 1, 2, 4, 6, 8 and 10 for RNA extraction, or protein extraction. Parallel cultures were stained with ORO and representative images of ORO stained cells on day 10 were quantified using MetaMorph Image analysis software (Nashville, TN).

Cells and transfection.

For each cell culture well, 3.5×10^5 3T3-L1 cells were plated and allowed to reach 80% confluence. Cells were then co-transfected with 2 μg [pGL4.10 (luc2/-500 C/EBP α)] and 0.2 μg of internal transfection control vector [pGL4.74 (hRluc/TK)], and transferred to growth medium. Cells were incubated 24 h, and allowed to reach 100% confluence. Two days post confluence cells (0 h) were treated with 1000 nM of retinoic acid plus differentiation medium, differentiation medium only, or growth medium only. Cells were harvested on 0, 12, 24, and 48 h, and assayed for firefly luciferase and renilla luciferase activities using the Dual Reporter Luciferase Assay System (Promega, Madison, WI) and a Wallac 1420 Multi Label Counter. Firefly luciferase activity units were normalized to units of renilla luciferase activity to correct for transfection efficiency.

Oil Red O (ORO) and Hematoxylin staining.

Accumulation of lipids was observed using ORO staining [21]. Oil Red O in isopropanol stock solution (3.5 mg/ml) was prepared, stirred overnight and filtered. Cells grown on cover slips in 24-well plates were used for lipid staining. On the day of the time point, culture medium was removed and cells were gently rinsed once with phosphate buffer saline (PBS). Cells were fixed in 10 % formaldehyde in PBS for 1 hr at RT. After fixation, cells were rinsed with PBS and then 60 % isopropanol. Oil Red O solution (6:4 v/v of stock solution and water) was added and incubated for 10 min at RT. Finally, cells were washed with distilled water, three times. Hematoxylin counter staining was done according to the manufacturer's instructions. Briefly, cells were incubated with filtered hematoxylin for two minutes and rinsed twice with tap water. Differentiation solution (0.25 % HCl in 70 %

alcohol) was added and cells were rinsed again with tap water. The glass cover slips were then removed from the wells and inverted on to a glass slide with mounting medium (Vecta Shield, Vector Labs, Burlingame, CA).

RNA extraction and cDNA synthesis.

Total RNA was extracted using Trizol according to the manufacturer's instructions. The RNA pellet was resuspended in nuclease-free water and stored at -80°C until further use. RNA was quantified using a Nanodrop ND-1000 UV-Vis Spectrophotometer (Nanodrop Technologies, Wilmington, DE). The quality of RNA was verified on 1% agarose gels. Two µg of RNA from each treatment was DNase treated. Synthesis of cDNA was conducted using a high capacity cDNA reverse transcription kit and random hexamers as primers according to the manufacturer's instructions. To ensure availability of cDNA sufficient to perform all real-time PCR reactions, cDNA synthesized from 2 µg of RNA was pooled for each sample. Pooled cDNA was diluted 1:10 using nuclease-free water for real-time PCR.

Real-time PCR.

Quantitative real-time PCR was performed using Taqman MGB primer/probe sets with an ABI 7500 Fast Real Time PCR system (Applied Biosystems, Foster City, CA). Primers and probes for all genes were designed using Applied Biosystems Primer Express 3.0 software. Primers (Integrated DNA Technologies, Coralville, IA) and probes (Life Technologies, Grand Island, NY) were designed to have a T_m of 58-60 °C and 69-70 °C, respectively. Primer-probe sets that span exon-junctions (trans-intronic positions) were

chosen for real-time PCR, to prevent binding to genomic DNA (Table 3.1). Eukaryotic translation elongation factor 2 (*EEF2*) was used as an endogenous control for gene expression. Probes were labeled with 6-FAM or VIC for all target genes or control (*EEF2*), respectively. Real-time PCR assays for each sample were conducted in duplicate wells with all genes including endogenous control on the same plate. Reactions contained Taqman Universal Fast PCR Master Mix, No AmpErase UNG (Applied Biosystems, Foster City, CA) (1X), forward primer (0.5 μ M), reverse primer (0.5 μ M), Taqman probe (0.125 μ M) and cDNA template made up to a final volume of 15 μ l in nuclease-free water. Real-time PCR cycle conditions included a holding time of 90 °C for 20 sec, followed by 40 cycles of 90 °C for 3 sec and 60 °C for 30 sec of melting and extension temperatures, respectively.

Data were analyzed using the relative C_T ($\Delta\Delta C_t$) method [22]. Average C_t values of endogenous control (*EEF2*) were subtracted from target gene average C_t values of each gene, to obtain ΔC_t values of each gene for each sample. For each gene, ΔC_t values in the control treatment at each time point were used to normalize ΔC_t values of corresponding time points of each treatment to obtain $\Delta\Delta C_t$ and mRNA fold expression values [$2^{(-\Delta\Delta C_t)}$].

Table 3.1: Primer-probe sets for real-time PCR. Primers and probe sequences used in real-time PCR listed 5' to 3': Forward primer (FP), reverse primer (RP) and Taqman probes for the following genes were designed from the corresponding GenBank accession numbers.

Accession No.	Gene name	Sequences
NM_007907.1	<i>Eukaryotic translation elongation factor 2 (Eef2)</i>	FP: CTGCCTGTCAATGAGTCCTTTG RP: GCCGCCGGTGTGGAT Probe: CTTACCGCTGATCTG
NM_011146.2	<i>Peroxisome proliferator activated receptor gamma (PPARγ)</i>	FP: GCTTCCACTATGGAGTTCATGCT RP: AATCGGATGGTTCTTCGGAAA Probe: TGAAGGATGCAAGGGTT
NM_007678.3	<i>CCAAT/enhancer binding protein alpha (C/EBPα)</i>	FP: CGCAAGAGCCGAGATAAAGC RP: GTCAACTCCAGCACCTTCTGTTG Probe: AACGCAACGTGGAGAC
NM_009883.3	<i>CCAAT/enhancer binding protein beta (C/EBPβ)</i>	FP: GCGCACCGGGTTTCG RP: GCGCTCAGCCACGTTTG Probe: ACTTGATGCAATCCGGA
NM_007679.4	<i>CCAAT/enhancer binding protein delta (C/EBPδ)</i>	FP: CTGTGCCACGACGAACTCTTC RP: GCCGGCCGCTTTGTG Probe: CGACCTCTTCAACAGC
NM_024406.1	<i>Fatty acid binding protein 4 (FABP4)</i>	FP: CCGCAGACGACAGGAAGGT RP: AGGGCCCCGCCATCT

		<i>Probe: AAGAGCATCATAACCC</i>
NM_010052.3	<i>Preadipocyte factor-1 (Pref-1)</i>	<i>FP: AATAGACGTTCTGGGCTTGCA</i> <i>RP: GGTCACGCAAGTTCCATTG</i> <i>Probe: CTCAACCCCCTGCGC</i>
NM_011480.3	<i>Sterol regulatory element binding transcription factor 1 (Srebf1)</i>	<i>FP: GCGGTTGGCACAGAGCTT</i> <i>RP: CTGTGGCCTCATGTAGGAATACC</i> <i>Probe: CGGCCTGCTATGAGG</i>
NM_009127.4	<i>Stearoyl-Coenzyme A desaturase 1 (Scd1)</i>	<i>FP: CAACACCATGGCGTTCCA</i> <i>RP: TGGGCGCGGTGATCTC</i> <i>Probe: AATGACGTGTACGAATGG</i>

Western Blot.

Protein extraction from 3T3-L1 preadipocytes and adipocytes was performed using cell lysis buffer with addition of phosphatase and protease inhibitors (Cell Signaling Technologies, Danvers, MA). The supernatant was extracted by centrifugation and protein concentration was determined by BCA protein assay according to manufacturer's protocol (Thermo Scientific, Rockford, IL). Ten μ g of whole cell lysate was resolved on SDS-PAGE (4-10% precise gels) and then transferred to PVDF membrane. Membranes were blocked with 5% non-fat milk in 1X TBST for 1h at room temperature. Membranes were incubated with anti-PPAR γ , anti-C/EBP α and anti- β -actin at 4 °C overnight, then washed with 1X TBST and incubated with AlexaFluor 680 conjugated anti-rabbit IgG and IRDye 800 conjugated anti-mouse IgG for 1 h at room temperature. After thorough washing, blots were scanned and quantified using an Odyssey Dual Infrared Imaging System (Li-Cor).

Microscopy.

Images were obtained using a Nikon 80i phase-contrast microscope, using a 20X objective lens. Image quantification was performed using MetaMorph Image analysis software (Nashville, TN). Area fractions were collected for each image. Images were collected in six to eight replicates from each culture well. Average area fractions of each of the six to eight replicates were used to calculate average area fraction of each treatment sample. Further, average area fraction values of each treatment were normalized to average area fraction values of corresponding controls.

Statistical analysis.

Statistical analysis software (SAS) 9.3 was used to perform all data analysis. Data were analyzed using a one-way analysis of variance (ANOVA) for each time point. Tukey's test was used to find the significant differences among the different means. Differences, when $p < 0.05$, were considered statistically significant. Gene expression data were analyzed by comparing log (base 2) transformed values of mRNA fold expression across treatments within each time-point. All data are reported as mean \pm SE (n = 3).

Results***Lipid accumulation is inhibited with RA treatments.***

3T3-L1 cells were cultured in standard hormonal differentiation medium, in the presence or absence of RA treatments. Cells treated with Basal growth medium only were considered the negative control. Cells treated with differentiation medium only were used as the positive control. Lipid accumulation was observed through ORO staining on days 0,

2, 4, 6, 8 (data not shown) and 10 (Supplementary Fig. 3.1). Image quantification analysis shows that with higher concentrations of RA (1000, 100, 10 nM) treatments, lipid accumulation in cells was inhibited, although remaining higher compared to negative control cells, but significantly lower compared to the positive control (Supplementary Fig. 3.1H). For the two lowest concentrations of RA treatment, cells showed higher lipid accumulation than negative control and the three highest RA treatments. Moreover, lipid accumulation was not significantly lower when compared to the positive control (Supplementary Fig. 3.1H). This suggests that RA treatment inhibited lipid accumulation and adipogenesis in a dose dependent manner, with a critical minimum concentration of approximately 10 nM.

Gene expression of *PPAR* γ is inhibited by high concentrations of RA.

Gene expression levels of *PPAR* γ in 3T3-L1 cells treated with the highest concentrations (1000 nM) of RA was significantly inhibited compared to the positive control (Fig. 3.1B-D) on days 4 – 8, but not on day 2 or 10. *PPAR* γ gene expression was not affected by RA treatments with all the concentrations at day 2 or day 10. In addition, 3T3-L1 cultures treated with low concentrations (10, 1 and 0.1 nM) of RA showed no significant differences in *PPAR* γ gene expression levels as compared to positive control cultures (Fig. 3.1A-E) at all time-points measured. On days 8, the highest concentration (1000 nM) of RA had the greatest inhibitory effect on *PPAR* γ mRNA expression levels (Fig. 3.1D), and the inhibitory effect had abated by day 10 (Fig. 3.1E). This suggests that *PPAR* γ gene expression levels were only marginally inhibited by RA, and RA had efficacy in inhibiting *PPAR* γ gene expression only at higher concentrations.

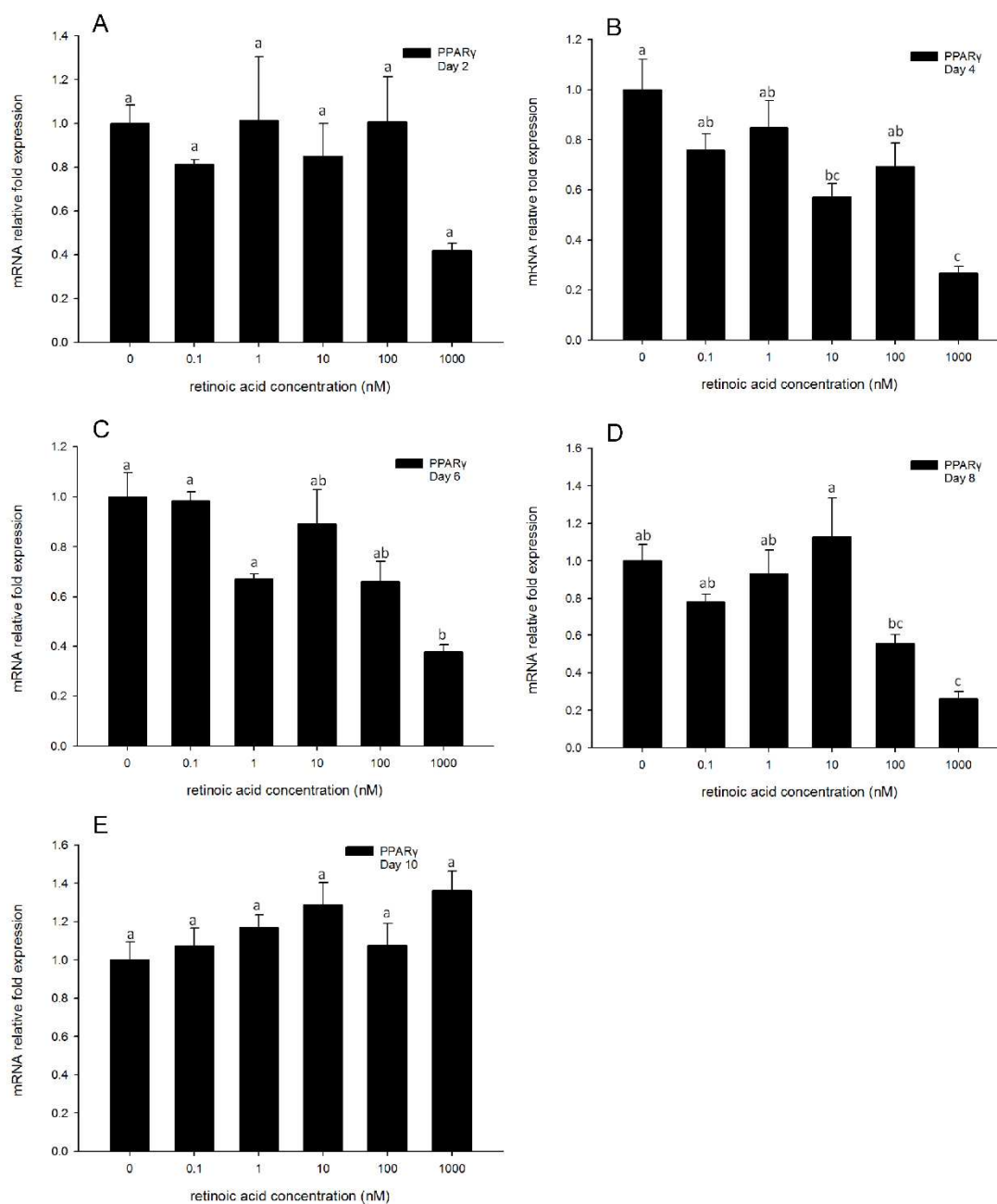


Figure 3.1 Real-time PCR quantification of PPAR γ gene expression in 3T3-L1 cells on days 2 (A), 4 (B), 6 (C), 8 (D) and 10 (E). Cells were treated with DM in the presence or absence of 0.1, 1, 10, 100, and 1000 nM RA and *EEF2* was used as endogenous control (Δ Ct). Data were normalized to PPAR γ gene expression of the positive control (DM) at the

corresponding time point ($\Delta\Delta\text{Ct}$). Data are means \pm SE ($n = 3$). Different letters represent treatment effects that were significantly different ($P < 0.05$).

To confirm the real-time PCR results, Western blots also were performed on whole cell lysates following treatment with 1000 or 10 nM of RA at all the time points. Differentiation medium (DM) and basal growth medium (GM) served as positive and negative controls, respectively. PPAR γ protein levels were not influenced by either high (1000 nM) or low (10 nM) concentrations of RA treatments at 6 and 12 h (Supplementary Fig. 3.2A-B), but thereafter the PPAR γ protein levels were reduced in the 1000 nM RA treated groups at day 1, 4, 8, and day 10 (Supplementary Fig. 3.2C, E, G and H), but remained high in 10 nM RA treated groups and DM only groups at all time-points (Supplementary Fig. 3.2B-H). At day 10, PPAR γ protein levels in both 1000 nM and 10 nM RA treatment groups remain low, however, in the DM only group, PPAR γ protein level still remained relatively high (Supplementary Fig. 3.2H). This suggests that RA treatments continuously inhibit PPAR γ protein levels from day 1 until day 10, but not the early time point, 6 h and 12 h. The results of above suggest that the highest concentration of RA treatment inhibits adipogenesis via reducing RNA expression levels of PPAR γ , and there appear to be no effects at protein levels of PPAR γ .

High concentrations of RA inhibit C/EBP α gene expression

Unlike the regulation of PPAR γ gene expression, 3T3-L1 cells treated with high concentrations (1000, 100, and 10 nM) of RA showed significant inhibition of C/EBP α expression as compared to the positive control for days 2 through 6 (Fig. 3.2A-C). No

significant changes in *C/EBP α* gene expression levels were observed in the cells treated with low concentrations (0.1 and 1 nM) of RA as compared to the positive control cells at all time-points measured (Fig. 3.2B-E), except day 2 (Fig. 3.2A).

Similarly to *PPAR γ* expression, *C/EBP α* gene expression levels was inhibited by the highest concentration (1000 nM) RA treatment until day 8 (Fig. 3.2D), and showed no significant difference between treatments groups and differentiation medium group on day 10 (Fig. 3.2E). This suggests that RA treatments had significant inhibitory effects on *C/EBP α* gene transcription, and this efficacy lasted until day 8.

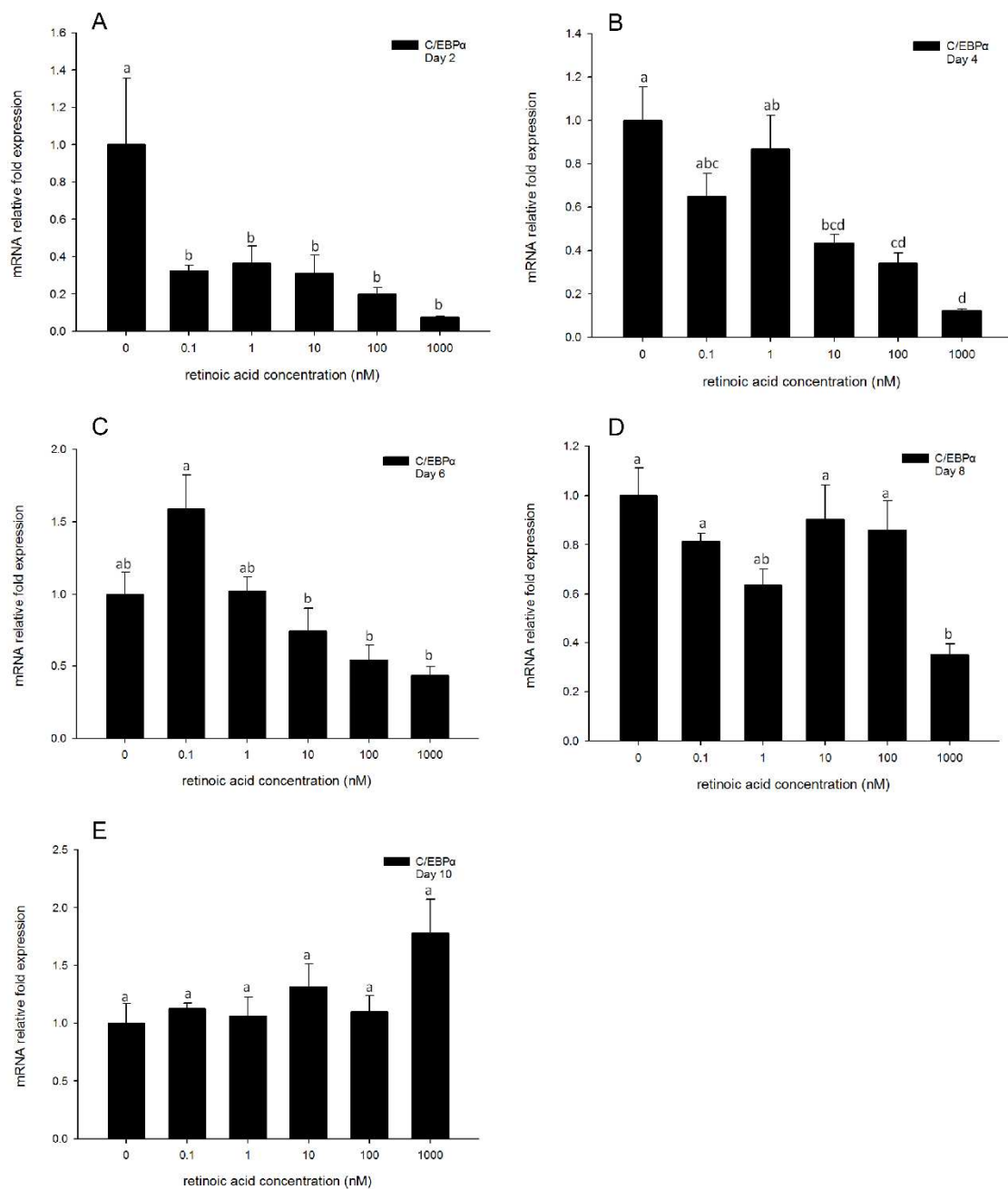


Figure 3.2 Real-time PCR quantification of *C/EBPα* gene expression in 3T3-L1 cells on days 2 (A), 4 (B), 6 (C), 8 (D) and 10 (E). Cells were treated with DM in the presence or absence of 0.1, 1, 10, 100, and 1000 nM RA and *EEF2* was used as endogenous control (ΔCt). Data were normalized to *C/EBPα* gene expression of positive control (DM) at the

corresponding time point ($\Delta\Delta\text{Ct}$). Data are means \pm SE ($n = 3$). Different letters represent treatment effects that were significantly different ($P < 0.05$).

Total cell protein levels of C/EBP α were also determined (Supplementary Fig. 3.3). In the early time points (6 and 12 h), C/EBP α protein levels were not changed in RA treatment groups and DM only group compared to negative control (Supplementary Fig. 3.3A-B). However, at day 1 and day 2, protein levels of C/EBP α in RA treated groups and DM groups were reduced comparing to negative control group (Supplementary Fig. 3.3C-D). Furthermore, in 3T3-L1 cells treated with 1000 nM RA, C/EBP α protein level was decreased at day 6 (Supplementary Fig. 3.3F), and continuously maintain low level until day 10 (Supplementary Fig. 3.3E-H). However, there were no changes in C/EBP α protein levels compared to DM only group to 1000 nM RA treated groups at day 4 (Supplementary Fig. 3.3E). The results suggest that both gene expression levels and total cellular protein levels of C/EBP α were influenced by RA treatment, and C/EBP α plays an important role in the mechanism of RA inhibiting adipogenesis.

There is no effect of RA treatments on C/EBP β and C/EBP δ gene expression levels.

Gene expression of C/EBP β was determined at 6, 12, 24 h and days 2, 4, 6, 8 10 by real-time PCR response to RA treatments, differentiation medium or growth medium. Unlike PPAR γ and C/EBP α , C/EBP β gene expression level was only impacted by 1000 nM RA compared to DM only group at day 2 (Supplementary Fig. 3.4D). Moreover, in the early time points, 6, 12 h and day 1 (Supplementary Fig. 3.4A-C) or from day 6 until day 10 (Supplementary Fig. 3.4F-H), all concentrations of RA showed no inhibitory effects on

C/EBPβ gene expression, suggesting that the inhibitory effect of RA treatments on *C/EBPβ* gene expression are transient and difficult to detect.

C/EBPδ is also induced in the early process of adipogenesis. Thus we quantified its gene expression levels at 6, 12, and 24 h, and continued to monitor its expression through days 2, 4, 6, 8, and 10, with or without RA treatments. *C/EBPδ* gene expression levels of RA treated cells were generally not inhibited compared to the DM only treated group (Supplementary Fig. 3.5A-H), even at the highest concentration of RA. This suggests that the inhibitory efficacy of RA in adipogenesis does not impact the expression of *C/EBPδ*.

Gene expression of FABP4 is highly responsive to RA treatments.

Gene expression of *FABP4* was strongly inhibited by the highest concentration (1000 nM) of RA treatments at all the time points, except day 10 (Fig. 3.3). Moreover, unlike *PPARγ* and *C/EBPα* expression levels, *FABP4* gene expression levels in response to 1 and 10 nM RA were also significantly inhibited compared to the positive control at day 2 (Fig. 3.3A) and day 6 (Fig. 3.3C). Moreover, the lowest concentration of RA (0.1nM) treatments had strong effect on *FABP4* gene expression on days 2 and 6 compared to the DM only group (Fig. 3.3A, C). However, on day 8, the high concentrations (1000 and 100 nM) of RA showed a significant inhibitory effect on *FABP4* gene expression (Fig. 3.3D). These effects were attenuated on day 10 (Fig. 3.3E). These results indicate that *FABP4* plays an important role during the inhibition of adipogenesis by RA.

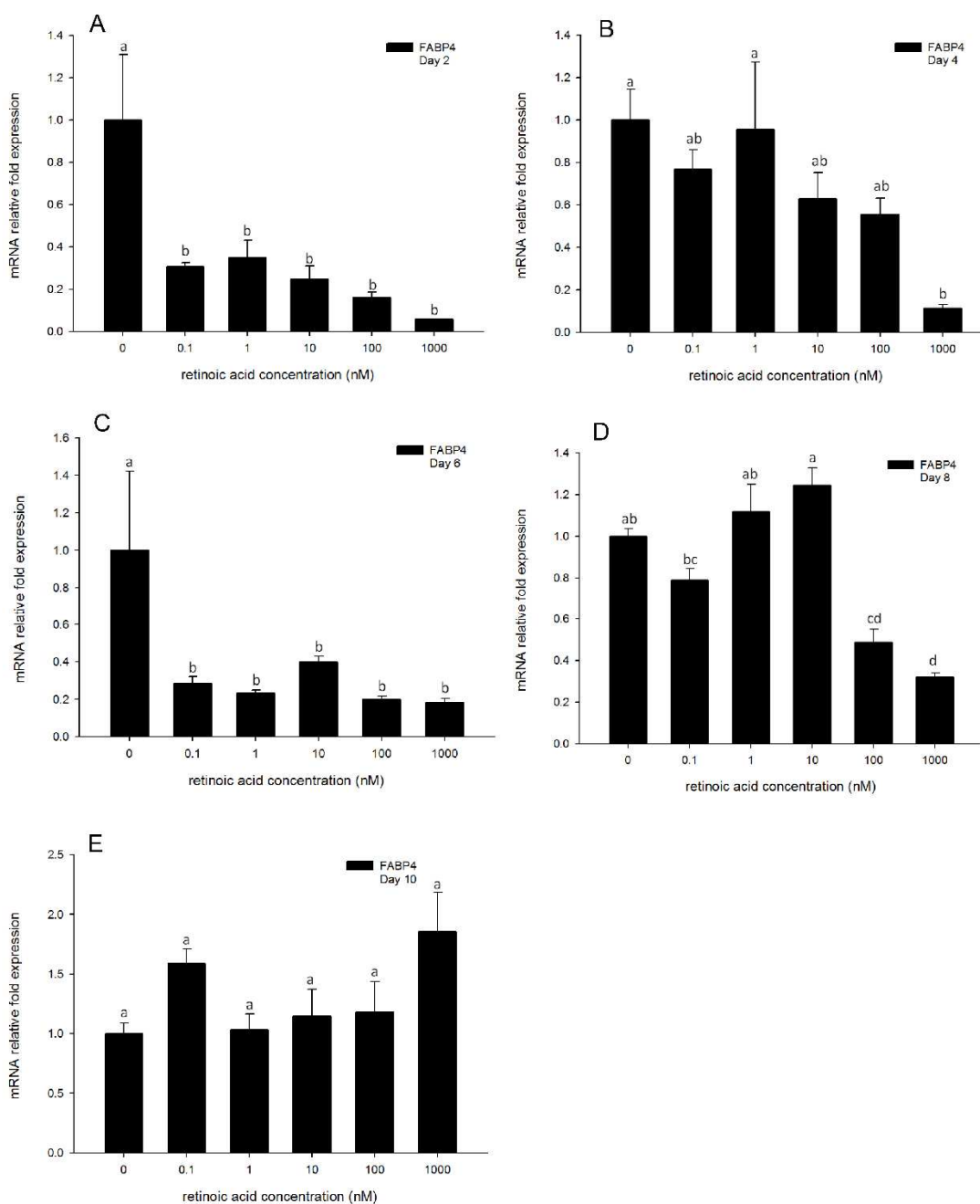


Figure 3.3 Real-time PCR quantification of FABP4 gene expression in 3T3-L1 cells on days 2 (A), 4 (B), 6 (C), 8 (D) and 10 (E). Cells were treated with DM in the presence or absence of 0.1, 1, 10, 100, and 1000 nM RA and *EEF2* was used as endogenous control (Δ Ct). Data were normalized to FABP4 gene expression of positive control (DM) at the

corresponding time point ($\Delta\Delta\text{Ct}$). Data are means \pm SE ($n = 3$). Different letters represent treatment effects that were significantly different ($P < 0.05$).

The inhibitory effect of RA on SREBP-1c gene expression levels was more gradual compared to C/EBP α or FABP4 expression.

In our previous studies, the expression pattern of *SREBP-1c* in adipocyte differentiation showed that it was induced to the maximum expression level on day 2, and then decreased quickly from days 4 to 10. Interestingly, on day 2, cells treated with 1000 nM and 0.1 nM RA showed significant inhibition of *SREBP-1c* gene expression as compared to the positive control (Fig. 3.4A). The inhibitory influence of RA coincides with the time point of maximum *SREBP-1c* expression, suggesting that RA has strong effects when *SREBP-1c* reached a high expression level. However, this effect was rapidly attenuated. *SREBP-1c* gene expression levels of RA treated cells were generally not different from the positive control at day 4 and 6 (Fig. 3.4B-C). However, the inhibitory effect of RA (all concentrations of treatments tested, 1000, 100, 10, 1, and 0.1 nM) on *SREBP-1c* gene expression was fleetingly showed again on day 8 (Fig. 3.4D), and declined at day 10 (Fig. 3.4E). These results suggest that *SREBP-1c* may also play an important role in the RA modulation pathway, and may have interaction with RA during the early stages of adipogenesis.

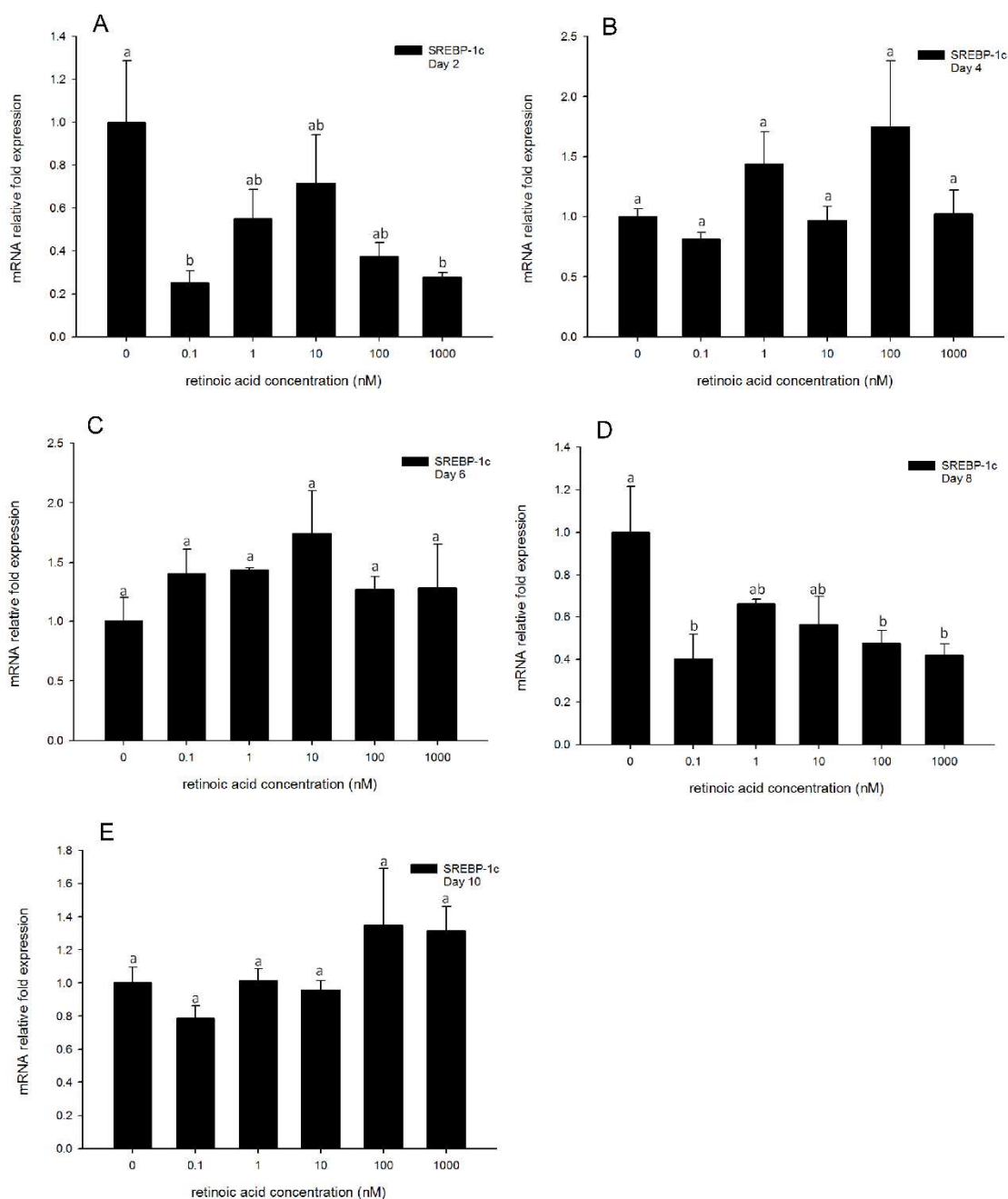


Figure 3.4 Real-time PCR quantification of *SREBP-1c* gene expression in 3T3-L1 cells on days 2 (A), 4 (B), 6 (C), 8 (D) and 10 (E). Cells were treated with DM in the presence or absence of 0.1, 1, 10, 100, and 1000 nM RA and *EEF2* was used as endogenous control (ΔCt). Data were normalized to *SREBP-1c* gene expression of positive control (DM) at the

corresponding time point ($\Delta\Delta\text{Ct}$). Data are means \pm SE ($n = 3$). Different letters represent treatment effects that were significantly different ($P < 0.05$).

Patterns of SCD-1 expression resembled PPAR γ expression, and was decreased by 1000 nM RA at days 4 to 8.

SCD-1 gene expression was not changed in response to any treatment concentrations of RA on day 2 (Fig. 3.5A). The inhibition of *SCD-1* gene expression was induced by the highest concentration of RA (1000 nM) on day 4 (Fig. 3.5B). The inhibitory effect of the highest concentration of RA (1000 nM) was most pronounced at day 4, and reached an inhibition effect greater than 90% of the positive control (Fig. 3.5B). Furthermore, at day 6, *SCD-1* was significantly inhibited by all concentrations of RA treatments, all showing a 70% inhibition effect at this time point (Fig. 3.5C). The inhibitory effect of 1000 nM RA continued to day 8 (Fig. 3.5D). The efficacy of RA to *SCD-1* gene expression was attenuated after day 8, and all the five concentrations of RA showed no significant inhibition on day 10 (Fig. 3.5E). This suggests *SCD-1* is intermittently responsive to RA during differentiation and may play an important role in the pathway of RA regulation of adipogenesis.

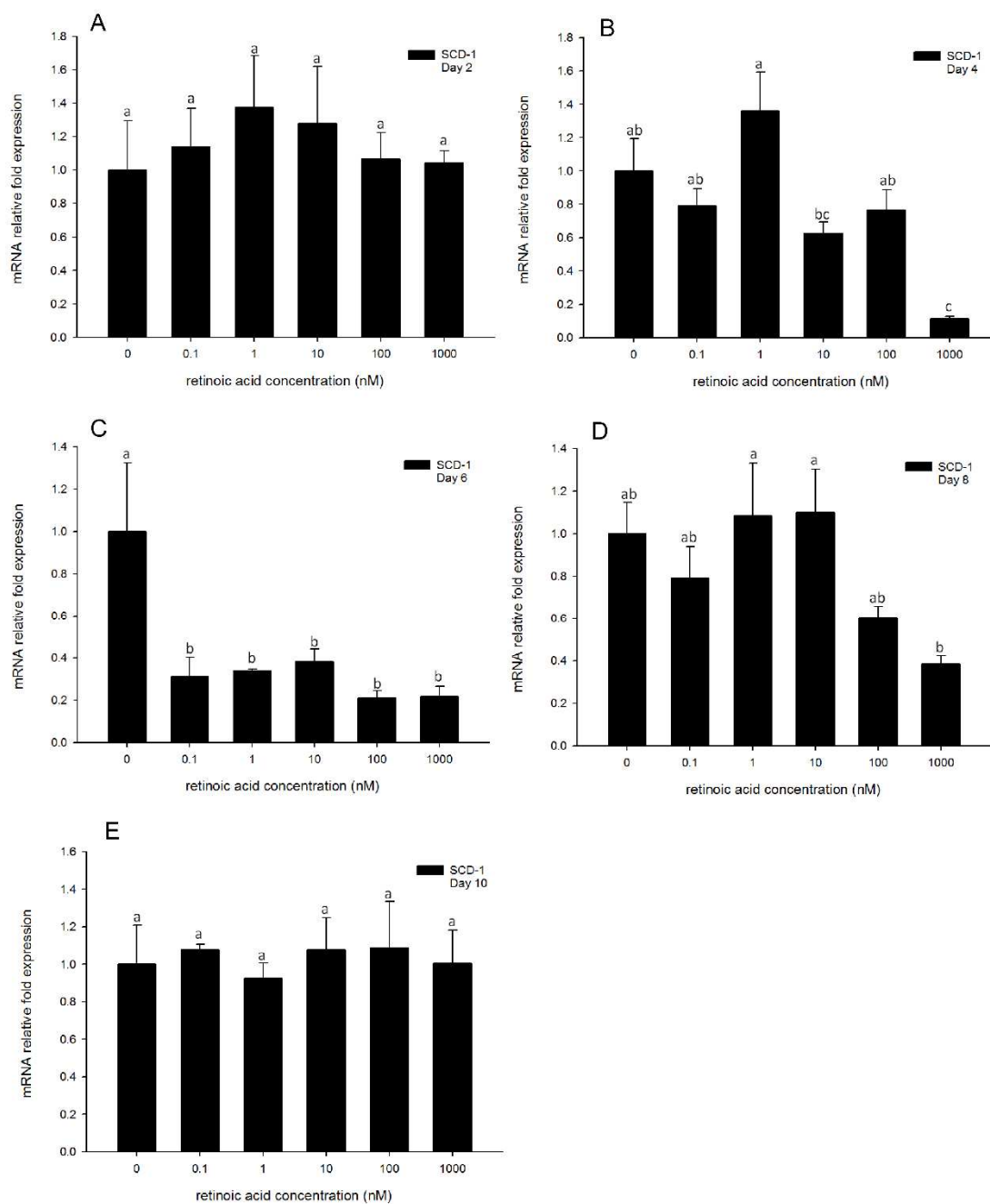


Figure 3.5 Real-time PCR quantification of *SCD-1* gene expression in 3T3-L1 cells on days 2 (A), 4 (B), 6 (C), 8 (D) and 10 (E). Cells were treated with DM in the presence or absence of 0.1, 1, 10, 100, and 1000 nM RA and *EEF2* was used as endogenous control (ΔCt). Data were normalized to *SCD-1* gene expression of positive control (DM) at the

corresponding time point ($\Delta\Delta\text{Ct}$). Data are means \pm SE ($n = 3$). Different letters represent treatment effects that were significantly different ($P < 0.05$).

Gene expression of *Pref-1* was altered in latter time-points, but only in response to high concentrations of RA.

Expression levels of *Pref-1* were not altered in any of the RA treated 3T3-L1 cells at days 2, 4, and 6 (Fig. 3.6A-C), gene expression relative values being similar to the positive control. Cells treated with the highest concentration of RA (1000 nM) showed a significant increase in *Pref-1* gene expression level at days 8 and 10 (Fig. 3.6D-E), suggesting greater retention of the preadipocyte phenotype. This result suggests that *Pref-1* expression responds only to high concentrations of RA in the latter stages of adipocyte differentiation, and may also play a role in the pathways of RA inhibited adipogenesis.

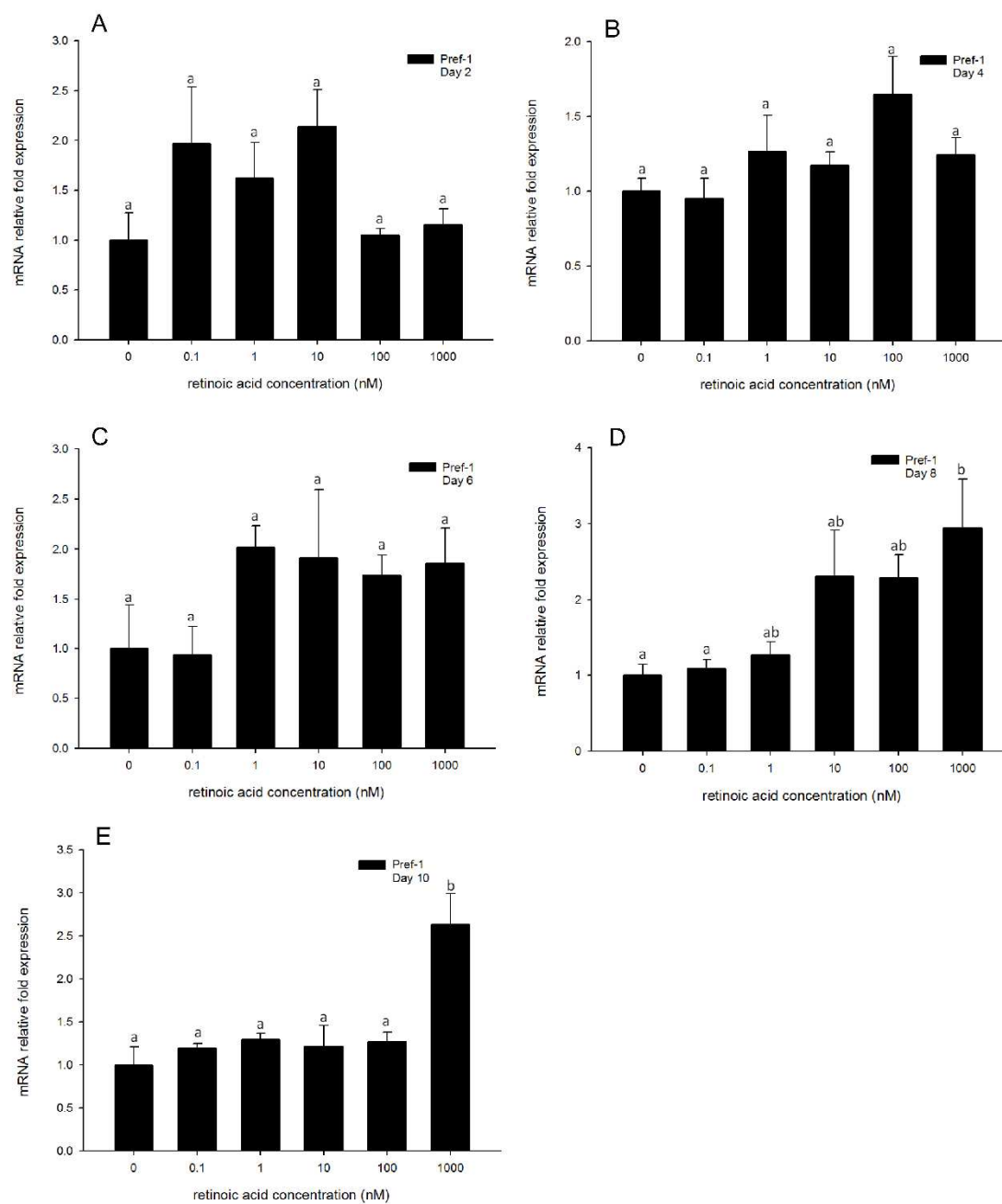


Figure 3.6 Real-time PCR quantification of *Pref-1* gene expression in 3T3-L1 cells on days 2 (A), 4 (B), 6 (C), 8 (D) and 10 (E). Cells were treated with DM in the presence or absence of 0.1, 1, 10, 100, and 1000 nM RA and *EEF2* was used as endogenous control (ΔCt). Data were normalized to *Pref-1* gene expression of positive control (DM) at the

corresponding time point ($\Delta\Delta\text{Ct}$). Data are means \pm SE ($n = 3$). Different letters represent treatment effects that were significantly different ($P < 0.05$).

Relative luciferase activity of C/EBP α promoter activity was not affected by RA treatment.

This study was conducted to investigate C/EBP α promoter activity in response to transient exposure of cells for 0, 12, 24 and 48 h to 1000 nM RA plus differentiation medium, differentiation medium only, and growth medium only. The data obtained with RA treatment indicate that C/EBP α promoter activity was increased relative to both the positive and negative controls, but only at the 48 h time-point. This may suggest that the RA-mediated reduction in C/EBP α gene expression observed from day 2 through day 8 may be due to the induction of a greater rate of C/EBP α mRNA degradation (Supplementary Fig. 3.6). The promoter activities of C/EBP α from cells treated with both differentiation medium and differentiation medium plus RA were significantly higher than growth medium alone (Supplementary Fig. 3.6), suggesting that the C/EBP α promoter is stimulated within the first 48 h of adipocyte differentiation.

Discussion

This study has shown at least three important observations: 1) high concentrations of RA have inhibitory effects on adipogenesis, and this effect persists through day 8, 2) not all of the key adipogenic genes (e.g. C/EBP δ) interact with RA, and 3) the pathway of RA mediated inhibition of adipogenesis may be mediated through C/EBP α mRNA degradation and is not related to a decrease in C/EBP α promoter activity. We demonstrate that RA plays a distinct metabolic role in adipocyte differentiation in vitro,

and when treated with high concentration, it inhibits lipid accumulation and some of adipogenic key gene expression.

The *C/EBP* family is a class of basic-leucine zipper transcription factors [23], and they have been shown to be regulators of adipocyte differentiation. Both *C/EBP β* and *C/EBP δ* mRNA and protein levels were reported to rise early and transiently in preadipocytes which have been induced to differentiate [9, 24, 25]. In the present study, RA treatments had a minimal inhibitory effect on *C/EBP β* after day 2, instead of in the early time points, and did not inhibit *C/EBP δ* expression at all the time points. These results are consistent with previous reports [26]. RA did not block the induction of endogenous *C/EBP β* early in adipogenesis, and *C/EBP β* is sufficient to induce adipogenesis. The effect of RA inhibition in adipogenesis appears to occur in a later phase of *C/EBP β* -induced adipogenesis.

The *PPAR* family is a group of transcriptional factors that heterodimerize with another nuclear hormone receptor, retinoid X receptor (RXR), binding to the response elements of target gene promoters and function as active transcriptional factors [27]. When PPARs are heterodimerized with RXR, the complex is activated and transported to the nucleus to bind to specific sequences in promoter regions (termed as *PPAR* response elements, PPREs) of downstream target genes, activating their transcription [13, 28, 29]. There are three major isoforms: *PPAR α* , *PPAR δ* , and *PPAR γ* [30], which have specific roles in lipid metabolism. Importantly, *PPAR γ* plays an important role in triglyceride synthesis and adipocyte differentiation [29]. As an important adipogenic

factor, *PPAR* γ expression is activated downstream of *C/EBP* β and *C/EBP* δ transcription during the cascade of adipogenesis, and upstream of *C/EBP* α . In the present study, gene expression of *PPAR* γ was only minimally affected by RA while *C/EBP* α gene expression was highly inhibited by RA, from day 2 until day 8 (Fig. 1, 2). These data indicate that RA induced inhibition of adipogenesis in 3T3-L1 cells was associated with an inhibition of *C/EBP* α gene expression. Previously studies reported that RA interferes with the transcriptional activity of *C/EBP* proteins, so that it blocks the *C/EBP* β -mediated induction of downstream genes [31]. This is consistent with our results, RA does not inhibit adipogenesis directly via *C/EBP* β , but through mechanisms active downstream. RA also strongly up-regulates the retinoic acid receptor γ (*RAR* γ) expression in 3T3-L1 preadipocytes, in the meantime it down-regulates retinoid receptor α (*RXR* α) expression [32,33]. This contributes to the inhibitory effect of RA on adipogenesis by favoring *RAR*: *RXR* heterodimer formation over *PPAR* γ : *RXR* formation. Although we observed only a marginal effect of RA on *PPAR* γ gene expression, it appears that when *PPAR* γ activation is delayed, it also has a negative mediation to downstream *C/EBP* α expression, and adipogenesis is inhibited. We observed that the *C/EBP* α promoter was upregulated in response to RA. This suggests that there may be counter-regulatory mechanisms at work, as the minimal effects of RA on *PPAR* γ might be expected to have little effect on *PPAR* γ feedback on up-regulation of *C/EBP* α expression. Thus, we hypothesize that the observed reduction in *C/EBP* α expression in response to RA may be mediated by mechanisms that up-regulate the degradation of *C/EBP* α mRNA. Clearly, further studies of these pathways are needed in order to understand these complex interactions.

In the present study, *SREBP-1c* gene expression was inhibited by high concentration (1000 and 100 nM) of RA treatment on days 2, coinciding with its maximum expression level in the positive control treatment. The inhibition were ameliorated after day 4. The low (0.1 and 0.01 nM) concentrations of RA has no inhibitory effect on *SREBP-1c* gene expression on all the time points. These data indicate that the inhibition of *SREBP-1c* gene expression by RA treatment was transient and corresponded with the d 2 time point. Thus, it is not clear whether *SREBP-1c* may be involved in the RA inhibition pathway of adipogenesis, showing a similar gene expression profile to *C/EBP δ* . These two genes are upstream of *PPAR γ* in the transcriptional activation of adipogenesis, therefore, the inhibition of adipogenesis caused by RA may be unrelated to mechanisms involving the transcriptional factors that are expressed in the early stages of adipogenesis.

Gene expression levels of *FABP4* and *SCD-1* were strongly inhibited by RA treatments. Gene expression of *FABP4* was strongly inhibited by the high concentrations of RA treatments from days 2 to 6. The inhibitory effects of RA treatments on *SCD-1* gene expression were gradual in comparison to effects on *FABP4* expression. Inhibition by high concentrations of RA began by day 4, and remained until day 8. However, at day 6, gene expression of *SCD-1* was inhibited by all concentrations of RA treatments tested, and comparable to effects on *FABP4*. In previous reports, *FABP4* has been shown to have a *PPAR γ* response element (PPRE) in its promoter region and *PPAR γ* regulates gene expression of *FABP4* [28, 34]. In RA treated cells, *PPAR γ* expression was inhibited, and this effect also negatively influenced *FABP4* expression. *SCD-1*

plays an important role in adipogenesis as well as *FABP4*. Its functions include incorporation of double bonds in fatty acids and synthesis of long chain fatty acids in adipocytes [35]. In the present study, *SCD-1* expression was significantly inhibited by RA, suggesting that *SCD-1* may play a role in the pathway of RA inhibited adipogenesis. Mechanisms of *FABP4* and *SCD-1* gene expression in response to RA still need to be explored further.

Preadipocyte factor 1 is a marker protein of preadipocytes and is not expressed in mature adipocytes [36]. During initiation of adipogenesis, the gene expression of Pref-1 decreases and the expression of key adipogenic genes increases [1]. We hypothesized that *Pref-1* expression would decrease in treatments with differentiation medium, and would remain at higher levels in treatments with RA when compared to in DM treated cells. In the present study, *Pref-1* gene expression was not significantly higher compared to DM only until day 10. These data support our hypothesis, and in RA treatments where *PPAR γ* , *C/EBP α* , *FABP4* and *SCD-1* gene expression levels were inhibited, the expression of *Pref-1* gene correspondingly remained significantly higher than in DM only treatments.

In conclusion, lipid accumulation and the expression of key adipogenic genes, *PPAR γ* , *C/EBP α* , *FABP4*, *SREBP-1c*, and *SCD-1* were significantly inhibited by RA treatments until day 8. In contrast, *C/EBP β* and δ expression were not changed in response to RA treatments. Our study has demonstrated that RA represses adipogenesis via up-regulating degradation of *C/EBP α* mRNA, but *C/EBP α* promoter activity, and hence,

the adipogenic-specific genes (*FABP4*, and *SCD-1*) downstream of *C/EBP α* during the transcriptional cascade of adipogenesis, were also inhibited. Future studies are needed to explore the mechanisms by which RA interacts with *C/EBP α* and regulates adipogenesis.

Acknowledgments

We thank Ann Norton of the Optical Imaging Center at the University of Idaho for assistance with the ORO image capture and analysis.

Supplementary information is in Chapter III, page 167-179.

References

1. Macdougald OA, Lane MD. Transcriptional Regulation of Gene-Expression During Adipocyte Differentiation. *Annual Review of Biochemistry* 1995; 64: 345-373.
2. Kawada T, Kamei Y, Fujita A, Hida Y, Takahashi N, and Sugimoto E. Carotenoids and retinoids as suppressors on adipocyte differentiation via nuclear receptors. *BioFactors* 2000; 13:103-109
3. Hirsch J, Batchelor B. Adipose tissue cellularity in human obesity. *Clin Endocrinol Metab* 1976; 5: 299-311.
4. Cheguru P, Chapalamadugu KC, Doumit ME, Murdoch GK, Hill RA. Adipocyte differentiation-specific gene transcriptional response to C18 unsaturated fatty acids plus insulin. *Pflugers Archiv-European Journal of Physiology*. 2012; 463: 429-447.
5. Tontonoz P, Hu E, Devine J, Beale EG, Spiegelman B M. PPARgamma 2 regulates adipose expression of the phosphoenolpyruvate carboxykinase gene. *Molecular and Cellular Biology* 1995; 15:351-357
6. Freytag SO, Paielli DL, Gilbert JD. Ectopic expression of the CCAAT/enhancer binding protein a promoters the adipogenic program in a variety of mouse fibroblastic cells. *Genes Dev* 1994; 8:1654-1663
7. Lin FT, Lane MD. CCAAT/enhancer-binding protein alpha is sufficient to initiate the 3T3-L1 adipocyte differentiation program. *Proc. Natl. Acad. Sci. USA* 1994; 91:8757-8761
8. Wu Z, Bucher NLR, Farmer SR. Conditional ectopic expression of C/EBPb in NIH-3T3 cells induces PPAR γ and stimulates adipogenesis. *Genes Dve* 1995; 9: 2350-2363

9. Yeh WC, Cao Z, Classon M, McKnight SL. Cascade regulation of terminal adipocyte differentiation by three members of the C/EBP family of leucine zipper proteins. *Genes Dev* 1995; 9: 168-181.
10. Rosen ED, Spiegelman BM. Molecular regulation of adipogenesis. *Annu Rev Cell Dev Biol* 2000; 16: 145-171.
11. Rosen ED, Hsu CH, Wang X, Sakai S, Freeman MW, Gonzalez FJ, et al. C/EBPalpha induces adipogenesis through PPARgamma: a unified pathway. *Genes Dev* 2002; 16: 22-26.
12. Gregoire FM, Smas CM, Sul HS. Understanding adipocyte differentiation. *Physiol Rev* 1998; 78: 783-809.
13. Rosen ED, Walkey CJ, Puigserver P, Spiegelman BM. Transcriptional regulation of adipogenesis. *Genes Dev* 2000; 14: 1293-1307.
14. Brown MS, Goldstein JL. The SREBP pathway: regulation of cholesterol metabolism by proteolysis of a membrane-bound transcription factor. *Cell* 1997; 89: 331-340.
15. Kim JB, Sarraf P, Wright M, Yao KM, Mueller E, Solanes G, et al. Nutritional and Insulin Regulation of Fatty Acid Synthetase and Leptin Gene Expression through ADD1/SREBP1. *J Clin Invest* 1998; 101: 1-9.
16. Kim JB, Spiegelman BM. ADD1/SREBP1 promotes adipocyte differentiation and gene expression linked to fatty acid metabolism. *Genes Dev* 1996; 10: 1096-1107.
17. Fajas L, Schoonjans K, Gelman L, Kim JB, Najib J, Martin G, et al. Regulation of peroxisome proliferator-activated receptor gamma expression by adipocyte differentiation and determination factor 1/sterol regulatory element binding protein

- 1: implications for adipocyte differentiation and metabolism. *Mol Cell Biol* 1999; 19: 5495-5503.
18. Ziouzenkova O, Orasanu G, Sharlach M, Akiyama TE, Berger JP, Viereck J et al. Retinaldehyde represses adipogenesis and diet-induced obesity. *Nature Medicine* 2007; 13:695-702.
19. Stao M, Hiragun A, Mitsui H. Preadipocytes possess cellular retinoid binding proteins and their differentiation is inhibited by retinoids. *Biochemical and Biophysical Research Communications* 1980; 95: 1839-1845.
20. Stone RL, Bernlohr DA. The molecular basis for inhibition of adipose conversion of murine 3T3-L1 cells by retinoic acid. *Differentiation* 1990; 45:119-127
21. Ramirezzacarias JL, Castromunozledo F, Kuriharcuch W. Quantitation of Adipose Conversion and Triglycerides by Staining Intracytoplasmic Lipids with Oil Red-O. *Histochemistry* 1992; 97: 493-497.
22. Pfaffl MW. A new mathematical model for relative quantification in real-time RT-PCR. *Nucleic Acids Research* 2001; 29: e45.
23. Li YC, Pirro AE, Amling M, Delling G, Baron R, Bronson R, et al. Targeted ablation of the vitamin D receptor: an animal model of vitamin D-dependent rickets type II with alopecia. *Proc Natl Acad Sci U S A* 1997; 94: 9831-9835.
24. Cao Z, Umek RM, McKnight SL. Regulated expression of three C/EBP isoforms during adipose conversion of 3T3-L1 cells. *Genes Dev* 1991; 5: 1538-1552.
25. Darlington GJ, Ross SE, MacDougald OA (1998) The role of C/EBP genes in adipocyte differentiation. *J Biol Chem* 1998; 273: 30057-30060.

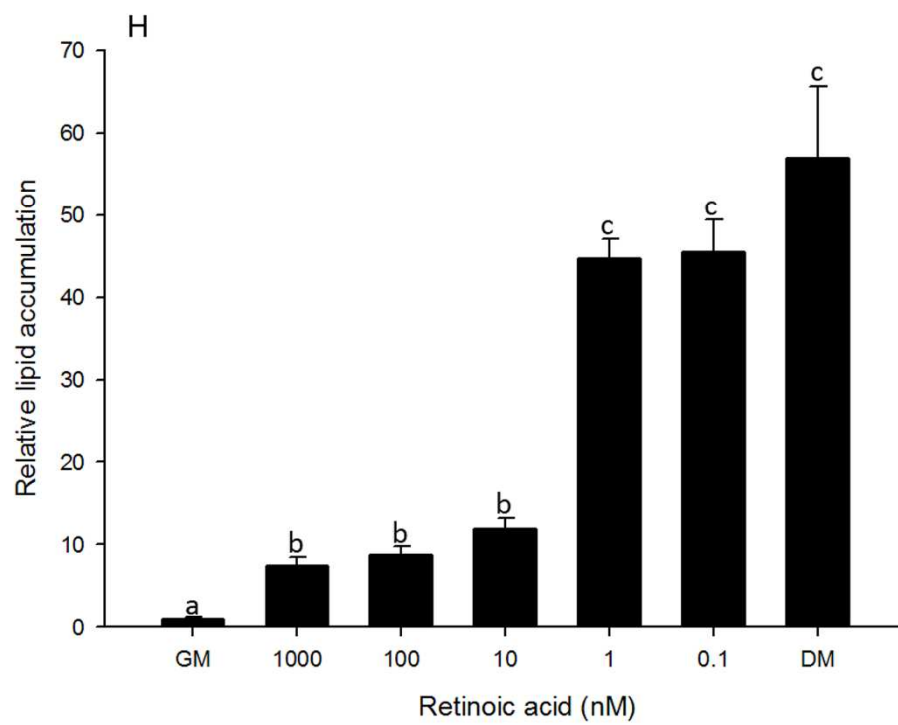
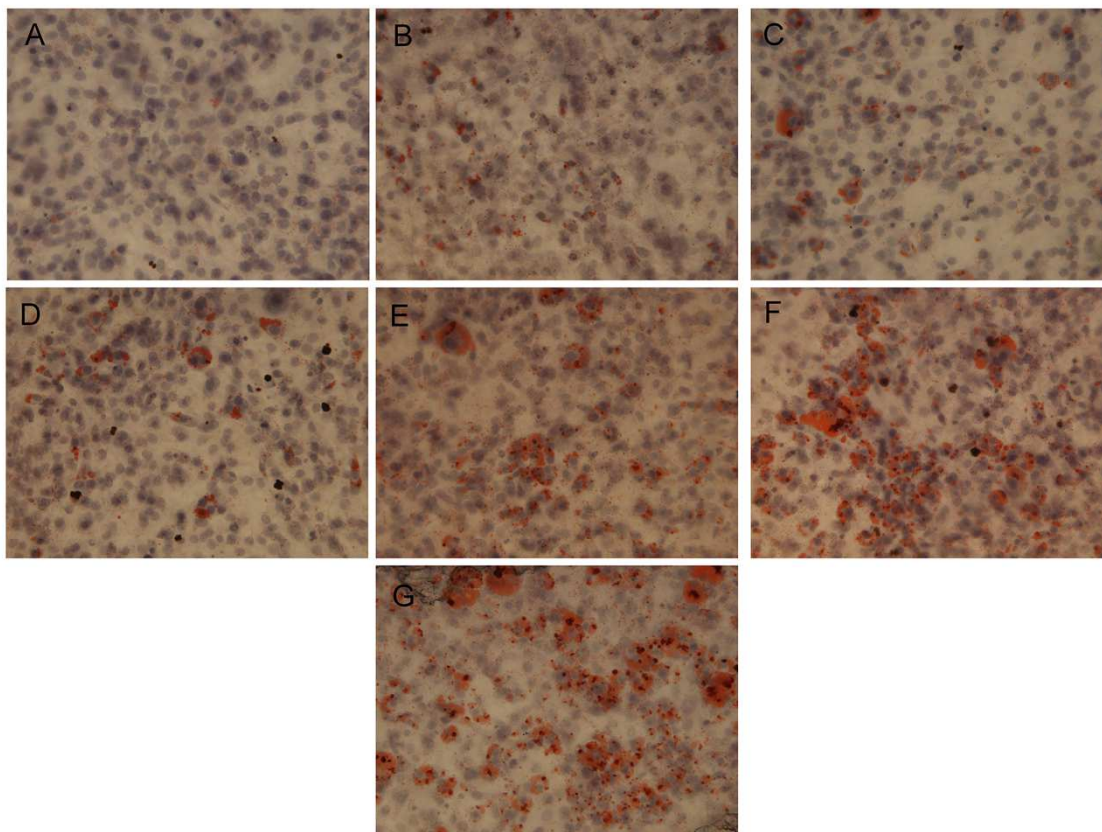
26. Schwarz EJ, Reginato MJ, Shao D, Krakow SJ, Lazar MA. Retinoic acid blocks adipogenesis by inhibiting C/EBP β -mediated transcription. *Molecular and Cellular Biology* 1997; Mar: 1552-1561
27. Laudet V, Hanni C, Coll J, Catzeflis F, Stehelin D. Evolution of the nuclear receptor gene superfamily. *EMBO J* 1992; 11: 1003-1013.
28. Berger J, Moller DE. The mechanisms of action of PPARs. *Annu Rev Med* 2002; 53: 409-435.
29. Rosen ED, Spiegelman BM. PPAR γ : a nuclear regulator of metabolism, differentiation, and cell growth. *J Biol Chem* 2001; 276: 37731-37734.
30. Desvergne B, Michalik, L. and Wahli, W. Transcriptional Regulation of Metabolism. *Physiol Rev* 2006; 86: 465-514.
31. Kamei Y, Kawada T, Mizukami J, Sugimoto E. The prevention of adipose differentiation of 3T3-L1 cells caused by retinoic acid is elicited through retinoic acid receptor alpha. *Life Sci* 1994; 55:307-312
32. Kamei Y, Kawada T, Kazuki R, Sugimoto E. Retinoic acid receptor gamma 2 gene expression is up-regulated by retinoic acid in 3T3-L1 preadipocytes. *Biochem. J* 1993; 293: 807-812
33. Kawada T, Kamei Y, Sugimoto E. The possibility of active form of vitamin A and D are suppressors on adipocyte development via ligand-dependent transcriptional regulators. *Int. J. Obes. Relat. Metab. Disord* 1996; 20: S52-S57
34. Tontonoz P, Hu E, Graves RA, Budavari AI, Spiegelman BM. mPPAR gamma 2: tissue-specific regulator of an adipocyte enhancer. *Genes Dev* 1994; 8: 1224-1234.

35. Enoch HG, Strittmatter P. Role of tyrosyl and arginyl residues in rat liver microsomal stearylcoenzyme A desaturase. *Biochemistry* 1978; 17: 4927-4932.
36. Sul HS. Minireview: Pref-1: role in adipogenesis and mesenchymal cell fate. *Mol Endocrinol* 2009; 23: 1717-1725.

Supplementary Information

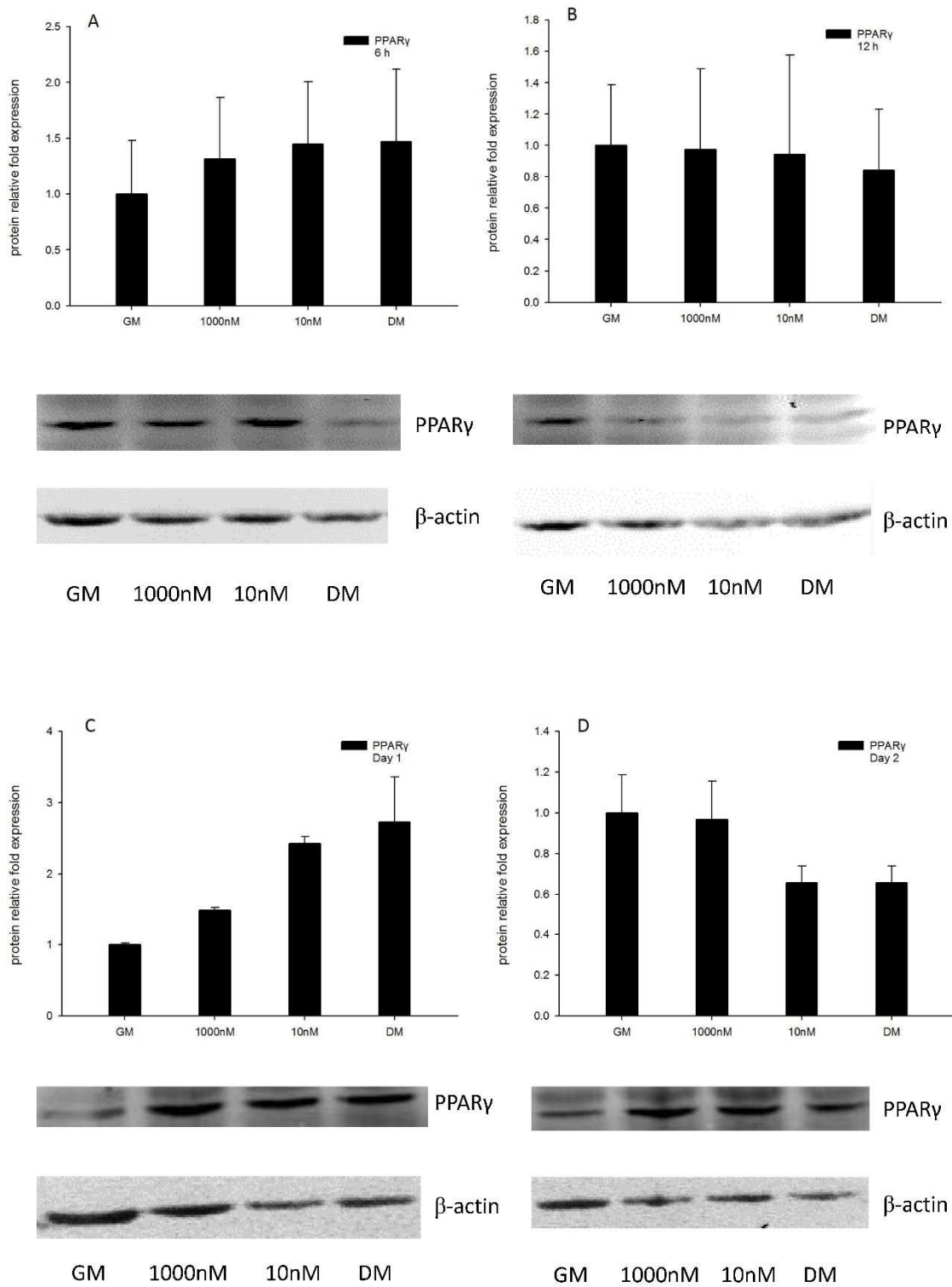
Adipogenesis and key adipogenic gene expression response to retinoic acid in 3T3-L1 cells

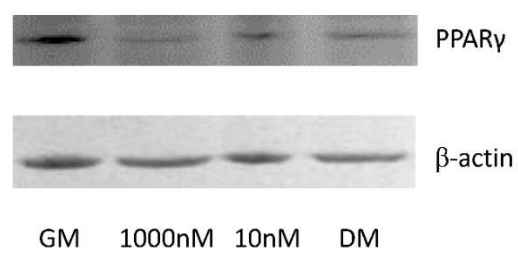
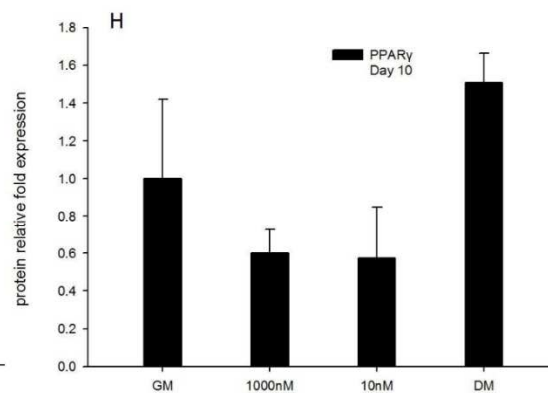
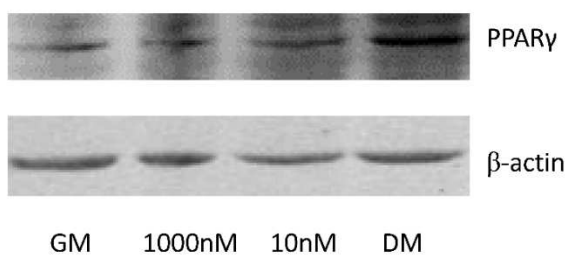
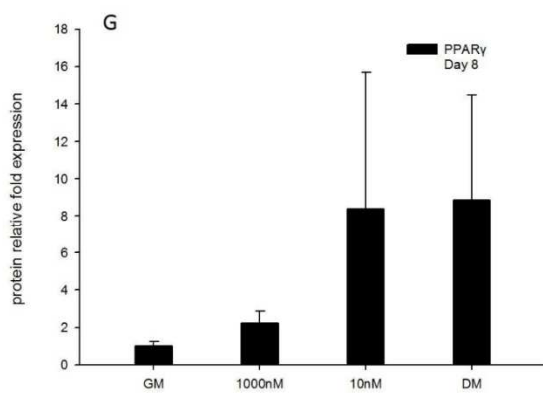
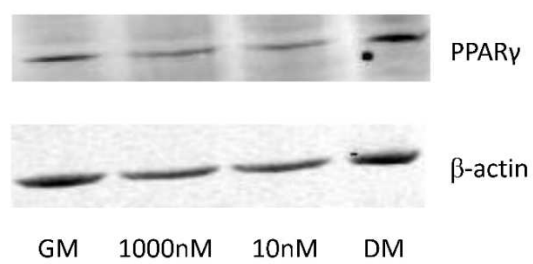
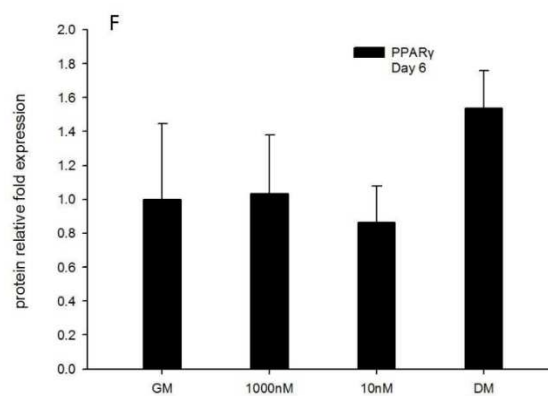
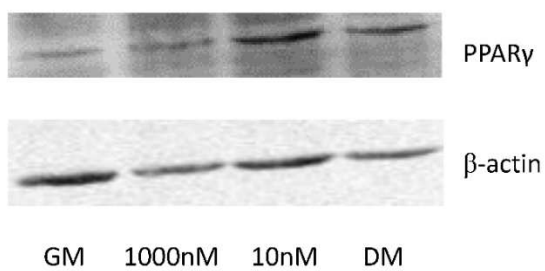
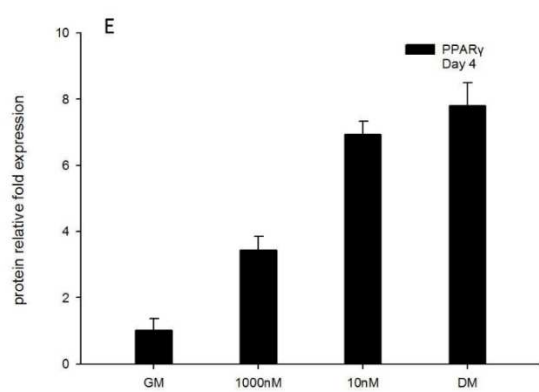
Supplementary Figure 3.1 Oil Red O staining in 3T3-L1 cells. Cells were treated with basal growth medium (GM) (A) or differentiation medium plus different concentrations of retinoic acid, 1000 nM (B), 100 nM (C), 10 nM (D), 1 nM (E) or 0.1 nM (F) or differentiation medium (DM) (G). Oil Red O staining was performed on days 2, 4, 6, 8 and 10. Representative day 10 images are shown. Images were collected at 400x magnification. (H): Quantification of lipid accumulation in 3T3-L1 cells. Lipid accumulation was quantified using MetaMorph Image analysis software. Area fractions were collected for each treatment and normalized to control of corresponding time point. Data are means \pm SE ($n = 3$). Different letters represent treatment effects that were significantly different ($P < 0.05$). The dose-response effect of retinoic acid treatment on lipid accumulation is illustrated.



Supplementary Figure 3.2 Western Blot quantification of PPAR γ protein expression.

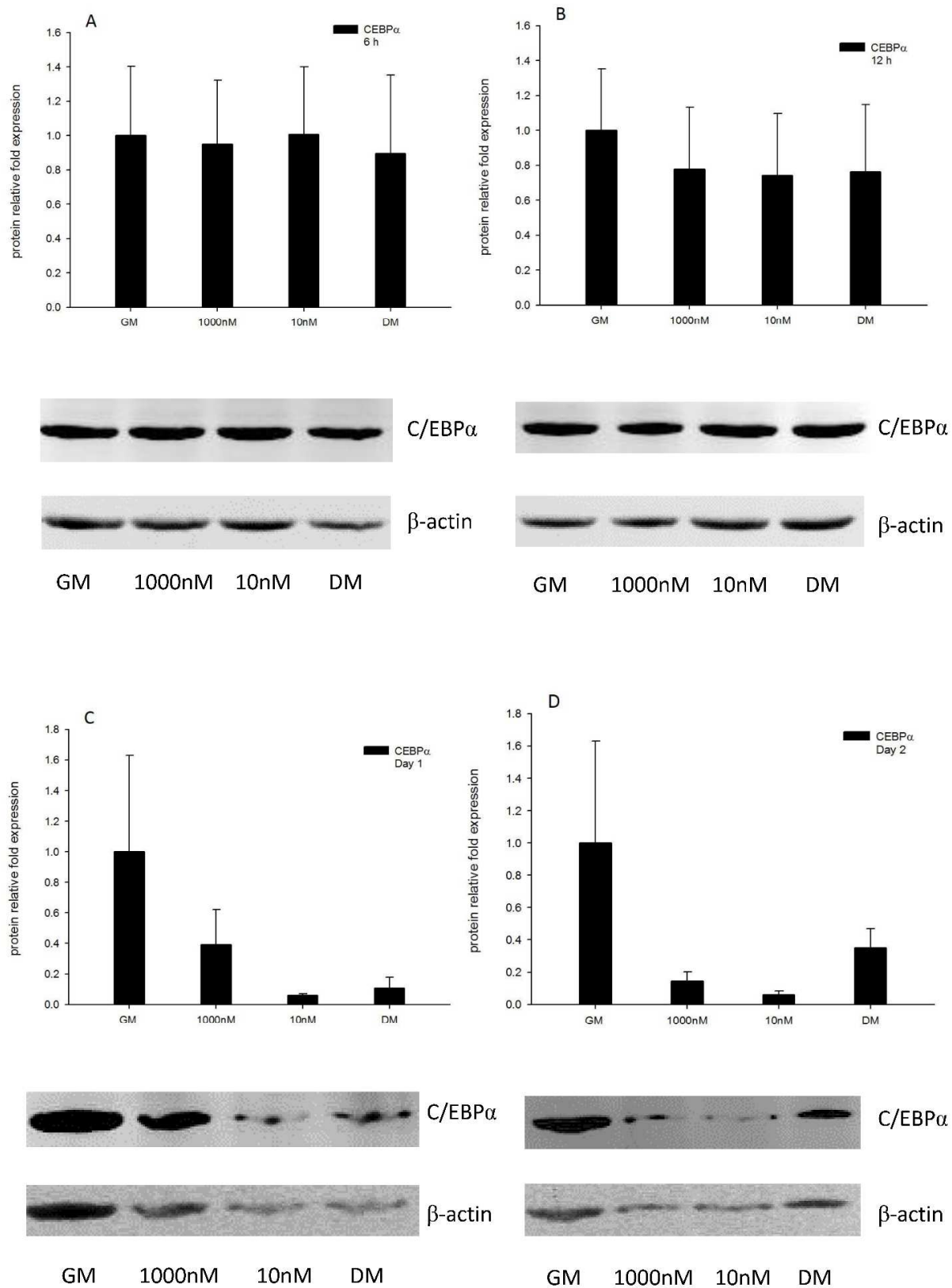
Representative images showing Western blot analysis (Odyssey® Dual Infrared Imaging System (Li-Cor)) of PPAR γ on 6 h (A), 12 h (B), days 1 (C), 2 (D), 4 (E), 6 (F), 8 (G) and 10 (H). Cells were treated with differentiation medium in the presence or absence of 1000 and 10 nM RA, and basal growth medium. β -actin was used as an internal protein loading control. Quantification of PPAR γ normalized to β -actin. Comparisons are with blank within day. Data are means \pm SE (n = 3).

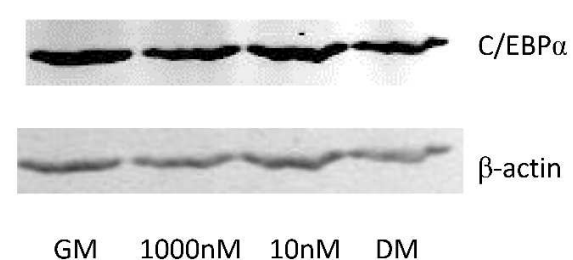
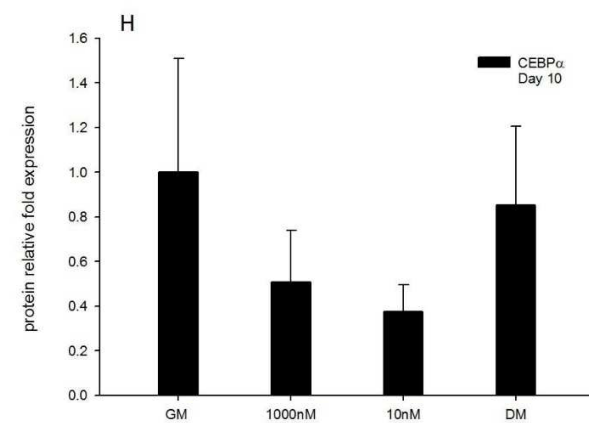
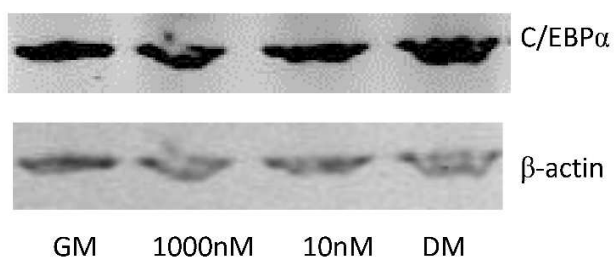
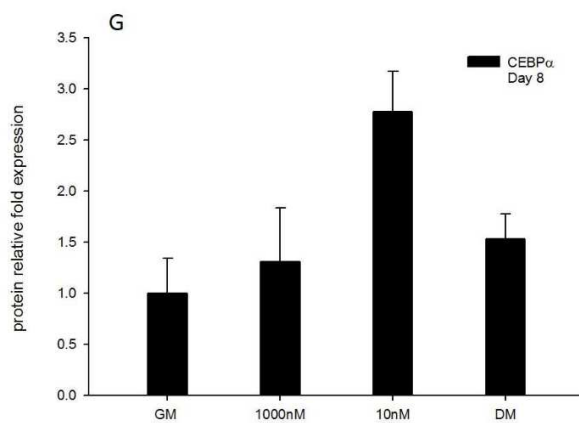
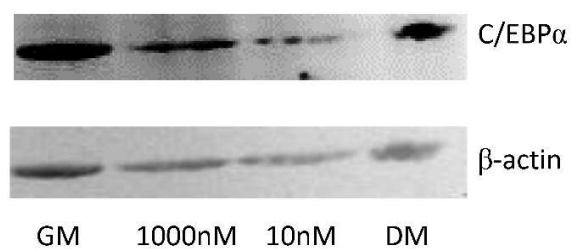
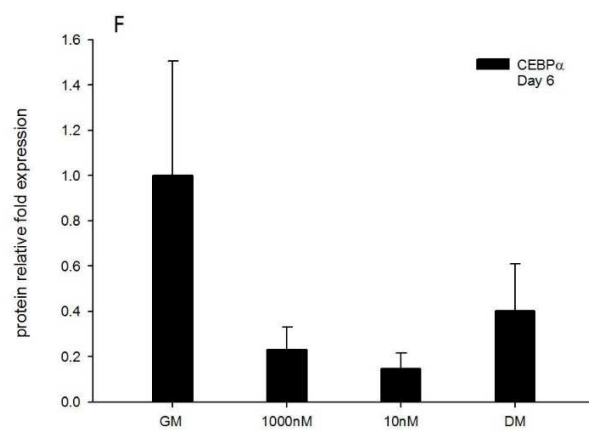
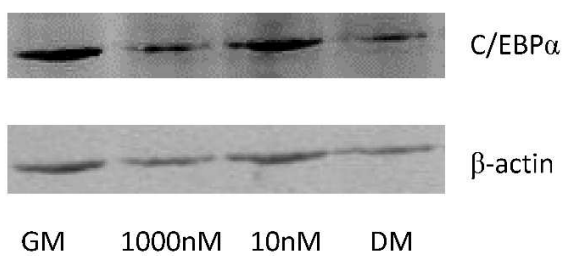
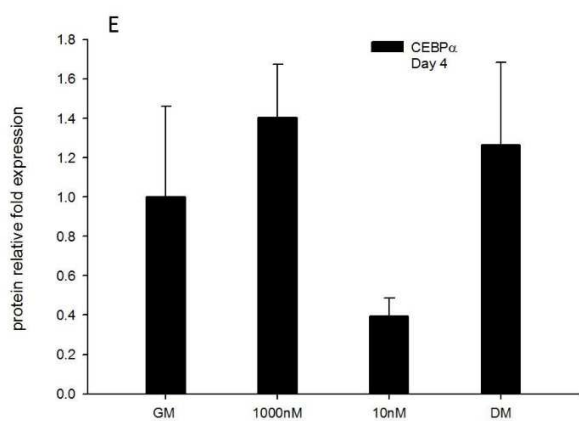




Supplementary Figure 3.3 Western Blot quantification of C/EBP α protein expression.

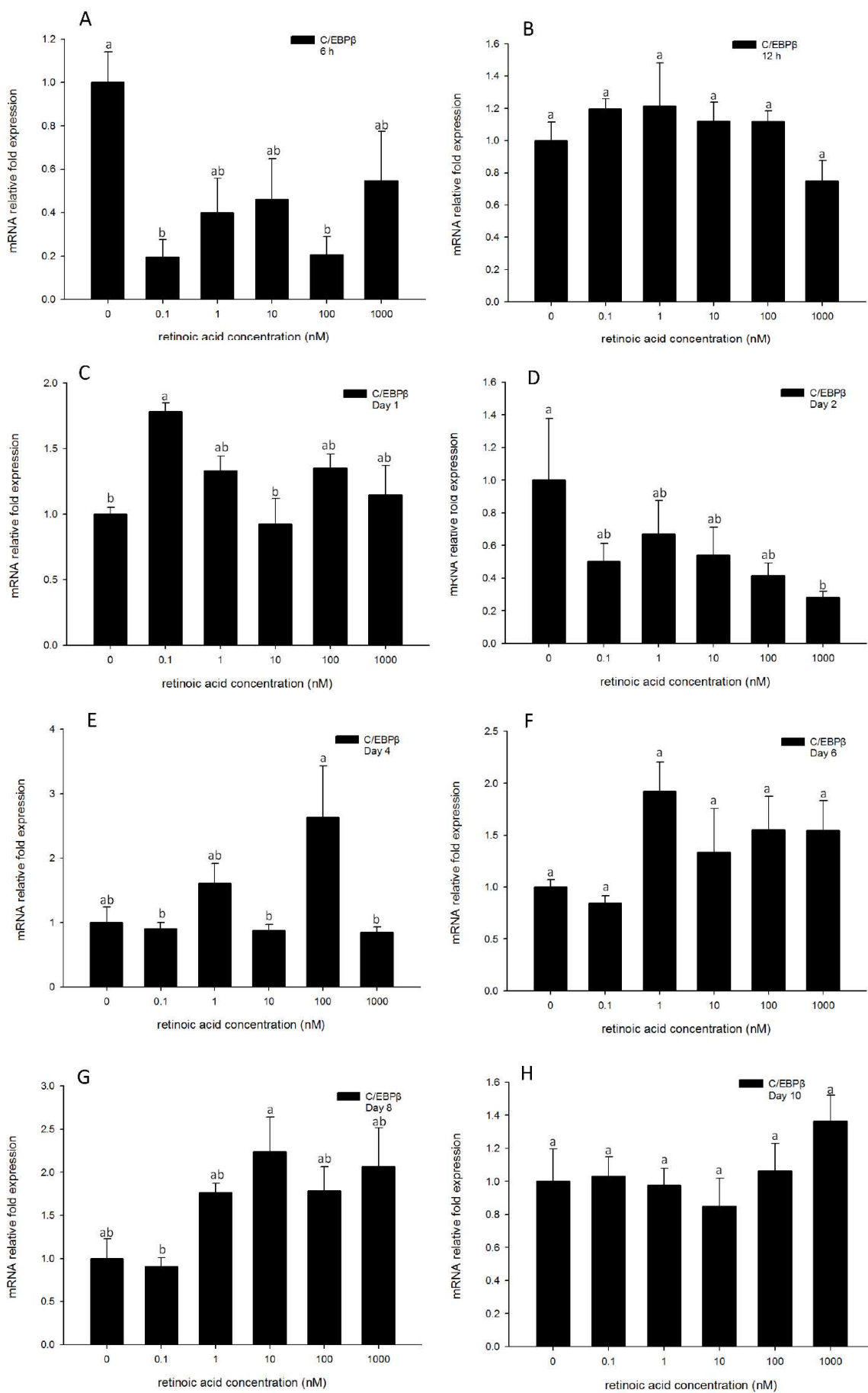
Representative images showing Western blot analysis (Odyssey® Dual Infrared Imaging System (Li-Cor)) of C/EBP α on 6 h (A), 12 h (B), days 1 (C), 2 (D), 4 (E), 6 (F), 8 (G) and 10 (H). Cells were treated with differentiation medium in the presence or absence of 1000 and 10 nM retinoic acid, and basal growth medium. β -actin was used as an internal protein loading control. Quantification of C/EBP α normalized to β -actin. Comparisons are with blank within day. Data are means \pm SE (n = 3).





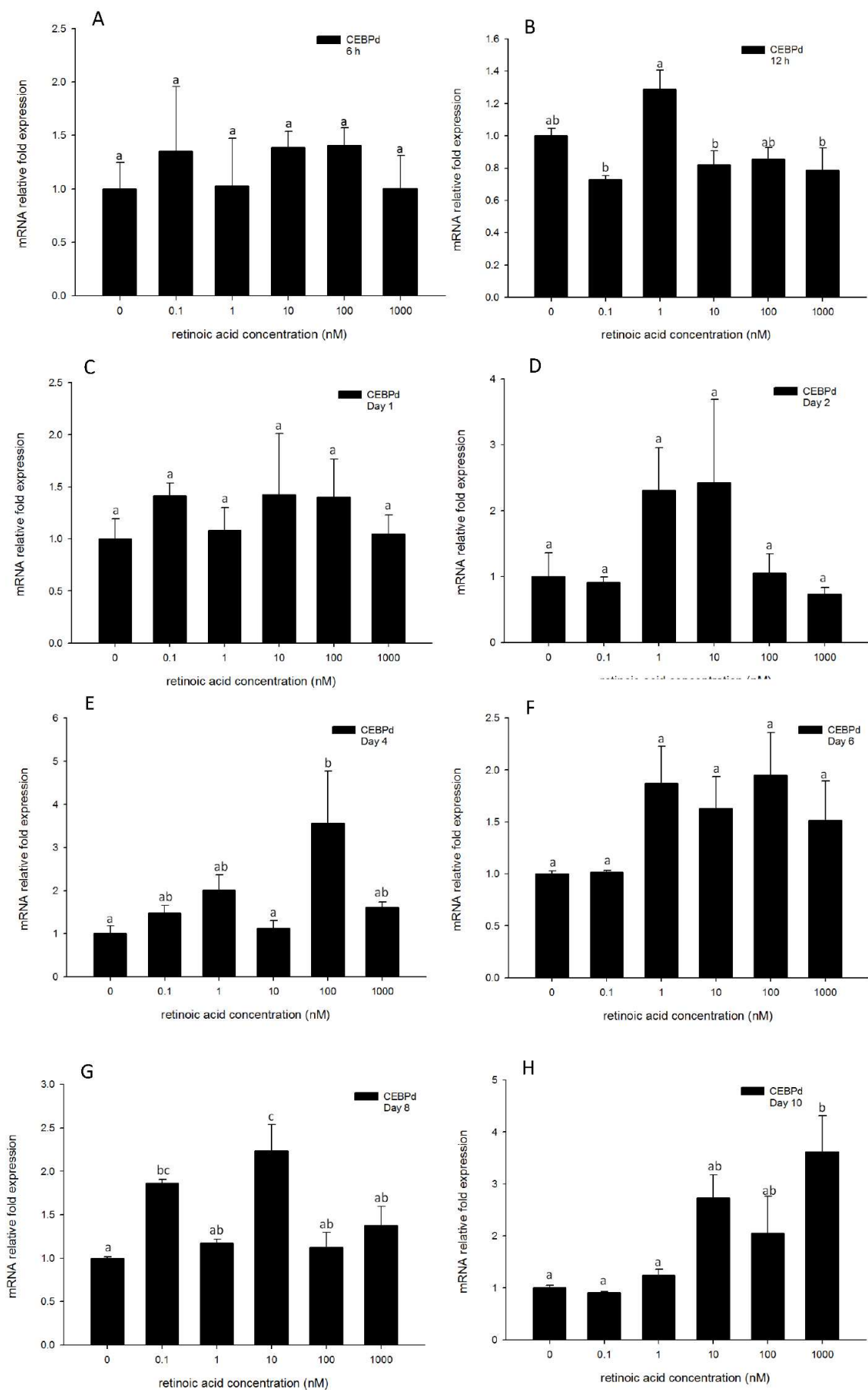
Supplementary Figure 3.4 Real-time PCR quantification of *C/EBPβ* gene expression in 3T3-L1 cells on 6h (A), 12h (B) and days1 (C), 2 (D), 4 (E), 6 (F), 8 (G) and 10 (H).

Cells were treated with DM in the presence or absence of 0.1, 1, 10, 100, and 1000 nM RA and *EEF2* was used as endogenous control (ΔCt). Data were normalized to *C/EBPβ* gene expression of positive control (DM) at the corresponding time point ($\Delta\Delta\text{Ct}$). Data are means \pm SE (n = 3). Different letters represent treatment effects that were significantly different ($P < 0.05$).

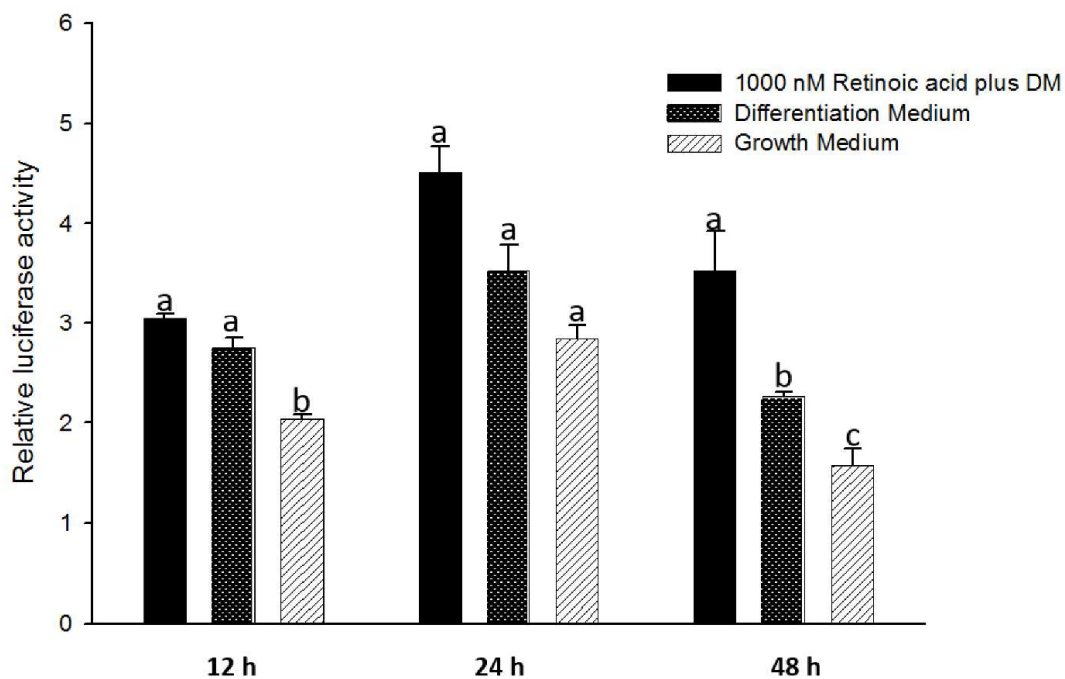


Supplementary Figure 3.5 Real-time PCR quantification of *C/EBPδ* gene expression in 3T3-L1 cells on 6h (A), 12h (B) and days1 (C), 2 (D), 4 (E), 6 (F), 8 (G) and 10 (H).

Cells were treated with DM in the presence or absence of 0.1, 1, 10, 100, and 1000 nM RA and *EEF2* was used as endogenous control (ΔCt). Data were normalized to *C/EBPδ* gene expression of positive control (DM) at the corresponding time point ($\Delta\Delta\text{Ct}$). Data are means \pm SE (n = 3). Different letters represent treatment effects that were significantly different ($P < 0.05$).



Supplementary Figure 3.6 Mouse 3T3-L1 cells were transfected with pGL4.10 (*luc2/-500CEBPa*) in triplicate. Following incubation with differentiation medium only, growth medium only, or differentiation medium with RA (1000 nM). Fire-fly and Renilla luciferase activity units were measured at 0, 12, 24 and 48 h. The firefly luciferase activity units were normalized to Renilla luciferase activity units. Data are normalized as fold activation relative to 0 h and shown as means \pm SE ($n = 3$). Different letters represent treatment effects that were significantly different ($P < 0.05$) within each time-point.



CHAPTER IV

GOLD-KDEL PEPTIDE-SIRNA NANOCONJUGATE-MEDIATED TRANSFECTION IN 3T3-L1 PREADIPOCYTES AND MATURE ADIPOCYTES

Abstract

To investigate the effect of gold-nanoconjugate delivering siRNA against CCAAT/enhancing binding protein α (C/EBP α , a key regulator of adipocyte differentiation) into pre-adipocytes and mature adipocytes, siRNA against C/EBP α was linked with gold nanoparticles (AuNPs, 20 nm) conjugated with cysteine terminated KDEL (Lys-Asp-Glu-Leu) peptide, and transfected into 3T3-L1 cells. Fluorescence microscopy analysis provided evidence of AuNP-peptide transfection in both undifferentiated 3T3-L1 preadipocytes and mature 3T3-L1 adipocytes. Unfortunately, no significant difference in C/EBP α expression between AuNP-delivered KDEL and siRNA group and negative control group was found. Basis on the transfection of the AuNP-delivered KDEL was observed with confocal microscopy, the reason that the expression of C/EBP α was not significantly reduced might be at day 0, C/EBP α expression was not induced yet, and at day 6, C/EBP α expression declined. However, the fluorescence microscopy data still indicates that AuNP-KDEL nanoconjugates can be transfected into post-differentiation

3T3-L1 (mature adipocytes), and a deeper understanding of the mechanisms regulating their uptake and intracellular trafficking is needed.

Introduction

Gold nanoparticles (AuNPs) have been reported as a supreme delivery tool in catalysis, biology and nanotechnology with unique characteristics compared to other vectors [1]. The characteristics of AuNP, enhanced cellular uptake, low cytotoxicity and flexibility in synthesis and functionalization, supporting that AuNPs could be used as nanocarriers for drug delivery and gene therapy, suggesting their promise for development and use in the clinic. Various modifications have been implemented on AuNP functionalization, such as AuNP conjugated to peptides [2-7], oligonucleotides (ONs) [8, 9], antibodies [10], various combinations of biomolecules [11-15], and also including biological passivating agents such as polyethylene glycol (PEG) [16-19], or oligoethylene glycol (OEG) [20, 21].

The carboxy-terminal sequence Lys-Asp-Glu-Leu (KDEL) in animal cells was first discovered as a retention signal for soluble proteins resident in the endoplasmic reticulum (ER) [22]. The KDEL signal is recognized by ERD2 receptors, targeting their ligands to the retrograde COPI-mediated transport pathway (23-25). Extracellular proteins and peptides having the C-terminal KDEL motif can be internalized, reaching Golgi-like structures within 30 min and the ER in 30-90 min [26].

Gene knockdown by siRNA has been showed to have high efficiency to control the transcriptional and translational level of genes and their products [27]. Delivery of siRNA

into cells has been conducted using various transfection methods such as electroporation, viral vector mediation and lipid (liposomal) mediation. Most of these *in vitro* transfections are attempted during the proliferative phase of the cells to enhance transfection efficiency [28]. However, the understanding and successful transfection of siRNA in differentiated cells remains limited and unclear. Various attempts have been made to deliver siRNA efficiently using AuNP nanoconjugates in both *in vivo* and *in vitro* models.

This study presents the use of AuNP as a delivery platform to deliver CCAAT/enhancer binding protein α (C/EBP α) siRNA to both undifferentiated 3T3-L1 preadipocytes and mature 3T3-L1 adipocytes. CEBP α plays an important role in the process of adipogenesis, and triggers the downstream adipogenic genes, such as FABP4. We hypothesize that the KDEL motif facilitates the cellular uptake and intracellular trafficking of C/EBP α siRNA as part of a multi-component AuNP nanoconjugates in mature adipocytes. This approach will provide an attractive alternative for delivery of siRNA in differentiated adipocytes avoiding the use of alternatives such as lipofectamine in high concentrations, which is cytotoxic. Further, this study provides a deeper understanding of the mechanisms involved in the intracellular transport of AuNP-based nanoconjugates in cell culture studies.

Materials and Methods

Peptide/siRNA design, sequences and synthesis

Sequences of peptides and siRNA are shown in Table 4.1. The peptide sequences were constructed as described previously [29]. KDEL peptide sequences were constructed with or without the fluorescent marker, rhodamine (New England Peptide, Gardner, MA) having

an N-terminal CGY motif. The peptide contains a KDEL motif at the C-terminus. The fluorophore-labeled peptides were used in most of the experiments. The siRNA sequence was designed with Custom Oligonucleotide design Software from Integrated DNA Technologies, Inc (Coralville, Iowa), and synthesized with a thiol modification at the 5' terminus. The antisense strand was unmodified.

siRNA protected thiol bond cleavage

Before resuspending the dry thiolated siRNA, sulfur cross-bridges were reversed (per the manufacturer's recommendations) to provide free thiols from binding to AuNP. Free sulfurs were capped using TCEP as described in the manufacturer's protocol (Piercenet, Rockford, IL). Briefly, 400 μ L of 3% TCEP was added to the dry oligonucleotide and vortexed until the sample was in solution, and was then incubated at room temperature for 1 h. After incubation, 50 μ L of 3 M sodium acetate and 500 μ L of 100 % ethanol were added followed by incubation at -80°C for 30 minutes. The solution was finally centrifuged at 13000 x g for 15 min and extra ethanol was removed using a vacuum lyophilizer. The dry pellet was resuspended in RNase free water to yield a final siRNA concentration of 20 μ M. To prevent bond reformation between strands and effective binding with AuNP this procedure was done on the day of nanoconstruct preparation.

Preparation of Au-peptide-siRNA nanoconjugates

AuNP-peptides nanoconjugates were prepared as described previously with slight modifications [29]. Citrate-capped Au NPs (20 nm) were purchased from SPI Supplies (West Chester, Pennsylvania). In order to bind approximately 50% of available AuNP sites,

twenty μL KDEL peptide (20 μM) was mixed with 1 mL AuNP (1.16 nM) and gently agitated for 24 h at room temperature (RT) and then centrifuged at 13,000 x g for 30 minutes to recover the nanoconjugates. The supernatant was carefully removed, and the conjugate pellet was resuspended in 0.5 mM sodium citrate buffer (pH 7.4). The stability and conjugation success of KDEL peptide nanoconjugates was consistent with observations reported in previous studies [29, 30]. Twenty μL of fluorophore labeled siRNA (20 μM) was then added to the solution and gently agitated for another 24 h at room temperature. The conjugates were centrifuged again as described above and washed with 1 X PBS, three times. Finally, the pellet was resuspended in 20 μL of 0.5 mM sodium citrate buffer (pH 7.4) and stored at 40C. Conjugates were prepared with or without rhodamine labeled peptide for different experiments.

Cell culture

Mouse 3T3-L1 preadipocytes were cultured at 37 °C with 5% CO₂ enriched air in DMEM with 10 % FBS, 100 I.U. /ml penicillin, 100 $\mu\text{g}/\text{ml}$ streptomycin (basal growth medium). To induce 3T3-L1 differentiation, after cells reached 100% confluence, cultures were then incubated for an additional 48 h, then the medium was changed to differentiation medium, including dexamethasone (1 μM), IBMX (500 μM) and insulin (1.7 mM) (standard hormonal differentiation medium, DMI). The DMI treatment was applied for the first 48 h followed by only insulin in basal growth medium throughout the remaining time points. Media were changed every 2 days for all treatments.

siRNA and nanoconjugate transfection

For transfection, 1×10^5 3T3-L1 cells were seeded into 6-well plates. After 24 h, when cells were at approximately 70% confluent. For Lipofectamine-mediated transfection, 10 μL of 20 μM siRNA was transfected using 4 μL of Lipofectamine (Invitrogen, Carlsbad, CA) in DM. For AuNP-mediated transfection, 20 μL of Au-siRNA-KDEL nanoconjugate was added to the medium. Equal concentrations of scrambled siRNA with lipofectamine or AuNP were transfected in parallel plates as controls. After 24 h, cells were extracted for imaging and gene expression analysis. Cells for days 2 and 6 were continuously cultured in differentiation media. On days 1 and 5, transfection was done following the protocol outlined for myoblasts above. Cells were extracted on days 2 and 6 (24 h transfection) for imaging and gene expression analysis.

Immunofluorescence Microscopy

For day 0 and day 6 staining, 3T3-L1 cells in 6-well plates were fixed using 4% paraformaldehyde for 15 minutes and laser confocal imaging was done using an Olympus Multiphoton/Confocal FluoView 1000 using a 40x water immersion lens (Center Valley, PA). All images were analyzed using FV10-ASW 3.1 software and/or Metamorph Image analysis software as described previously [31]. All images were standardized during acquisition and analysis of all comparable groups. Images were quantified from at least 6-8 individual images from triplicate wells per treatment.

RNA extraction and cDNA synthesis

Total RNA extraction was performed using the Trizol extraction method as recommended by the manufacturer (Invitrogen) as previously described [32]. Extracted RNA was resuspended in nuclease free water and stored at -80°C until further use. Each RNA sample was quantified using a Nanodrop® ND-1000 UV-Vis spectrophotometer (Nanodrop Technologies, Wilmington, DE). Samples were further treated with Turbo DNase free to remove DNA contamination. First strand cDNA synthesis was performed using 2 µg RNA for each sample using a high capacity cDNA reverse transcription kit according to the manufacturer's instructions (Invitrogen).

Real-time PCR

Total Quantitative Real Time PCR (qRT-PCR) was performed using Taqman MGB® primer/probe sets with an ABI 7500 Fast Real Time PCR system (Applied Biosystems, Foster City, CA) as described previously [33]. Primers and probes used for PCR were as follows: C/EBPα; F. primer: CGCAAGAGCCGAGATAAAGC, R. primer: GTCAACTCCAGCACCTTCTGTTG, probe: AACGCAACGTGGAGAC, and Eef2; F. primer: CTGCCTGTCAATGAGTCCTTTG, R. primer: GCCGCCGGTGTGGAT and probe: CTTACCGCTGATCTG. Primers and probes for all genes were designed using Applied Biosystems Primer Express 3.0 software. Real-time PCR assays for each sample were conducted in duplicate wells on the same plate for both C/EBPα and the Eef2 endogenous control. Negative controls for all genes were run without reverse transcriptase. Reactions contained Taqman Universal Fast PCR Master Mix, No AmpErase® UNG (Applied Biosystems, Foster City, CA), forward primer (0.5 µM), reverse primer (0.5 µM),

Taqman probe (0.125 μ M) and cDNA template made up to a final volume of 15 μ L in nuclease-free water. Real-time PCR cycle conditions included a holding time of 90 °C for 20 sec, followed by 40 cycles of 90 °C for 3 sec and 60 °C for 30 sec of melting and extension temperatures, respectively.

Data were analyzed using the relative CT ($\Delta\Delta$ Ct) method [34]. Average Ct values of endogenous control (Eef2) were subtracted from C/EBP α gene average Ct values, to obtain Δ Ct values for each sample. Finally, Δ Ct values of samples from the control treatment at each time point were used to normalize Δ Ct values of corresponding time points of each treatment to obtain $\Delta\Delta$ Ct and mRNA fold expression values [$2^{-\Delta\Delta$ Ct}].

Statistical Analysis

For qRT-PCR, data are expressed as fold change of means \pm SE from at least three independent experiments. All other assays were conducted in triplicate. Statically analysis was performed using one-way ANOVA test (SAS 9.3- Cary, NC). When $P < 0.05$, differences were considered statistically significant.

Table 4.1 Sequences and purities of peptides and siRNA used to form nanoconjugates

Name	Sequence
Peptide A	H2N-CGYRQSDIDTHNRIKDEL-COOH
Fluorescent Peptide A	H2N-CGY[KRhod]RQSDIDTHNRIKDEL-COOH
C/EBP α siRNA	5'-GCCAGGCUGCAGGUGCAUGGUGGUC-3' 5'-5ThioMC6-D-GACCACCAUGCACCUGCAGCCGUUC

Results

Au-peptide nanoconjugates were transfected into both pre- (day 0) and post (day 6) adipocytes.

For day 0 and day 6 staining, 3T3-L1 cells in 6-well plates were fixed using 4% paraformaldehyde for 15 minutes and laser confocal imaging was done using an Olympus Multiphoton/ Confocal FluoView 1000. The fluorescence images strongly support that AuNPs-peptide nanoconjugates had been transfected into both the preadipocytes (day 0) (Fig. 4.1A) and mature adipocytes (day 6) (Fig. 4.1B).

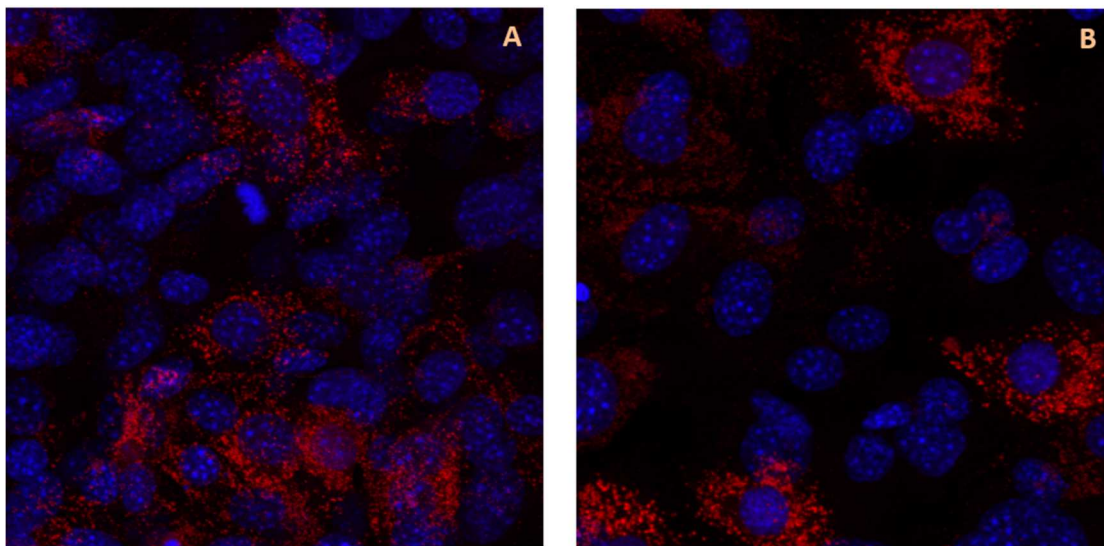


Figure 4.1 Fluorescence image of Au-nanoconjugates in 3T3-L1

3T3-L1 cells transfected with AuNPs-peptide nanoconjugates on day -1 and day 5, respectively, and incubated for 24 h. Fluorescence staining was performed on day 0 (A), and day 6 (B). Images was collected at 40x water immersion lens.

Gene knockdown efficacy of AuNP nanoconjugates.

To further investigate the transfection efficacy of AuNP-mediated siRNA delivery, we studied at the mRNA expression of *C/EBP α* in both undifferentiated 3T3-L1 and mature adipocytes. Unfortunately, there was no *C/EBP α* knockdown observed in neither undifferentiated preadipocytes nor differentiated adipocytes with lipofectamine-mediated siRNA transfection or AuNP nanoconjugates transfection (Fig. 4.2). However, at day 2 and day 6, in the control groups (blank and scrambled siRNA), *C/EBP α* expression was induced compared to day 0.

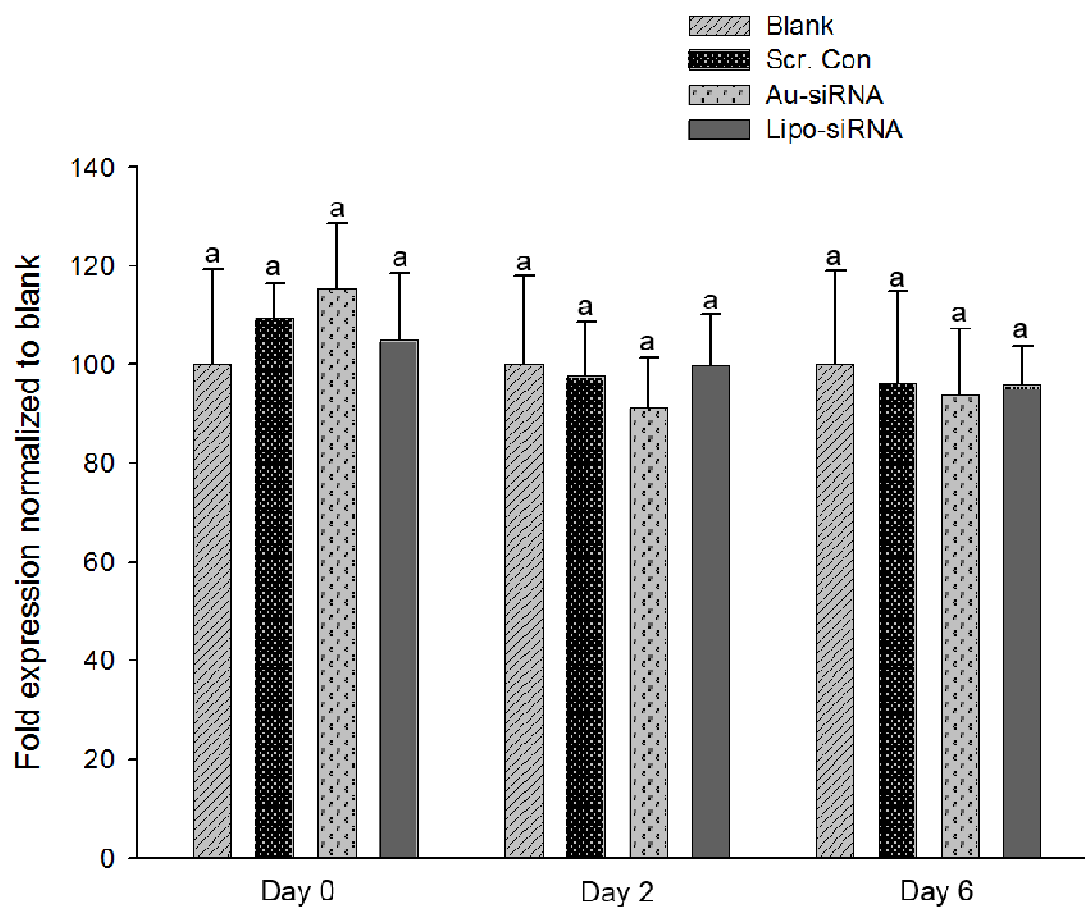


Figure 4.2 mRNA knockdown of C/EBP α by Au-nanoconjugates

Real-time PCR quantification of C/EBP α gene expression in 3T3-L1 cells on days 0, 2 and 6 of differentiation. Cells were treated with siRNA scrambled control, siRNA C/EBP α or Au-KDEL-siRNA nanoconjugates on days-1, 1, and 5. Comparisons are made with the blank within day. Data are means \pm SE (n=3). Bars with different letters represent statistically significant differences (P<0.05).

Discussion

Lipofectamine is a cationic lipid formulation that has relatively high efficacy in terms of delivery of siRNA to cells, especially in cultures during exponential growth phase. However, Lipofectamine has been observed to delay growth and possess cytotoxic effects on transfected cells [35]. Although, attempts have been made to improve these cationic lipids to render them less cytotoxic and more efficient, they still possess some level of cytotoxicity [36, 37]. In addition, effective transfection of non-proliferating cells such as mature adipocytes has been a challenge even with the use of these cationic lipids. Therefore, there is a need for a delivery vector that is less cytotoxic and that can efficiently deliver oligonucleotides or peptides to differentiated cells.

AuNP have emerged as a promising vector for delivery of peptides, molecular markers, oligonucleotides, and drugs to undifferentiated cells [38]. However, higher concentrations of AuNP may have cytotoxic effects, concentrations of 20 nM or lower have been found to be compatible with cells without any adverse effects [39]. In our experiments, the final concentration of nanoconjugates was less than 1 nM, and at this concentration we did not

observe any adverse effects on the cells. We started with studies of AuNP-peptide conjugates to understand the cellular uptake of the peptides. Consistent with previous experiments, we observed significant uptake of AuNP-peptide conjugates in 3T3-L1 preadipocytes and also the mature adipocytes. Effective delivery into these cells also provides presumptive evidence that transfection of adipose tissue in vivo may be enhanced using this approach. Our data provides preliminary evidence for the use of AuNP nanoconjugates functionalized with KDEL peptides as an efficient delivery vector for siRNA to differentiated mature adipocytes.

To estimate the efficacy of siRNA gene knockdown in mature adipocytes is one of the objectives of the present study. We performed comparative mRNA expression analysis between Lipofectamine-mediated delivery and AuNP nanoconjugate delivery of siRNA using highly specific Taqman PCR reactions. However, we did not observe C/EBP α gene knockdown in either the lipofectamine delivery group or the AuNP nanoconjugate delivery group. This is a little disappointing, however, it might be because the siRNA against C/EBP α did not work out as expected. Another hypothetical explanation is that siRNA could be degraded through lysosomes, and to investigate this hypothesis, further studies will be conducted in intracellular trafficking and co-localization of siRNA against C/EBP α labeled with fluorophores.

In the previous studies, AuNP-KDEL nanoconjugates were reported to be effective in transfection into Sol8 [29, 30] and C2C12 muscle cells [32]. In the present study, we also observed AuNP-KDEL nanoconjugates were successfully transfected into differentiated

3T3-L1 adipocytes. These observations suggest that AuNP-KDEL nanoconjugates transfection is effective. However, since the transfection with AuNP-KDEL nanoconjugates is effective, there may be some other explanations for why gene knock-down was not achieved as expected. First of all, the timing of transfection timing is very important. Another reason is that during the process of adipogenesis, C/EBP α expression level is changed from the beginning to the late phase of the process, and this may also impact to choose the optimal timing of transfection. Even though in the present study three time points have been chosen, we may still miss the optimized time point for gene knock. In the next step of this study, transfection timing will need be optimized and choose shorter time interval, 0, 12 h, and days 1, 2, and 6. The siRNA against C/EBP α will also be optimized in the next step studies. We will design several other sequences of siRNA against C/EBP α , test for the best gene knock down efficiency, and use it to link with AuNP nanoconjugates.

References

1. Daniel, M.C. and Astruc, D., *Gold nanoparticles: assembly, supramolecular chemistry, quantum-size-related properties, and applications toward biology, catalysis, and nanotechnology*. Chem Rev, 2004. **104**(1): p. 293-346.
2. Porta, F., et al., *Gold nanoparticles capped by peptides*. Materials Science and Engineering B-Solid State Materials for Advanced Technology, 2007. **140**(3): p. 187-194.
3. Xie, H., et al., *Critical flocculation concentrations, binding isotherms, and ligand exchange properties of peptide-modified gold nanoparticles studied by UV-visible, fluorescence, and time-correlated single photon counting spectroscopies*. Anal Chem, 2003. **75**(21): p. 5797-805.
4. Levy, R., et al., *Rational and combinatorial design of peptide capping Ligands for gold nanoparticles*. Journal of the American Chemical Society, 2004. **126**(32): p. 10076-10084.
5. Nativo, P., Prior, I.A., and Brust, M., *Uptake and intracellular fate of surface-modified gold nanoparticles*. ACS Nano, 2008. **2**(8): p. 1639-44.
6. Chithrani, B.D., Ghazani, A.A., and Chan, W.C., *Determining the size and shape dependence of gold nanoparticle uptake into mammalian cells*. Nano Lett, 2006. **6**(4): p. 662-8.
7. de la Fuente, J.M. and Berry, C.C., *Tat peptide as an efficient molecule to translocate gold nanoparticles into the cell nucleus*. Bioconjug Chem, 2005. **16**(5): p. 1176-80.

8. Alivisatos, A.P., et al., *Organization of 'nanocrystal molecules' using DNA*. Nature, 1996. **382**(6592): p. 609-11.
9. Mirkin, C.A., et al., *A DNA-based method for rationally assembling nanoparticles into macroscopic materials*. Nature, 1996. **382**(6592): p. 607-9.
10. El-Sayed, I.H., Huang, X., and El-Sayed, M.A., *Surface plasmon resonance scattering and absorption of anti-EGFR antibody conjugated gold nanoparticles in cancer diagnostics: applications in oral cancer*. Nano Lett, 2005. **5**(5): p. 829-34.
11. Nam, J.M., Jang, K.J., and Groves, J.T., *Detection of proteins using a colorimetric bio-barcode assay*. Nat Protoc, 2007. **2**(6): p. 1438-44.
12. Liu, Y. and Franzen, S., *Factors determining the efficacy of nuclear delivery of antisense oligonucleotides by gold nanoparticles*. Bioconjug Chem, 2008. **19**(5): p. 1009-16.
13. Tkachenko, A.G., et al., *Cellular trajectories of peptide-modified gold particle complexes: Comparison of nuclear localization signals and peptide transduction domains*. Bioconjugate Chemistry, 2004. **15**(3): p. 482-490.
14. Patel, P.C., et al., *Peptide antisense nanoparticles*. Proc Natl Acad Sci U S A, 2008. **105**(45): p. 17222-6.
15. Sandhu, K.K., et al., *Gold nanoparticle-mediated transfection of mammalian cells*. Bioconjug Chem, 2002. **13**(1): p. 3-6.
16. Liu, Y., et al., *Synthesis, stability, and cellular internalization of gold nanoparticles containing mixed peptide-poly(ethylene glycol) monolayers*. Anal Chem, 2007. **79**(6): p. 2221-9.

17. Lee, S.H., et al., *Amine-functionalized gold nanoparticles as non-cytotoxic and efficient intracellular siRNA delivery carriers*. Int J Pharm, 2008. **364**(1): p. 94-101.
18. Oishi, M., et al., *Smart PEGylated gold nanoparticles for the cytoplasmic delivery of siRNA to induce enhanced gene silencing*. Chemistry Letters, 2006. **35**(9): p. 1046-1047.
19. Seferos, D.S., et al., *Polyvalent DNA nanoparticle conjugates stabilize nucleic acids*. Nano Lett, 2009. **9**(1): p. 308-11.
20. Giljohann, D.A., et al., *Gene Regulation with Polyvalent siRNA-Nanoparticle Conjugates*. Journal of the American Chemical Society, 2009. **131**(6): p. 2072-+.
21. Giljohann, D.A., et al., *Oligonucleotide loading determines cellular uptake of DNA-modified gold nanoparticles*. Nano Lett, 2007. **7**(12): p. 3818-21.
22. Munro, S. and Pelham, H.R.B., *An Hsp70-Like Protein in the Er - Identity with the 78 Kd Glucose-Regulated Protein and Immunoglobulin Heavy-Chain Binding-Protein*. Cell, 1986. **46**(2): p. 291-300.
23. Lewis, M.J. and Pelham, H.R.B., *Ligand-Induced Redistribution of a Human Kdel Receptor from the Golgi-Complex to the Endoplasmic-Reticulum*. Cell, 1992. **68**(2): p. 353-364.
24. Pelham, H.R., *Recycling of proteins between the endoplasmic reticulum and Golgi complex*. Curr Opin Cell Biol, 1991. **3**(4): p. 585-91.
25. Sonnichsen, B., et al., *Sorting by COP I-coated vesicles under interphase and mitotic conditions*. Journal of Cell Biology, 1996. **134**(6): p. 1411-1425.

26. Majoul, I.V., Bastiaens, P.I.H., and Soling, H.D., *Transport of an external Lys-Asp-Glu-Leu (KDEL) protein from the plasma membrane to the endoplasmic reticulum: Studies with cholera toxin in Vero cells*. *Journal of Cell Biology*, 1996. **133**(4): p. 777-789.
27. Filipowicz, W., et al., Post-transcriptional gene silencing by siRNAs and miRNAs. *Curr Opin Struct Biol*, 2005. 15(3): p. 331-41.
28. Gavrillov, K. and W.M. Saltzman, Therapeutic siRNA: principles, challenges, and strategies. *Yale J Biol Med*. 85(2): p. 187-200.
29. Wang, G., et al., Gold-peptide nanoconjugate cellular uptake is modulated by serum proteins. *Nanomedicine*, 2011. 8(6): p. 822-32.
30. Wang, G., et al., KDEL peptide gold nanoconstructs: promising nanoplatforms for drug delivery. *Nanomedicine : nanotechnology, biology, and medicine*, 2013. 9(3): p. 366-374.
31. Majmundar, A.J., et al., O(2) regulates skeletal muscle progenitor differentiation through phosphatidylinositol 3-kinase/AKT signaling. *Mol Cell Biol*, 2012. 32(1): p. 36-49.
32. Acharya, S., et al., Change in Nox4 expression is accompanied by changes in myogenic marker expression in differentiating C2C12 myoblasts. *Pflugers Arch*, 2013.
33. Cheguru, P., et al., Adipocyte differentiation-specific gene transcriptional response to C18 unsaturated fatty acids plus insulin. *Pflugers Arch*, 2012. 463(3): p. 429-47.

34. Pfaffl, M.W., A new mathematical model for relative quantification in real-time RT-PCR. *Nucleic Acids Research*, 2001. 29(9): p. e45.
35. Romoren, K., et al., Transfection efficiency and cytotoxicity of cationic liposomes in salmonid cell lines of hepatocyte and macrophage origin. *Biochim Biophys Acta*, 2004. 1663(1-2): p. 127-34.
36. Zhong, Y.Q., et al., [Toxicity of cationic liposome Lipofectamine 2000 in human pancreatic cancer Capan-2 cells]. *Nan Fang Yi Ke Da Xue Xue Bao*, 2008. 28(11): p. 1981-4.
37. Lv, H., et al., Toxicity of cationic lipids and cationic polymers in gene delivery. *J Control Release*, 2006. 114(1): p. 100-9.
38. Han, G., P. Ghosh, and V.M. Rotello, Functionalized gold nanoparticles for drug delivery. *Nanomedicine (Lond)*, 2007. 2(1): p. 113-23.
39. Soenen, S.J., et al., Cytotoxic effects of gold nanoparticles: a multiparametric study. *ACS Nano*. 6(7): p. 5767-83.

CHAPTER V

CONCLUSIONS AND FUTURE DIRECTIONS

Adipogenesis plays an important role in lipid accumulation and adipose tissue development. Understanding the underlying regulatory mechanisms of adipogenesis is important to improve meat quality for the beef industry, and it is also may be important for human obesity therapy. There are several transcriptional factors (such as PPAR γ , C/EBP α , C/EBP β , C/EBP δ , SREBP-1c) which are induced as a cascade regulating the process of adipogenesis. These factors are all crucial in adipogenesis. Some nutrient molecules, for example, vitamin A and D have also been reported to regulate adipogenesis.

In the present studies, 1,25-dihydroxyvitamin D (1,25-(OH) $_2$ D $_3$) and retinoic acid (RA) were studied as regulators of adipogenesis. Both of them inhibited aspects of adipogenesis and lipid accumulation possibly through regulation of adipogenic transcriptional factors. The inhibitory effect of 1,25-(OH) $_2$ D $_3$ on lipid accumulation occurred at high concentrations (100, 10, and 1 nM) of 1,25-(OH) $_2$ D $_3$ through 10 days of testing. The gene expression of PPAR γ and C/EBP α was inhibited by 1,25-(OH) $_2$ D $_3$ treatments through 10 days of testing. FABP4 and SCD-1 expression levels were also suppressed by 1,25-(OH) $_2$ D $_3$ from day 2 to day 10. However, expression of C/EBP β and C/EBP δ was not influenced by 1,25-(OH) $_2$ D $_3$. The promoter activity of C/EBP α was not impacted by 1,25-(OH) $_2$ D $_3$. These results suggest that 1,25-(OH) $_2$ D $_3$ inhibits adipogenesis not directly

through C/EBPs, but via repressed PPAR γ gene expression level or PPAR γ activity. When PPAR γ is inhibited, the downstream transcriptional adipogenic factors, such as C/EBP α , will also be inhibited. RA treatments (high concentrations, 1000 and 100 nM) have greater inhibitory effect on the gene expression of C/EBP α compared to PPAR γ . Similarly to 1,25-(OH) $_2$ D $_3$, C/EBP β and C/EBP δ do not respond to RA at any concentration tested. On the other hand, *FABP4* gene expression was inhibited by all the concentrations of RA. Gene expression of *SCD-1* was inhibited gradually by high concentrations of RA compared to *FABP4*. These results indicate that the pathway of RA inhibition on adipogenesis involves C/EBP α , but not C/EBP β or C/EBP δ . However, the activity of C/EBP α promoter is not affected by RA, so maybe RA inhibiting adipogenesis is via up-regulating degradation of C/EBP α mRNA, but does not influence the promoter activity.

AuNP-nanoconjugates linked with KDEL peptide were used to deliver siRNA against C/EBP α into 3T3-L1 preadipocytes and mature adipocytes. Confocal microscopy images showed that AuNP-nanoconjugates were transfected into both preadipocytes and mature adipocytes. These interesting results indicate that AuNP nanoconjugates are transfected differentiated adipocytes, consistent with previous studies which demonstrated that AuNP-nanoconjugates transfection into mature myotube cells were high effective. In conclusion, the present studies systematically report 1,25-(OH) $_2$ D $_3$ and RA regulation of adipogenesis and the expression of key adipogenic genes. The studies focus on C/EBP α promoter activity response to 1,25-(OH) $_2$ D $_3$ and RA show that the inhibitory effect of vitamin A and D on adipogenesis does not involve C/EBP α promoter. The AuNP-nanoconjugate

experiments report transfection of gold-KDEL-nanoconjugates into mature adipocytes, and might present a potential delivery tool for mature adipocytes.

Future studies will focus on the following aspects: 1) the mechanisms of $1,25\text{-(OH)}_2\text{D}_3$ regulation on adipogenesis through $\text{PPAR}\gamma$; 2) the pathway of retinoic acid regulation on adipogenesis via $\text{C/EBP}\alpha$; 3) $\text{C/EBP}\alpha$ gene knock-down with AuNP-nanoconjugates, and AuNP-nanoconjugates intracellular trafficking and co-localization in 3T3-L1 cells. For $1,25\text{-(OH)}_2\text{D}_3$, future studies should focus on the interaction between the activity of $\text{PPAR}\gamma$ promoter and $1,25\text{-(OH)}_2\text{D}_3$, to investigate the deeper mechanisms of $1,25\text{-(OH)}_2\text{D}_3$ regulation on adipogenesis. For retinoic acid, future studies should focus on both $\text{C/EBP}\alpha$ mRNA and protein level. To investigate the hypothesis of the mechanisms of RA inhibition on adipogenesis via up-regulating degradation of $\text{C/EBP}\alpha$ mRNA or reducing $\text{C/EBP}\alpha$ protein transport into nucleus, nucleic protein could be isolated, and tested in the short interval time course experiments. $\text{C/EBP}\alpha$ mRNA could also be measured accordingly to the same time course experiments as protein. In future $\text{C/EBP}\alpha$ gene knock-down studies, the optimal time points for AuNP-nanoconjugate transfection for intracellular trafficking and co-localization of AuNP-nanoconjugates could be a focus.